

2013

Analysis of Small Molecule Inhibitors Aimed at Bacterial Virulence

Paul Daniel Dossa

Follow this and additional works at: http://digitalcommons.rockefeller.edu/student_theses_and_dissertations

 Part of the [Life Sciences Commons](#)

Recommended Citation

Dossa, Paul Daniel, "Analysis of Small Molecule Inhibitors Aimed at Bacterial Virulence" (2013). *Student Theses and Dissertations*. Paper 239.



ANALYSIS OF SMALL MOLECULE INHIBITORS

AIMED AT BACTERIAL VIRULENCE

A Thesis Presented to the Faculty of

The Rockefeller University

in Partial Fulfillment of the Requirements for

the degree of Doctor of Philosophy

by

Paul Daniel Dossa

June 2013

© Copyright by Paul Daniel Dossa 2013

ANALYSIS OF SMALL MOLECULE INHIBITORS AIMED AT BACTERIAL VIRULENCE

Paul Daniel Dossa, Ph.D.
The Rockefeller University 2013

The emergence of antibiotic-resistant bacterial pathogens and the discovery of new bacterial pathogens have motivated the development of novel antibacterials. One recently proposed strategy is to target pathogenic bacteria specifically by inhibiting virulence mechanisms as opposed to killing bacteria indiscriminately, which includes commensal strains. Due to the increased appreciation for the role commensal bacteria play in the immune response and the importance for maintaining a healthy microbiota, specifically targeting pathogenic bacteria is a desirable goal to attain. Genetic and biochemical studies have highlighted type III secretion systems (T3SSs) as essential components for infection of host cells by Gram-negative bacterial pathogens. Small molecules that target type III protein secretion may therefore represent a new class of antibacterial agents and provide a platform for evaluating an anti-virulence approach.

The salicylidene acylhydrazides (SAHs) are a class of compounds that prevent secretion of bacterial effector proteins through the T3SS and attenuate infection from various species of Gram-negative pathogens; however, the molecular target(s) of these compounds remains unknown, and the potency of these compounds is not optimal. To discover the molecular target(s) of the SAHs in *Salmonella typhimurium* and determine their mechanism of action, I synthesized several alkynyl SAH analogs and employed bioorthogonal labeling techniques for proteomic analysis of their

protein-binding partners. Through structure-activity relationship (SAR) analysis of the alkynyl analogs, I discovered important features for the inhibitory activity of the SAHs and observed that they covalently modify many *S. typhimurium* proteins; however, the protein targets responsible for the inhibitory activity of SAHs remains to be determined.

Repurposing chemical inhibitors to target host enzymes required for infection has emerged as an alternative approach to subvert rapid antibiotic resistance in bacterial pathogens. Towards this goal, the isoquinolinesulfonamide H-89 was reported to limit *Salmonella* replication in macrophages through inhibition of Akt, a host kinase that is activated during infection. However, more potent Akt-specific inhibitors are less effective at inhibiting bacterial replication, suggesting an alternative mechanism of action for H-89. I discovered that H-89 does not target Akt in host cells to restrict bacterial replication, but more likely prevents bacterial replication by inhibiting the expression of *S. typhimurium* T3SS components and effector proteins required for bacterial invasion and replication in host cells. As H-89 does not interfere with bacterial growth in liquid culture, these results highlight isoquinolinesulfonamides as a new class of lead compounds for targeting bacterial virulence.

To my parents,
who have supported me the whole way
and sacrificed to get me where I am today.

ACKNOWLEDGMENTS

I would first like to thank my advisor Howard for cultivating a lab atmosphere conducive to learning and for helping me grow as a scientist over the years. It's difficult to see progress on a day-by-day or even month-by-month basis, but looking back where I was five years ago and where I am today, it's obvious I've come a long way and learned a great deal. I'd like to thank my committee: Tarun Kapoor, Derek Tan, and Erec Stebbins for giving helpful feedback on my projects and even providing reagents to do some experiments. I especially appreciate the original members of the Hang lab for always being there and helping me over the years. Kelvin Tsou, Jacob Yount, Markus Grammel, Mingzi Zhang, Guillaume Charron, and Kavita Rangan all helped me a lot during my graduate career - answering chemistry questions, providing reagents, teaching me how to do biology, and even having some fun while trudging through graduate school. I've enjoyed working with the current lab members as well, especially Lisa Ambrosini-Vadola who has helped me during the later years of my graduate career. The members of the Proteomics Resource Facility at Rockefeller have always been extremely helpful and patient with me, and their service is greatly appreciated. I'm glad I was given the opportunity to be a part of the Tri-Institutional Training Program in Chemical Biology (TPCB) and appreciate its financial and academic support. I wouldn't have made it this far without having some fun outside of lab as well, so a special shout out goes to my friends and family.

TABLE OF CONTENTS

CHAPTER 1 – Introduction	1
1.1 Targeting virulence as an alternative strategy to antibiotics.....	1
1.2 Bacterial virulence mechanisms can be targeted with small molecule inhibitors.....	3
1.3 Type III secretion systems (T3SSs) are essential to infection	7
1.4 Inhibitors of T3SSs in Gram-negative pathogens.....	13
1.4.1 Salicylidene acylhydrazides	13
1.4.2 2-Imino-5-arylidene Thiazolidinones	20
1.4.3 Other chemotypes from HTSs	22
1.4.4 Natural Products	26
1.5 Additional assays for monitoring T3SSs.....	30
1.6 Identifying the target of the SAHs in <i>Salmonella typhimurium</i>	32
1.7 Strategies for target identification of small molecules	33
CHAPTER 2 – Efforts Towards Target Identification of the Salicylidene Acylhydrazides	39
Abstract.....	39
Introduction.....	40
Results	41
2.1 Synthesis and biological activity of photocrosslinking alkynyl SAH	41
2.2 Synthesis and biological activity of alkynyl SAHs	47
2.3 SAR analysis of alkynyl SAHs for inhibitory activity and covalent labeling.....	50
2.4 Effect of SAHs on <i>Salmonella</i> transcription	55
2.5 Proteomic identification of SAH protein-binding partners	56
2.6 SAH inhibition of <i>Salmonella</i> invasion of HeLa cells	58
Discussion	59
CHAPTER 3 – The Repurposed Kinase Inhibitor H-89 Targets Bacterial Virulence Pathways to Limit Infection	61
Abstract.....	61
Introduction.....	62
Results	64
3.1 H-89 inhibits bacterial replication through Akt-independent mechanism	64
3.2 H-89 inhibits expression of <i>Salmonella</i> virulence genes required for bacterial infection	67
3.3 H-89 decreases the levels of bacterial effectors secreted during <i>S. typhimurium</i> replication in host cells	68
3.4 H-89 also antagonizes the SPI-1 T3SS and inhibits <i>Salmonella</i> invasion of epithelial cells.....	70
Discussion	75
CHAPTER 4 – Discussion and Future Outlook	78
CHAPTER 5 – Materials and Methods	85
Compounds.....	85
5.1 Synthesis of T3SS inhibitor INP-0007 (2.1).....	85
5.2 Synthesis of photocrosslinking-alkynyl-INP (PC-alk-INP) (2.2).....	86
5.3 Synthesis of inactive SAH analog	90
5.4 Synthesis of alkynyl SAHs.....	90
5.5 Bacterial strains and eukaryotic cell lines for SAH experiments.....	96
5.6 Isolation of secreted SPI-1 effector proteins.....	96

5.7 Characterization of secreted effector proteins.....	97
5.8 Bacterial lysis.....	97
5.9 Click chemistry protocol and in-gel fluorescence analysis.....	98
5.10 Transcriptional profiling of <i>S. typhimurium</i>.....	99
5.11 Secretion and expression of SopE2-CPG2-HA	99
5.12 Proteomic identification of modified proteins.....	100
5.12.1 Bacterial lysis	100
5.12.2 Click chemistry reaction with azido-biotin	101
5.12.3 Binding the protein to streptavidin beads.....	101
5.12.4 Eluting the protein from the beads and concentrating the sample.....	102
5.12.5 Separating the sample by SDS-PAGE and preparing it for mass spec analysis.....	103
5.13 <i>S. typhimurium</i> invasion of HeLa cells	103
5.14 Bacterial strains, plasmids, and eukaryotic cell lines for H-89 experiments.....	104
5.15 Bacterial replication in macrophages	105
5.16 Western blotting for Akt during macrophage infection.....	105
5.17 Imaging macrophages and secreted SseJ-HA during infection.....	106
APPENDIX.....	107
¹ H and ¹³ C NMR spectra	107
REFERENCES.....	147

LIST OF FIGURES

1.1 Antibiotic deployment and resistance

1.2 Bacterial virulence mechanisms to target

1.3 Structures of anti-virulence compounds

1.4 T3SS needle apparatus

1.5 Assays for bacterial effector secretion and HTSs

1.6 Bioorthogonal labeling strategy

2.1 Structure of INP-0007 and PC-alk-INP

2.2 Synthesis of INP-0007 and PC-alk-INP

2.3 Proteomic analysis of secreted SPI-1 effectors

2.4 Secretion profile and protein labeling of T3SS inhibitor and PC-alk-INP probe

2.5 Structures of INP-0007, a negative control, and their alkynyl analogs

2.6 Synthesis of alkynyl salicylidene acylhydrazide analogs

2.7 Activity of initial SAH analogs on T3S and covalent labeling of proteins

2.8 Panel of alkynyl SAH analogs synthesized

2.9 Effect of T3SS inhibitors and probes on SPI-1 effector secretion

2.10 In-gel fluorescence analysis of proteins labeled by alkynyl SAHs

2.11 Plot correlating covalent labeling and inhibitory activity

2.12 Reaction scheme for small molecule binding to proteins

2.13 Effects of SAHs on expression of *Salmonella* virulence-related genes

2.14 Effects of SAHs on *Salmonella* invasion of HeLa cells

- 3.1 Structures and activity of isoquinolinesulfonamides on *Salmonella* and Akt**
- 3.2 H-89 inhibits bacterial replication through Akt-independent mechanism**
- 3.3 Compound effects on gene expression**
- 3.4 Imaging of SseJ-HA during *Salmonella* infection**
- 3.5 H-89's decrease of secreted effectors correlates with inhibition of expression**
- 3.6 Levels of secreted SPI-1 effectors in bacterial culture supernatants**
- 3.7 Dose-dependent decrease of secreted SPI-1 effectors**
- 3.8 H-89 blocks *S. typhimurium* invasion of HeLa cells**

LIST OF TABLES

1.1 Compound structures of salicylidene acylhydrazides and assays tested

1.2 Compound structures of 2-imino-5-arylidene thiazolidinones and assays tested

1.3 Summary of other T3SS inhibitors and their reported inhibitory activities

2.1 Proteomic identification of secreted *Salmonella* proteins

2.2 High-confidence proteins pulled down by alkynyl SAHs

LIST OF ABBREVIATIONS

ABC	Ammonium bicarbonate
ACN	Acetonitrile
AHL	Acyl-homoserine lactone
az-Rho	Azido-Rhodamine
BCA	Bicinchoninic acid
BME	β -mercaptoethanol
BOC	Di- <i>tert</i> -butyl dicarbonate
CB	Coomassie blue
CFU	Colony forming unit
CPG2	Carboxypeptidase G2
CuACC	Copper-catalyzed azide-alkyne cycloaddition
DCM	Dichloromethane
DIEA	Diisopropylethylamine
DMF	Dimethylformamide
DMSO	Dimethyl sulfoxide
EHEC	Enterohaemorrhagic <i>E. coli</i>
EPEC	Enteropathogenic <i>E. coli</i>
EtOAC	Ethyl acetate
EtOH	Ethanol
FBS	Fetal bovine serum
FCC	Flash column chromatography
GFP	Green fluorescent protein
Glu	Glutamate
HCl	Hydrochloric acid
HTS	High-throughput screen
LB	Luria-Bertani broth
LC-MS	Liquid chromatography-mass spectrometry
MOI	Multiplicity of infection
NMR	Nuclear Magnetic Resonance
PBS	Phosphate-buffered saline
pi	Post-infection
PyBOP	Benzotriazol-1-yl-oxytripyrrolidinophosphonium hexafluorophosphate
RT-PCR	Reverse transcriptase polymerase chain reaction
SAH	Salicylidene acylhydrazide
SAR	Structure-activity relationship
SCV	<i>Salmonella</i> -containing vacuole
SDS-PAGE	Sodium dodecyl sulfate-polyacrylamide gel electrophoresis
SPI	<i>Salmonella</i> pathogenicity island
T3SS	Type III secretion system
TBTA	<i>Tris</i> [(1-benzyl-1H-1,2,3-triazol-4-yl)methyl]amine
TCA	Trichloroacetic acid
TCEP	<i>Tris</i> (2-carboxyethyl)phosphine
TEM	A fragment of β -lactamase
TFA	Trifluoroacetic acid

THF
Yops

Tetrahydrofuran
Yersinia outer proteins

CHAPTER 1 – Introduction

1.1 Targeting virulence as an alternative strategy to antibiotics

The emergence of multidrug-resistant bacterial strains and new microbial pathogens necessitates that novel antimicrobial strategies are developed to replenish our waning antibiotic arsenal [1,2]. The rate at which bacteria acquire resistance to antibiotics is faster than we are developing new ones. The widespread use of antibiotics over the years has applied selective pressure that gives a competitive advantage to bacteria containing resistance mechanisms [3]. Despite the increase in antibiotic-resistant strains, unfortunately there has been a decrease in the number of new drugs to combat them (**Fig. 1.1**). Over the last 40 years, there has been a major lull in the deployment of new antibiotics, and antibiotic resistance has quickly developed. A new approach to antibacterials is necessary if we hope to keep up with the ever-evolving bacteria. The discovery of antibiotics has been one of the most impactful events to benefit human health [4], but currently we are regressing towards the pre-antibiotic era.

Not all bacteria are harmful; however, as an increasing number of studies have been begun to reveal specific beneficial mechanisms of commensal bacteria on host immunity [5-9]. Thousands of bacterial species make up the microbiota that inhabit the gastrointestinal tract of humans [7]. These bacteria establish colonization resistance to infection by pathogenic bacteria and are crucial for the proper development of the immune system [6]. They stimulate intestinal epithelial cells to secrete antimicrobial peptides [7], affect the number and activity of dendritic cells [10], and even single

bacterial species are capable of restoring the balance of T helper cells in germ-free mice [11,12].

Antibiotic disruption of bacterial communities can alter host immunity and exacerbate microbial infections [13]. Most antibiotics indiscriminately kill bacteria, including beneficial commensals. Since they play a large role in homeostasis of the immune system, antibiotic treatment depletes many of the beneficial effects commensals bestow onto their hosts. Treatment with antibiotics completely changes the composition of the normal microbiota, and these effects are long-lasting [13,14]. This not only paves the way for opportunistic pathogens to establish infection [15] but also renders the host more susceptible to other enteric infections [16,17].

Therapeutic strategies that target bacterial virulence rather than growth have thus received considerable attention [1,2], as these approaches are proposed to selectively disarm pathogens while preserving the integrity of the host microbiome. It is also hypothesized that anti-virulence compounds could apply less selective pressure to develop resistance mechanisms, but as of now it is unsubstantiated.

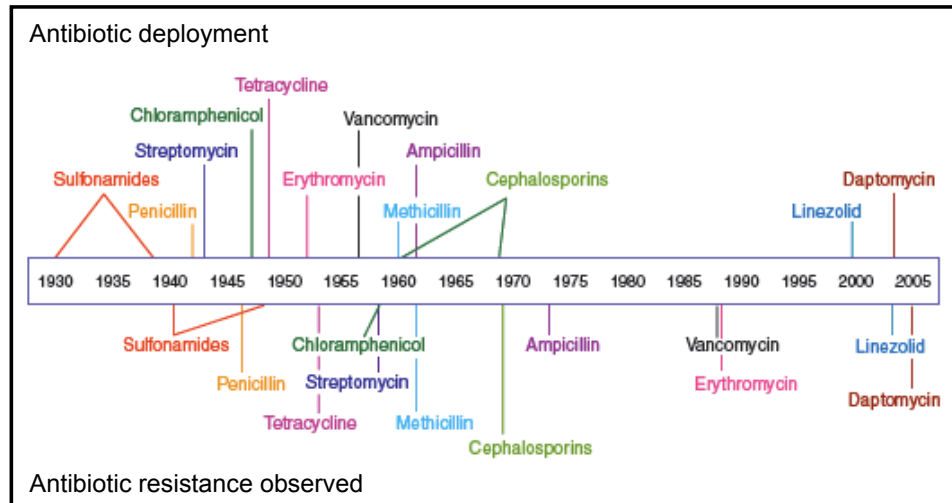


Figure 1.1 Antibiotic deployment and resistance. Taken from [2], this timeline shows the relationship between when an antibiotic was first deployed (top) and when resistance to that antibiotic was first observed (bottom).

1.2 Bacterial virulence mechanisms can be targeted with small molecule inhibitors

The discovery of many bacterial virulence mechanisms including virulence gene regulation, adhesins, protein secretion systems, and associated toxins are new targets for anti-virulence strategies [1,2] (**Fig. 1.2**). At the start of infection, bacteria sense their environment and up-regulate the expression of virulence genes, which primes the bacteria for establishing infection. This leads to the production of toxins and effector proteins that disrupt host cell functions and cause disease. Bacteria then use specialized secretion systems to deliver these toxins and effectors into the host cells to which they have adhered. Disrupting any one of these aspects of pathogenesis can lead to attenuated infection.

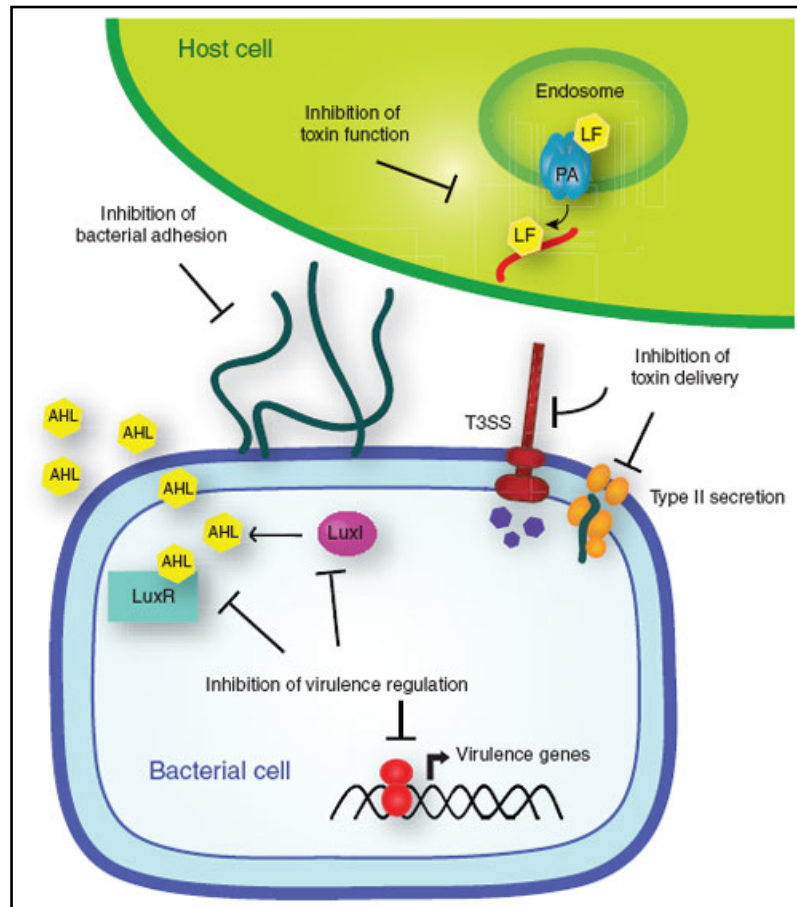


Figure 1.2 Bacterial virulence mechanisms to target. Taken from [2], bacterial virulence mechanisms can be targeted with small molecule inhibitors. Inhibition of virulence gene regulation, bacterial adhesion to host cells, delivery of toxins, or toxin function could lead to decreased infection.

Bacteria themselves are not inherently harmful; the toxins they produce are what cause disease. Inhibiting toxin activity is therefore a direct method for inhibiting virulence. This is the principle behind antitoxin development. This approach can be achieved by inhibiting toxin activity directly or altering the host response [18]. One difficulty with this approach is that many bacterial effectors exert their function by mimicking host factors; blocking this interaction could also block the endogenous

activity of host proteins [19]. Anthrax lethal factor can be inhibited by a small molecule (**Fig. 1.3A**) that binds its active site or by adding soluble Anthrax receptors that compete for binding [20,21].

Many bacterial species sense their environment and communicate to each other on a population level through a process called “quorum sensing” [22]. It is a method for bacteria to communicate between species and also to evaluate its own population density. The external environment and population density regulate virulence gene expression. When pathogens sense they are in an appropriate situation to cause infection, they can up-regulate expression of virulence genes. Many Gram-negative pathogens use acyl-homoserine lactones (AHLs) as the signaling molecules that mediate quorum sensing [22,23]. Though many species share a similar pathway, the receptors can be selective for their specific signaling molecule [22]. Halogenated furanones (**Fig. 1.3B**) are analogs that have been used *in vitro* to inhibit the signaling process stimulated by AHLs [24], and in a mouse model of *P. aeruginosa* infection, they were shown to inhibit quorum sensing and increase survival from a lethal dose of bacteria [25], validating the potential of this approach.

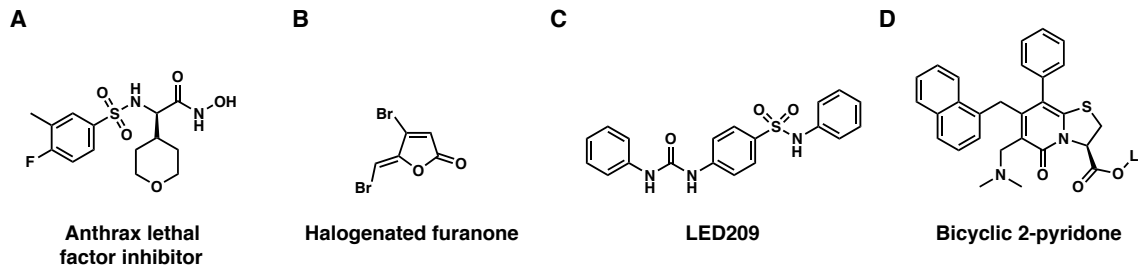


Figure 1.3 Structures of anti-virulence compounds. **A)** Structure of compound that inhibits Anthrax lethal factor. **B)** Halogenated furanones disrupt quorum sensing. **C)** LED209 inhibits QseC two-component signaling. **D)** Bicyclic 2-pyridones inhibit pilus assembly, preventing adhesion.

Bacteria also utilize two-component signaling pathways to sense their environment and respond accordingly [22]. Targeting two-component sensory systems led to the discovery of a compound that inhibits QseC-dependent virulence gene activation in enterohemorrhagic *Escherichia coli* [26]. QseC is a histidine kinase sensor that is conserved amongst several pathogens and regulates transcription of virulence genes. The compound LED209 (**Fig. 1.3C**) prevents transcription of virulence genes and secretion of effectors without inhibiting bacterial growth. It also increased the lifespan of mice infected with *S. typhimurium* and *F. tularensis* [26].

For bacteria to establish infection, they first attach to host cells. They do so with adhesins that recognize cell surface receptors on the host cells [27]. Small molecule inhibitors could be developed to prevent either the formation of the adhesins or the binding to host cell receptors. The bicyclic 2-pyridones are a class of compounds that prevents the formation of the adhesins that recognize and bind to host cells [28,29] (**Fig.**

1.3D). They were shown to prevent adhesion of *E. coli* in an *ex vivo* model of infection [28].

1.3 Type III secretion systems (T3SSs) are essential to infection

After bacteria adhere to host cells, they use specialized secretion systems to deliver the toxins and effector proteins into the host cell. One example is the type III secretion system (T3SS), which is a molecular syringe that is common to many Gram-negative pathogens including *Chlamydia*, *E. coli*, *Pseudomonas*, *Salmonella*, *Shigella*, and *Yersinia* [30]. These pathogens use the T3SS to inject effector proteins from the bacteria into the host cytosol. Amongst the many bacterial virulence mechanisms that have been discovered, protein secretion systems appear to be prime targets for small molecule inhibition of infection [31-33].

The highly conserved T3SS is central to the virulence of many human Gram-negative pathogens [30,34,35]. Mutants defective in T3SS activity are attenuated in their ability to cause infection [36]. These two aspects make targeting T3SSs an attractive strategy; inhibitors can have a marked effect on infection with the potential for broad-spectrum activity. The T3SS is a transmembrane machine comprised of about 20 proteins that assemble into a needle-like complex (**Fig. 1.4A**) that spans the bacterial membranes and functions in a highly regulated manner to transport effector proteins from the bacterial cytoplasm directly into host cells (**Fig. 1.4B**) [37-40]. Construction of T3SSs requires both structural components and ancillary proteins for the assembly process [41,42]. The basal body spans the inner (IM) and outer (OM) membranes of the bacteria [41,42]. The rings that span the IM are brought to the envelope by a Sec-dependent

pathway and anchored by N-terminal lipidation [34]. A short rod connects the IM rings to the OM components, which belong to the secretin family of pore-forming proteins [42]. The needle, which varies in length between species and strains, is a polymer of helical proteins that protrudes from the bacterial surface and delivers protein effectors outside the bacteria [41,42]. The tip of the needle is composed of a complex known as the “translocon,” which can insert itself into the host cell membranes [30,41]. The T3SS is activated by environmental cues, and upon contact with host cells, secretes and translocates protein effectors into the host cytoplasm (**Fig. 1.4B**) [30]. T3SSs thus facilitate highly coordinated and regulated secretion of specific bacterial protein effectors during infection [43].

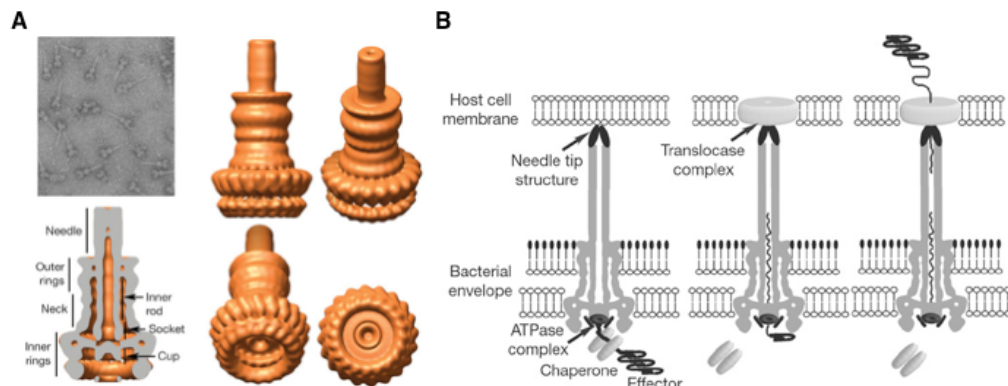


Figure 1.4 T3SS needle apparatus. **A)** Electron micrograph and models of T3SS needle apparatus. **B)** Diagram for translocation of effector proteins into host cells. Figures taken from [30].

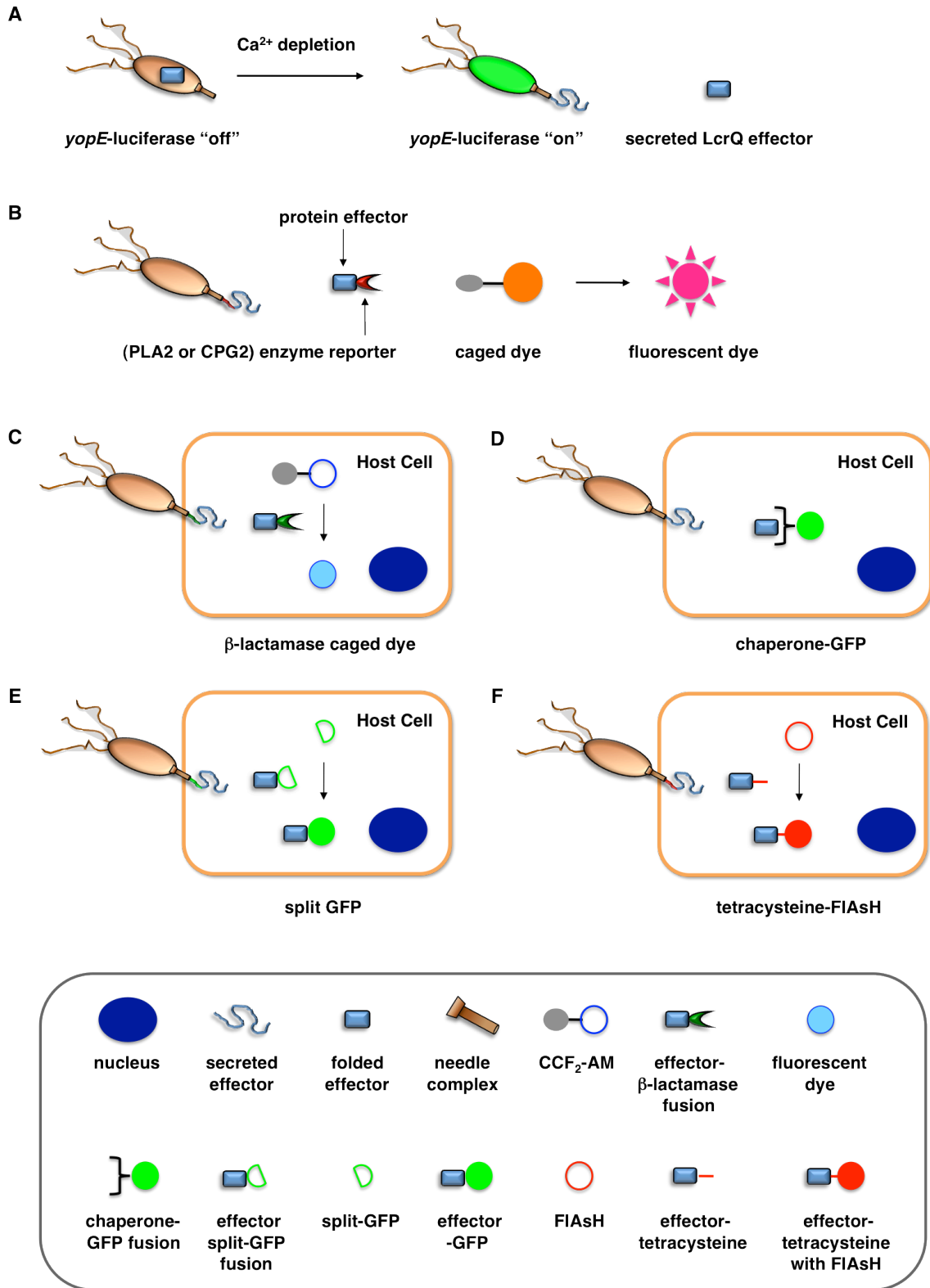
Hundreds of effector proteins among diverse bacterial pathogens have been identified as potential substrates of T3SSs, with as many as 30 different effector proteins being secreted from a single pathogen [35]. Several bacterial effectors can directly induce host cell death to facilitate bacterial pathogenesis [44,45]. Other bacterial effectors mimic host signaling proteins and enzymes to alter cellular signaling pathways. This allows bacteria to enter and replicate within the host cells while evading detection and destruction by the host immune system [46]. Depending on the bacterial pathogen, T3SSs can thus facilitate bacterial entry and replication in host cells or cause host cell death directly. Even though many detailed molecular mechanisms regarding the biogenesis of T3SSs and bacterial effector functions are still under investigation, genetic and biochemical studies of many Gram-negative bacterial pathogens have revealed that effector translocation by T3SSs is crucial for infection [42]. Despite normal *in vitro* growth rates, T3SS bacterial mutants can not deliver protein effectors into host cells, which renders the pathogens avirulent and significantly attenuated in their ability to cause disease in animals [42]. Moreover, directly blocking the injection of protein effectors into host cells through active or passive immunization using specific antibodies further supports T3SSs as key virulence mechanisms for infection.

T3SSs have emerged as attractive targets for small molecule anti-virulence therapeutics and have motivated several high-throughput screens (HTSs) in search for specific chemical inhibitors that block the secretion and translocation of bacterial effector proteins [31-33]. As T3SSs have not been reconstituted *in vitro*, the search for small molecule inhibitors has largely employed cell-based assays for protein secretion coupled to sensitive and high-throughput readouts (**Fig. 1.5**) or targeted screens against the

enzymatic activity of the ATPase required for protein secretion. Several classes of small molecules have now been identified from these screens (**Tables 1.1, 1.2, and 1.3**), which are summarized below with their potential mechanisms of action and prospects for clinical development [47].

Figure 1.5. Assays for bacterial effector secretion and HTSs. **A)** Whole cell HTS using a *Yersinia pseudotuberculosis* (*yopE:luxAB*) strain [48] that utilizes a transcriptional readout linked to secretion. **B)** Whole-cell HTSs were performed using an effector-enzyme fusion where the enzymatic activity can be monitored by fluorescence [49,50]. **C)** A bacterial effector is fused with β -lactamase (β la) that cleaves a β -sensitive FRET probe, CCF₂-AM, in the host cells [51]. **D)** GFP-labeled chaperones were used as probes to visualize translocation of bacterial effectors by imaging effector accumulation in the cytosol of the host cells [52]. **E)** Upon T3SS effector translocation, the association of the two fragments, the small 13-amino-acid 11th strand of the GFP β -barrel and the complementary fragment of the first 10 GFP strands, leads to GFP fluorescent-tagging of the effector population in the host cells [53]. **F)** The fluorescein-based biarsenical dye FAsH in the host cells allows the labeling of effectors with a genetically encoded sequence containing the tetracysteine repeat motif as the tag [54-56].

Figure 1.5



1.4 Inhibitors of T3SSs in Gram-negative pathogens

1.4.1 Salicylidene acylhydrazides

The salicylidene acylhydrazides (SAHs) were the first class of small molecules identified from a T3SS effector screen [48]. Kauppi et al. developed a whole cell HTS using a *Yersinia pseudotuberculosis* reporter strain that utilizes a transcriptional readout linked to secretion (**Fig. 1.5A**) [48]. They engineered the luciferase *luxAB* gene under the control of the effector *yopE* promoter. When grown at 37 °C in Ca²⁺-rich media, LcrQ prevents T3SS gene expression. Upon contact with a eukaryotic cell or depletion of Ca²⁺, LcrQ is secreted via the T3SS, thus releasing transcriptional repression of type III secretion genes such as *yopE* [57]. Under these conditions, this strain will then express luciferase and luminescence can be used to monitor *yopE* expression. Using this assay, Kauppi et al. screened 9,400 compounds for their ability to block expression of luciferase activity. Luminescence was measured after bacteria were incubated with compound in Ca²⁺-depleted media. In wells with inactive compounds, LcrQ would be secreted and luciferase would be expressed. For compounds that block T3S, LcrQ would remain in the cell and repress expression of the luciferase gene. Since this assay monitors loss of signal on a transcriptional level, follow-up assays are required to assess the activity of compounds on type III secretion directly. Compounds that affect the growth of the bacteria are excluded, and compounds with effects on transcription would also result in hits by indirectly affecting type III secretion.

Three notable classes of compounds were discovered to prevent type III secretion at low micromolar concentrations without affecting growth of the bacteria: the

sulfonylamino-benzanilides, salicylanilides, and salicylidene acylhydrazides. Incubation of bacteria with each class resulted in decreased levels of secreted effectors into culture supernatant, confirming the transcriptional readout. The individual compounds have varying effects on transcription and motility, which suggests they have different targets and mechanisms of action. The flagellar system is related to the type III secretion machinery, so compounds that affect one could also target the other. The sulfonylamino-benzanilides did not affect motility or general transcriptional regulation of the T3SS, but only one follow-up study has been done, potentially due to their limited solubility [58]. The salicylanilides have no effect on motility and likely work upstream of a transcriptional activator of the Yops, potentially by affecting two-component signaling, thus indirectly affecting type III secretion. There are other reports confirming their effect on transcription [59,60]. The salicylidene acylhydrazides, specifically INP-0007 from this study, affected both secretion and motility without generally affecting transcription (**Table 1.1**, entry 1). This suggests a conserved component between the two systems as a potential target. Inhibiting secretion and motility is advantageous for an anti-virulence compound, making this class a good candidate for follow-up studies.

Since the initial discovery of the salicylidene acylhydrazides displaying T3SS inhibitory activity in *Yersinia*, follow-up studies in *Yersinia* demonstrated INP-0007 blocks secretion in a constitutively secreting mutant and prevents bacterial invasion of HeLa cells [61]. Compounds in this class have since been shown to have T3SS inhibitory activity in several Gram-negative pathogens including *E. coli* [62,63], *Chlamydia* [64-69], *Salmonella* [50,70-72], and *Shigella* [73], which results in an attenuation of infection. Various INP-0007 derivatives were shown to prevent invasion of *Yersinia*,

Salmonella, and *Shigella*, disrupt the infectious cycle in *Chlamydia*, and decrease the number of attachment and effacement lesions in a bovine epithelial cell line when infected with *E. coli* [62]. INP-0007 and INP-0403 were shown to inhibit T3SS-induced hemolysis in erythrocytes and decrease the secretory and inflammatory responses *in vivo* with a bovine intestinal ligated loop model when infected with *Salmonella* (**Table 1.1**, entries 1 and 5), but the caveat for drug development is that these protective effects were only observed when the bacteria were pre-treated with inhibitor [70]. In *Chlamydia*, however, even when inhibitor was added 24 hours post-infection to HeLa cells, it still had a significant impact on bacterial replication [68]. This led to some pre-clinical studies and *in vivo* experiments with *Chlamydia*-infected mice [74]. Gylfe et al. used mice injected with compound to analyze the pharmacokinetics of two of the most potent inhibitors of *Chlamydia* replication. The most potent compound displayed poor pharmacokinetic parameters, so they applied it topically to mice inoculated intravaginally with *C. trachomatis*. They saw a significant decrease in the number of inclusion forming units (IFUs) for compound-treated mice over the 4 weeks monitored. Moreover, they did not observe any noticeable effect on strains of lactobacilli: commensals that are essential for maintaining the balance of the vaginal microflora. These results demonstrate the utility of the SAHs to be used *in vivo* to treat *Chlamydia* infection.

More recently, the SAHs have been shown to have antiviral effects as well [75]. Forthal et al. screened 25 SAHs for anti-HIV-1 activity and focused on 4 that had IC₅₀ values in an infection assay in the single-digit micromolar range and were not cytotoxic to cells. They were effective against several strains of HIV-1 and were active in a vaginal and semen simulant, demonstrating their potential as a topical applicant for inhibiting the

transmission of sexually transmitted diseases.

While there is variability in the exact structure of active SAHs between species, there is a common core scaffold. One study used statistical molecular design (SMD) and quantitative structure-activity relationships (QSAR) on 50 compounds tested in *Yersinia* to make predictions about untested compounds [76]. Of eight candidate compounds, they were able to correctly predict that three would be inactive, but only three of the five predicted to be active demonstrated inhibitory activity. Though there was no obvious consensus motif that confers activity, the authors found that the pKa of the phenol was the most important property in the model and that the electrostatic potential of the carbon atoms in that aromatic ring may play a key role.

Though there have been several studies using the salicylidene acylhydrazides in various bacterial species, the precise target(s) and mechanisms of action remain unclear. Since these compounds have broad-spectrum inhibitory activity, it is likely that they target something conserved among the species. It was initially proposed that the compounds act directly on the T3SS machinery, and one report in *Shigella* suggests that incubation with INP-0400 affected needle assembly [73] (**Table 1.1**, entry 4). Further support for this notion is that the T3SS needle complex is related to the flagellar assembly, and motility is affected in *Yersinia* [48] and *Salmonella* [71]. Several reports have examined the effects these compounds have on transcription. In *Chlamydia*, Wolf and co-workers found that INP-0007 down-regulates some virulence genes, and while levels of needle components are unaffected, effectors accumulate intracellularly [66]. Another study performed RT-PCR of virulence genes during infection of HeLa cells where compound was added at the time of infection [68]. They also observed that only

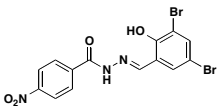
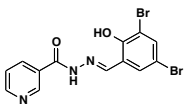
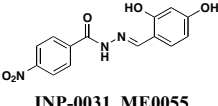
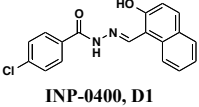
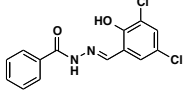
some virulence genes are down-regulated when incubated with active compound, and importantly, they used an inactive compound as a negative control and saw no differences between that and the DMSO sample. In *E. coli*, four compounds with varying potency all down-regulated genes in the locus for enterocyte effacement, but there was large variation between strains [62]. When the transcriptome in *Salmonella* incubated with various inhibitors was examined, the needle complex ATPase InvC and the HilD regulator were down-regulated, but no major effects on HilA or the effectors themselves were observed [72]. Taken together, it is clear the salicylidene acylhydrazides have some transcriptional effects; however, it is not obvious if this is a direct effect and the cause of secretion inhibition or the result of a feedback loop.

In *Chlamydia* [68] and *Salmonella* [72], it has been reported that adding exogenous iron to the cultures can prevent the inhibitory effects of the SAHs acylhydrazides, suggesting iron restriction as a potential mechanism of action. Iron transport and acquisition genes are up-regulated in *Salmonella* upon treatment with several inhibitors, however, neither the up-regulation of iron-related genes nor an effect from adding exogenous iron is observed in *Yersinia*. Also, an inactive compound was shown to bind iron to the same extent as an active compound [68], thus casting doubt on an iron-restriction mechanism.

Roe and co-workers attempted to identify the targets of the salicylidene acylhydrazides using a biochemical approach [63]. They synthesized two analogs of ME0052 (**Table 1.1**, entry 2) and ME0055 (**Table 1.1**, entry 3) for affinity purification of binding partners from *E. coli* lysate. After trypsinization and LC-MS/MS analysis, 16 proteins were identified, and three were suggested binding partners by Far Western

analysis using a biotinylated version of a much less active compound: Tpx (thiol peroxidase), WrbA (NAD(P)H quinine oxidoreducase), and FolX (dihydroneopterin-tri-P-epimerase). Knockouts of each gene results in down-regulation of flagellar components and up-regulation of T3SS genes, the opposite of what is observed with compound treatment. Deletion mutants of Tpx and WrbA secrete more effectors, and they are as virulent in infecting macrophages, but adding ME0052 can still inhibit both processes. The authors thus suggest the inhibition of T3SS activity is due to a polypharmacological effect on proteins involved in metabolism, which then results in a dis-regulation of bacterial virulence. Given the diverse pharmacological effects of salicylidene acylhydrazides that have been reported, the precise mechanism of action for these compounds remains unclear.

Table 1.1 Compound structures of salicylidene acylhydrazides and assays tested.

Compound	Regulation	Secretion/Translocation	T3SS IC ₅₀	Infection	Other Pathways	Ref
<p>1</p>  <p>INP-0007, D8</p>	<p><i>C. trachomatis</i>: Down-regulates transcription of late-cycle virulence genes</p>	<p><i>C. trachomatis</i>: Prevents IncA secretion during infection</p> <p><i>S. typhimurium</i></p> <p><i>Y. pseudo-tuberculosis</i></p> <p><i>Y. pseudo-tuberculosis</i>: Prevents YopH translocation into HeLa</p>	<p>~15 μM</p> <p>~5 μM</p>	<p><i>C. trachomatis</i>: Inhibits replication in HeLa</p> <p><i>S. typhimurium</i>: Reduces hemolysis of erythrocytes, invasion of HeLa, and immune response in bovine ligated loop model</p> <p><i>Y. pseudo-tuberculosis</i>: Inhibits invasion of HeLa</p>	<p><i>Y. pseudo-tuberculosis</i>: Inhibits motility</p>	<p>48, 50, 61, 66, 70,</p>
<p>2</p>  <p>INP-0010, D9, ME0052</p>	<p><i>EHEC</i>: Down-regulates transcription of LEE but not iron-related genes</p> <p><i>C. pneumoniae</i>, <i>S. typhimurium</i>: Down-regulates transcription of some virulence genes</p>	<p><i>EHEC</i>: Inhibits Tir and EspD secretion</p> <p><i>S. typhimurium</i></p>	<p>~25 μM</p>	<p><i>C. trachomatis</i>: Inhibits replication in mammalian cell lines</p> <p><i>S. typhimurium</i>: Inhibits invasion of MDCK cells and replication in macrophages</p> <p><i>Y. pseudo-tuberculosis</i>: Reduces macrophage cytotoxicity</p>		<p>62, 67, 71,</p>
<p>3</p>  <p>INP-0031, ME0055</p>	<p><i>EHEC</i>: Down-regulates transcription of LEE but not iron-related genes and up-regulates flagellum expression</p>	<p><i>EHEC</i>: Inhibits Tir and EspD secretion</p>	<p>~25 μM</p>	<p><i>EHEC</i>: Reduces number of A/E lesions on bovine epithelial cells</p>		<p>62</p>
<p>4</p>  <p>INP-0400, D1</p>	<p><i>S. flexneri</i>: Affects needle complex assembly</p>	<p><i>S. typhimurium</i></p> <p><i>S. flexneri</i></p>		<p><i>C. trachomatis</i>: Inhibits replication in HeLa and McCoy cells</p> <p><i>S. typhimurium</i>: Reduces HeLa cytotoxicity</p> <p><i>S. flexneri</i>: Reduces invasion of HeLa and macrophage cytotoxicity</p>		<p>65, 68, 71, 73</p>
<p>5</p>  <p>INP-0403, D4</p>	<p><i>S. typhimurium</i>: Down-regulates transcription of invC and hilD but not hilA or effectors</p>	<p><i>S. typhimurium</i></p>	<p>~25 μM</p>	<p><i>S. typhimurium</i>: Reduces hemolysis of erythrocytes, invasion of HeLa, and immune response in bovine ligated loop model</p>	<p><i>S. typhimurium</i>: Effects reversed with exogenous iron</p>	<p>70, 71, 72,</p>

1.4.2 2-Imino-5-arylidene Thiazolidinones

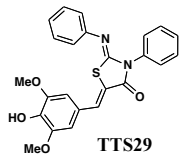
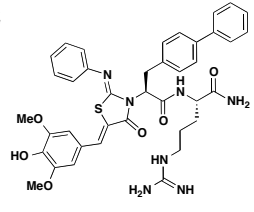
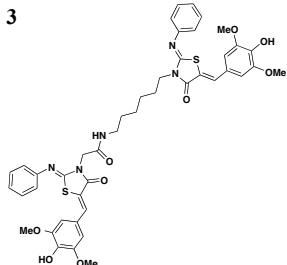
A whole-cell HTS in *Salmonella* identified the 2-imino-5-arylidene thiazolidinones as broad inhibitors of T3S [49]. The screen was performed by engineering a *Salmonella* strain where the secreted effector SipA was fused to a portion of a *Yersinia* protein YplA, that contained phospholipase A2 activity (**Fig. 1.5B**). The phospholipase A2 activity could then be measured with a fluorogenic substrate. Using this strain, they screened 92,000 small molecules from natural and synthetic libraries. After ruling out compounds that affected growth or were unsuitable for drug development, they followed up on 25 compounds. Excluding compounds that had an effect on general transcription, translation, or Sec-dependent secretion left seven molecules for follow-up studies. Six of these were found to affect T3SS gene expression, leaving one that might specifically target the T3S process or assembly directly.

The one compound Felise et al. pursued was a 2-imino-5-arylidene thiazolidinone (TTS29) (**Table 1.2**, entry 1), and it was shown to have T3SS inhibitory effects in *Yersinia*, *Pseudomonas aeruginosa*, and *Francisella novicida*, demonstrating broad-spectrum inhibitory activity. By purifying the needle complexes of *Salmonella*, they found that compound-treated samples had lower levels of needle components, but whole-cell and membrane fraction levels were unchanged, suggesting that the compound disrupts needle complex assembly. No effect was observed on motility or the levels of flagellar components, suggesting the effect was specific to the T3SS. They also discovered that TTS29 affects type II secretion (T2S) and the related type IV pili assembly. After examining what is common to all of the affected systems and not present in the flagellar system, it was proposed that TTS29 acts by disrupting secretin

interactions, thus affecting needle complex assembly or stability but not the flagellar system. These effects on the T3SS carried over into an infection setting, as the compound was able to prevent *Salmonella*-induced lysis of macrophages and the hypersensitivity response in tobacco plants from the plant pathogen *Pseudomonas syringae*.

One major drawback is the low potency of TTS29, as several hundred micromolar is required to have an inhibitory effect. Subsequent SAR analysis demonstrated the importance of the imino nitrogen, its aryl group, and the substitution pattern on the arylidene ring while the amido nitrogen tolerated modification. A TTS29-analog in this study displayed higher potency in every assay tested without affecting bacterial growth (**Table 1.2**, entry 2). This led to further modification of the amido nitrogen, with several analogs containing a dipeptide chain displaying low micromolar IC₅₀ values for inhibition of SipA [77]. Tethered thiazolidinone dimers (**Table 1.2**, entry 3), some of which are linked with a peptide, displayed similar potencies [78]; however, no follow-up studies have been reported with these compounds.

Table 1.2 Compound structures of 2-imino-5-arylidene thiazolidinones and assays tested. IC₅₀ values are reported based on the inhibition of SipA secretion as determined by Western blot.

Compound	Regulation	Secretion/Translocation	T3SS IC ₅₀	Infection	Other Pathways	Ref
<p>1</p>  <p>TTS29</p>	<p><i>S. typhimurium</i>: Inhibits needle complex assembly, No effect on general transcription</p>	<p><i>S. typhimurium</i> <i>Y. enterocolitica</i> <i>F. tularensis</i></p>	83 μM	<p><i>P. syringae</i>: Prevents HR response in tobacco leaves <i>S. typhimurium</i>: Reduces macrophage cytotoxicity</p>	<p><i>S. typhimurium</i>: No effect on flagellar system or motility <i>P. aeruginosa</i>: Inhibits T4-dependent motility & T2S</p>	49, 77, 78
<p>2</p>  <p>TTS29-analog</p>	<p><i>S. typhimurium</i>: No effect on general transcription</p>	<p><i>S. typhimurium</i></p>	3 μM	<p><i>S. typhimurium</i>: Reduces macrophage cytotoxicity</p>	<p><i>P. aeruginosa</i>: Inhibits T2S</p>	49, 77, 78
<p>3</p> 		<p><i>S. typhimurium</i>: Inhibits secretion of SipA</p>	5 μM			78

1.4.3 Other chemotypes from HTSs

A few other HTSs have revealed several other classes of T3SS inhibitors. Janssen Pharmaceuticals employed an assay which measures levels of the secreted effector protein ExoU from *P. aeruginosa* and SipA and SopE from *S. typhimurium* as the readouts of T3SS inhibition [79]. The majority of the inhibitors that exhibited low micromolar potencies were comprised of a common N-acyl *p*-Cl phenylalanine moiety (Table 1.3, entry 1). However, this class of compounds lacks the broad-spectrum anti-

T3SS activity across different Gram-negative pathogens, and no further development has yet been reported.

Microbiotix Pharmaceuticals has identified five inhibitors from a library of 80,000 compounds through two distinct functional bioassays [80]. First, compounds were screened against a transcriptional fusion of the *Photorhabdus luminescens luxCDABE* operon to the *P. aeruginosa exoT* effector gene. The compounds were then selected based on the inhibition of the secretion of a *P. aeruginosa* ExoS effector- β -lactamase fusion protein (**Fig. 1.5C**) and also of native ExoS by the SDS-PAGE analysis of culture supernatants. To demonstrate the broad-spectrum efficacy of the compounds, they were found to also antagonize *Yersinia* T3S and one compound, MBX1641, also targeted *Chlamydia* T3S (**Table 1.3**, entry 2). Interestingly, contrary to typical HTS hits, Microbiotix compounds contained chiral centers and through a series of synthetic efforts, it was shown that the *R* enantiomer was the preferred stereochemistry. With a stringent structure activity relationship, these compounds might see many obstacles moving forward; however, other scaffolds identified in the screen could be explored in the future.

Harmon et al. devised a HTS to identify compounds that inhibit the T3S-dependent translocation of *Yersinia* effector proteins, Yops, into host cells [51]. This translocation-monitoring FRET-based system employed a chimeric protein, E-TEM, which encodes the first 100 amino acids of YopE, containing the secretion and translocation signals, fused to a fragment of β -lactamase (TEM) (**Fig. 1.5C**). The substrate, CCF₂-AM, consists of two fluorophores conjugated by a lactam ring. Normally, the substrate fluoresces green due to FRET between the fluorophores. TEM can cleave the lactam ring between the fluorophores, leading to the loss of FRET and

resulting in blue fluorescence. If *Y. pseudotuberculosis* translocates E-TEM into host cells, the substrate will be cleaved and the cells will fluoresce blue. The green-to-blue ratio was measured to determine whether the compounds could block the translocation of E-TEM. Notably, they have identified six compounds that specifically inhibit translocation of Yops into mammalian cells but not Yop synthesis or secretion (**Table 1.3**, entry 3). These six diverse compounds lacked a consensus pharmacophore, yet they inhibited translocation of effectors into the host cell while not affecting the synthesis of T3SS components or effectors, assembly of the T3SS, or secretion of effectors. Interestingly, C20 reduced adherence of *Y. pseudotuberculosis* to target cells. Additionally, the compounds were shown to cause leakage of Yops into the supernatant during infection and reduced polarized translocation. Furthermore, several molecules also inhibited *P. aeruginosa* ExoS-mediated cell rounding, suggesting that the compounds target factors that are conserved between these two pathogens.

Similar to the reported *yopE:luxAB* strain [48], Pan et al. screened a collection of 70,966 compounds using a *Y. pestis* luciferase reporter strain [81]. Four new compounds were identified to inhibit secretion of *Y. pestis* T3SS effector proteins YopD, YopH, and YopM at micromolar concentrations without affecting bacterial growth. Moreover, two of the four compounds (Compounds 1 and 2, **Table 1.3**, entry 4) also attenuated T3SS-mediated secretion of EPEC effector proteins. In all, compounds discovered from this library are likely to have different mechanisms of action and targets from each other.

Li and co-workers adopted a cell-based assay that measures the T3S-dependent secretion of a chimeric SopE- β -lactamase fusion and identified a class of triazine-based compounds (**Table 1.3**, entry 5) as inhibitors of T3S [82]. Active compounds can

selectively reduce the level of SipB in the supernatant fraction of *Salmonella* culture without affecting the production of SipB intracellularly. Moreover, these compounds also diminished the level of ExoU in the supernatant of *P. aeruginosa* cultures. No further development has been reported since the patent.

In an effort to identify compounds that protect Chinese hamster ovary (CHO) cells against the T3S-dependent cytotoxic effects of the *P. aeruginosa* effector ExoU, Lee et al. reported pseudolipasin A as a specific inhibitor for the phospholipase A2 activity of ExoU with an IC₅₀ of 7 μM (**Table 1.3**, entry 6) [83]. They found that pseudolipasin A did not prevent the type III secretion of ExoU or its translocation into CHO cells but inhibited the phospholipase A2 activity of ExoU directly and specifically. A collection of structural analogs was used to demonstrate a conserved pharmacophore for phospholipase A2 inhibitory activity.

Starting with an *in silico* screen, a number of *N*-hydroxybenzimidazole-based scaffolds was synthesized to block the binding of the *Yersinia* transcription factor LcrF to DNA (**Table 1.3**, entry 7) [84]. LcrF regulates the expression of the *Yersinia* T3SS. With more detailed SAR studies, a number of novel compounds potently inhibited the secretion of Yops. They also demonstrated that these compounds were capable of protecting macrophages from *Y. pseudotuberculosis*-induced cytotoxicity, decreasing the bacterial burden in a mouse infection model, and increasing survival from a lethal dose of bacteria [85].

Swientnicki et al. has recently reported *in silico* studies to identify inhibitors to target the *Yersinia pestis* T3SS ATPase YscN (**Table 1.3**, entry 8) [86]. The authors validated YscN as a therapeutic target by deleting the catalytic domain of the *yscN* gene

in *Y. pestis* CO92 and showed a reduction of over three million-fold of bubonic plague in the Swiss-Webster mouse model. The validated but diverse inhibitors had IC₅₀ values below 20 μM in an *in vitro* ATPase assay and were also found to inhibit the homologous BsaS protein from the *Burkholderia mallei* animal-like T3SS at similar potency. Moreover, these compounds inhibited YopE secretion and attenuated *Y. pestis* toxicity in mammalian cells. These data demonstrate the possibilities of targeting and inhibiting ATPases of T3SSs in other pathogens.

1.4.4 Natural Products

In addition to synthetic chemical libraries, natural product extracts have been surveyed for compounds with T3SS inhibitory activity. Bioassay-guided fractionation of the extracts from the marine sponge *Caminus sphaeroconia* led to the isolation of a series of lipidated pentasaccharides that possess potent anti-T3SS activity (**Table 1.3**, entry 9) [87,88]. Analysis of EPEC culture supernatants showed that caminoside A selectively diminished the level of a T3S-dependent effector protein EspB while not affecting the level of EspC, a type V-dependent effector. The potency of caminoside A is approximately 20 μM without affecting the growth of the pathogens [87], yet further development of the caminosides has not been reported. Alternatively, guadinomines isolated from *Streptomyces sp.* K-01-0509 were reported to inhibit EPEC T3S-dependent lysis of sheep blood erythrocytes with an IC₅₀ value of 20 nM in a whole cell assay (**Table 1.3**, entry 10) [89,90]. Even though this class of natural products might be the most potent inhibitors to date, major synthetic efforts are needed to produce pure material for further studies [91].

From a screen of monitoring T3SS-mediated hemolysis from enteropathogenic *E. coli* (*EPEC*), Abe and co-workers identified aurodox, a linear polyketide from *Streptomyces*, as a specific T3SS inhibitor [92]. Aurodox potently inhibited T3SS-mediated hemolysis with an IC₅₀ value of 1.5 µg/ml without affecting bacterial growth (**Table 1.3**, entry 11). By Coomassie blue staining and Western analysis of the supernatant fraction, aurodox specifically diminished the levels of effector proteins such as EspB, EspF, and Map without affecting the expression of the housekeeping protein GroEL. Moreover, aurodox allowed mice to survive a lethal dose of *Citrobacter rodentium*, a model bacterium for human pathogens such as *EPEC*. Beyond the antibacterial drug development, the discovery of aurodox highlights the possibility that microbes may produce small molecules that can antagonize T3SSs in chemical ecology.

Without the use of a HTS, Li et al. discovered that cytosporone B (**Table 1.3**, entry 12) and its analogs can effectively prevent the secretion of SPI-1 effectors without affecting growth or the levels of the flagellar proteins in *Salmonella typhimurium* [93]. Cytosporone B is a reported agonist for the nuclear orphan receptor Nur77 [94]. This group scanned their library for compounds that could inhibit SPI-1 secretion by SDS-PAGE analysis. Treatment of bacteria with cytosporone B also prevented the SPI-1-dependent invasion of HeLa cells. Its potency was in the low micromolar range, comparable to most other reported T3S inhibitors. By RT-PCR analysis, they found that it acted upstream of HilD and HilA, up-regulating the nucleoid proteins Hha/H-NS that inhibit their expression. By up-regulating inhibitors of the SPI-1 regulators, cytosporone B down-regulated the expression of SPI-1 genes to inhibit type III secretion in *Salmonella*.

Table 1.3 Summary of other T3SS inhibitors and their reported inhibitory activities.

Specific bacterial effectors antagonized by the inhibitors are noted in parentheses.

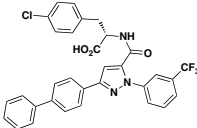
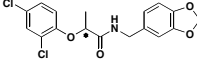
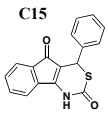
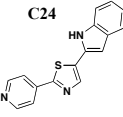
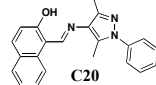
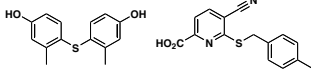
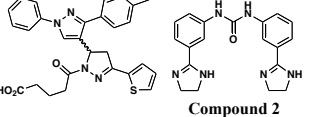
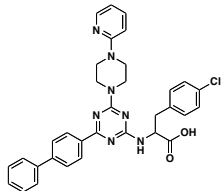
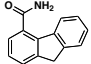
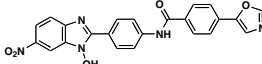
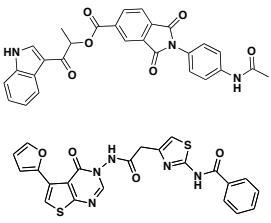
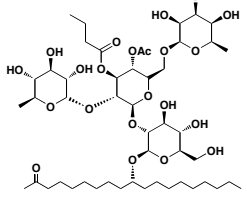
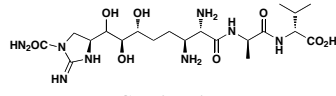
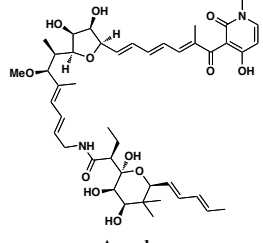
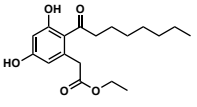
Representative compounds	Regulation	Secretion/Translocation	T3SS IC ₅₀	Infection	Other Pathways	Ref
<p>1</p> 		<p><i>S. typhimurium</i> (SipA, SopE)</p> <p><i>P. aeruginosa</i> (ExoU)</p>				44
<p>2</p> 	<p><i>P. aeruginosa</i>: Inhibits <i>exoT</i> transcription</p>	<p><i>P. aeruginosa</i></p> <p><i>Y. pestis</i> (YopE-βla)</p>	<p>12.5 μM for ExoS</p> <p>22 μM for YopE</p>	<p><i>P. aeruginosa</i>: Inhibits ExoU-dependent CHO cytotoxicity</p> <p><i>C. trachomatis</i>: Inhibits growth in Hep-2 cells</p>	<p><i>P. aeruginosa</i>: No effect on type II-mediated elastase secretion</p>	80
<p>3</p> <p>C15  C24 </p> <p>C20 </p>	<p><i>Y. pseudo-tuberculosis</i>: No effect on needle assembly</p>	<p><i>Y. pseudo-tuberculosis</i>: Prevents translocation of YopE-βla</p> <p><i>P. aeruginosa</i></p>		<p><i>P. aeruginosa</i>: Reduces Hep-2 cell-rounding by</p>	<p><i>Y. pseudo-tuberculosis</i>: Increases Yop leakage, and C20 reduces adherence of Hep-2 cells</p>	51
<p>4</p> <p>Compound 1 </p> <p>Compound 2 </p>	<p><i>EPEC</i>: No effect on OmpA level</p>	<p><i>Y. pestis</i></p> <p><i>Y. pestis</i>: Prevents translocation of YopE-βla</p> <p><i>EPEC</i> (Tir)</p>	<p>10 - 15 μM for Yops</p>	<p><i>Y. pestis</i>: Reduces HeLa cell toxicity</p>		81
<p>5</p> 		<p><i>S. typhimurium</i> (SipB)</p> <p><i>P. aeruginosa</i> (ExoU)</p>	<p>20 - 80 μM for SipB</p> <p>>100 μM for ExoU</p>			82
<p>6</p> <p>Pseudolipasin A </p>		<p><i>P. aeruginosa</i>: No effect on T3S secretion</p>		<p><i>P. aeruginosa</i>: Protects CHO cells and <i>Dictyostelium discoideum</i>, from ExoU cytotoxicity</p> <p>Inhibits ExoU-mediated killing of <i>Saccharomyces cerevisiae</i></p>		83
<p>7</p> 		<p><i>Y. pseudo-tuberculosis</i></p>		<p><i>Y. pseudo-tuberculosis</i>: Reduces macrophage cytotoxicity and increases mouse survival</p>		85

Table 1.3 continued.

Representative compounds	Regulation	Secretion/Translocation	T3SS IC ₅₀	Infection	Other Pathways	Ref
<p>8</p> 		<i>Y. pestis</i> (YopE)	20 μM	<i>Y. pestis</i> : Reduces mammalian cell cytotoxicity	Inhibits ATPase activity of BsaS protein from <i>Burkholderia mallei</i>	86
<p>9</p>  <p>Caminoside A</p>	<i>EPEC</i> : No effect on type-V effector EspC	<i>EPEC</i> (EspB)	20 μM			87, 88
<p>10</p>  <p>Guadinomines</p>		<i>EPEC</i>	20 nM in hemolysis assay	<i>EPEC</i> : Prevents hemolysis of erythrocytes		89, 91
<p>11</p>  <p>Aurodox</p>	<i>EPEC</i> : No effect on expression of GroEL	<i>EPEC</i> (EspA, EspB, EspD)	1.5 μg/ml in hemolysis assay	<i>EPEC</i> : Prevents hemolysis of erythrocytes <i>Citrobacter rodentium</i> Protects mice from infection		92
<p>12</p>  <p>Cytosporone B</p>	<i>S. typhimurium</i> : down-regulates HilD, HilA, and effectors	<i>S. typhimurium</i>		<i>S. typhimurium</i> : Prevents invasion of HeLa cells		93

1.5 Additional assays for monitoring T3SSs

To facilitate the analysis of T3SSs and small molecule inhibitor discovery, new assays have been developed to more efficiently and precisely visualize protein secretion and translocation. Our laboratory recently described a carboxypeptidase G2 (CPG2)-based reporter system for fluorescence and visible detection of type III protein secretion from *Salmonella* (**Fig. 1.5B**) [50]. The orthogonal specificity of CPG2 presents an attractive enzyme-reporter system to monitor bacterial protein secretion. CPG2 is a 43 kDa metalloprotease found in rare *Pseudomonas syringae* strains that selectively cleaves glutamate (Glu) from small molecule metabolites [95]. Importantly, the glutamyl-carboxypeptidase activity of CPG2 is not present in most species of bacteria or higher eukaryotes. The ability of CPG2 to hydrolyze urea analogues of Glu provides a unique enzymatic activity to uncage fluorogenic dyes. Based upon the tunable, photostable, and fluorescent properties of 2-dicyanomethylene-3-cyano-2,5-dihydrofuran (CyFur) fluorophores [96-98], a Glu-modified derivative of CyFur (Glu-CyFur) was synthesized as a potential fluorogenic substrate for CPG2. The time-dependent uncaging of Glu-CyFur with CPG2 can be readily observed by the naked eye with or without UV-excitation. In *S. typhimurium*, SopE2-CPG2-HA was cloned into the pWSK29 plasmid driven by the SopE2 promoter. *S. typhimurium* deficient in a structural component of the SPI-1 T3SS needle complex (Δ *invA*) did not secrete SopE2-CPG2-HA and, consequently, did not exhibit CPG2 activity in the growth media, confirming that this assay measures secretion through the T3SS.

The SopE2-CPG2-HA:Glu-CyFur reporter system can differentially measure the activity of T3SS inhibitors. An INP-0007 analog lacking the dibromophenol motif

showed no inhibitory activity as compared to INP-0007, which suggests that the dibromophenol motif of INP-0007 is crucial for potent inhibition of T3SSs. Moreover, INP-0007 is ~4 times more potent in blocking SopE2-CPG2-HA secretion than 2-imino-5-arylidene-thiazolidinone with IC₅₀ values of 5.5 and 22.6 μ M, respectively. These experiments highlight the utility and sensitivity of the CPG2:Glu-CyFur reporter system in measuring differential inhibitory activity of small molecules targeted at T3SSs. The CPG2:Glu-CyFur reporter system provides a robust and sensitive method for monitoring protein expression and secretion. This system is complementary and orthogonal to other enzyme reporter systems such as luciferase and β -lactamase, making it potentially useful for dual-imaging applications in the future.

Green fluorescent protein (GFP)-based systems have been employed to monitor type III protein secretion. While direct translational fusions of GFP to bacterial effectors have not been successful, GFP-labeled effector chaperones can be used as probes to visualize translocation of bacterial effectors into the host cells (**Fig. 1.5D**). This approach allows the imaging of effector accumulation in the cytosol of the host cells by detecting clustering or accumulation of the fluorescently labeled chaperones. Schlumberger et al. used this strategy to monitor the injection of the *Salmonella* effector SipA into the host cytosol and concurrent depletion from the bacterial cytosol in real time [52]. Alternatively, Palmer and co-workers recently reported a split GFP system to image T3S. They fused the small 13-amino-acid 11th strand of the GFP β -barrel to *Salmonella* effectors and expressed the complementary fragment of the split GFP *in trans* in the host cells (**Fig. 1.5E**) [53]. Upon T3SS effector translocation, the association of the two split GFP fragments leads to fluorescent tagging of the effector population in the host cells.

The authors used this method to directly label and visualize the dynamics of the T3SS-dependent SPI-2 effectors PipB2, SteA, and SteC during bacterial replication in host cells. Rather than GFP-based systems, smaller protein tags such as tetracysteine sequences can also be used with fluorescein-based biarsenical dye FLAsH to image bacterial effector translocation into mammalian cells (**Fig. 1.5F**) [54-56]. It would be interesting to employ these assays to evaluate the precise effects of the reported T3SS inhibitors on bacterial effector translocation into mammalian cells.

1.6 Identifying the target of the SAHs in *Salmonella typhimurium*

Though there has been much focus recently on T3SSs as potential therapeutic targets, clear mechanisms of action for inhibitors of T3S are still lacking. The SAHs were the first class of T3SS inhibitors reported and are one of the most potent to have broad-spectrum inhibitory activity (**Table 1.1**). There are several reports on the activity of SAHs in various pathogens and reports on *in vivo* activity, but though target identification is an important step for drug development, no clear mechanism of action exists. The potential for the SAHs makes them an attractive class to study, so we set out to identify their molecular targets and determine their mechanism of action in *Salmonella typhimurium*.

Salmonella is a Gram-negative pathogen that affects millions of people each year [71,99-102] and causes gastroenteritis in a variety of hosts and typhoid fever in humans [99]. Hosts become infected after ingesting contaminated food or water. Pathogenic strains of *Salmonella* are able to establish infection by evading host defenses in the gut and invading intestinal epithelial cells [99]. Once the bacteria have successfully invaded

the host, they migrate to macrophages and reside in a special compartment called the *Salmonella* containing vacuole (SCV). While in the SCV, the bacteria are able to avoid degradative enzymes and gather nutrients to replicate and disseminate to other tissues [99]. There are two *Salmonella* pathogenicity islands (SPI-1 and SPI-2) that encode for virulence factors required for bacterial invasion and subsequent replication, respectively [99]. Both loci encode proteins for type III secretion systems (T3SSs), which are essential components of bacterial infections *in vivo* [30]. Upon contact with host cells, *Salmonella* injects effector proteins through the T3SS into the host cytosol, where these bacterial effector proteins alter host cell signaling to establish and propagate infection.

1.7 Strategies for target identification of small molecules

Given the potential utility of inhibiting T3SSs, our aim was to identify the targets and determine the mechanism of action of the SAHs, one of the most potent classes of inhibitors of T3S with broad-spectrum reactivity. The gold standard for target identification of antibacterials is selecting for mutants that are resistant to small molecule treatment and using sequencing techniques to discover what confers resistance [103,104]. Since anti-virulence compounds do not affect bacterial viability, there is no easy way to select for resistant mutants because resistance does not confer any competitive advantage. So although genetic strategies are very powerful for target identification, sequencing resistant mutants does not apply in this case due to the inability to select for them.

Another commonly used approach for target ID of small molecules is affinity chromatography [105,106]. Small molecules are attached to an affinity matrix and immobilized. The matrix is then exposed to cell lysate so that the protein targets can bind

the small molecule. Proteins that do not bind will be washed away, and the protein-binding partners can be eluted by competition with active compound or a physical perturbation such as heating. The eluted proteins can be identified by MS-based methods, including quantitatively [107-109], to generate a list of potential targets. The targets must be validated as binding-partners and confirmed to play a role in the phenotype observed. For example, Ito and co-workers used an affinity chromatography strategy to identify the target(s) of the drug thalidomide [105]. Thalidomide is a drug used to treat leprosy and multiple myeloma, but it is also the causative agent of birth defects. They chemically modified it and conjugated it to beads to pull down its targets from HeLa cell extracts. After washing, they eluted the bound proteins by adding free thalidomide and separated them by SDS-PAGE. Two proteins were identified by mass spec, and when recombinantly expressed, only one of them bound to the beads: CRBN, which exhibits ubiquitin ligase activity. Using a zebrafish model, they demonstrated that adding zCRBN mRNA could rescue the developmental defects observed with thalidomide treatment.

A major drawback to the affinity chromatography method is that attaching a small molecule to a bulky affinity matrix can be synthetically challenging and potentially render the molecule inactive. There can also be high background from non-specific interactions with the matrix. Apart from losing activity due to the small molecule modification, potentially the biggest drawback is that the molecule binds proteins in an unnatural environment. Proteins can lose their activity or specific interactions after lysis, and solubility is a concern, especially for membrane proteins.

Because T3S is a dynamic process occurring inside cells, we would like to use live cells in their natural environment for our targeting approach as opposed to cell lysate.

The T3SS is a large protein complex that spans the bacterial membranes [30], so maintaining its integrity when looking at inhibitors of the process it performs could be essential for discovering the inhibitors' target(s). Given that we can not use the classic genetic approach, chemical methods are more suitable, but there are major disadvantages to the standard affinity chromatography. The criteria for our strategy are as follows:

- We use a small chemical modification that allows the molecule to retain its activity.
- We use live cells because we are looking at inhibitors of a dynamic process.
- We have the ability to pull down membrane proteins.

Given these criteria, our focus is to create a cell-permeable molecule that retains its inhibitory activity in cells and allows for retrieval of proteins following cell lysis, including membrane proteins.

A bioorthogonal labeling strategy is ideally suited for this type of problem (**Fig. 1.6**). A bioorthogonal reaction is one that can occur exclusively between two groups within a cellular environment. The two groups must be selective for each other and inert to all other chemical reactions occurring in a cell. An example of a bioorthogonal reaction is the Huisgen [3+2] Cu(I)-catalyzed azide-alkyne cycloaddition (CuACC), which has been termed a “click chemistry” reaction [110]. The general strategy is that a small molecule can be modified with an azide or an alkyne, which is a relatively small modification, and incubated with cells. During the incubation, the small molecule reacts with its targets or is incorporated onto its substrates as it would normally. After cell lysis, a tag containing the corresponding reactive group can be selectively reacted with the small molecule probe to detect its reactivity with proteins (**Fig. 1.6A**). The detection tag can be a fluorophore for visualization or a biotin tag for selective retrieval and proteomic

identification (**Fig. 1.6B**) [111,112]. This approach has been extensively used by our laboratory and others, and there are several examples in the literature of azide- and alkyne-functionalized chemical probes that allow for labeling of proteins in their native cellular environments [113-118]. Major advantages of this technique are its orthogonality to biological systems, relatively small chemical handle, efficiency, and ability to be used in live cells [118]. These characteristics make it a valuable technique that is central to our target identification strategy.

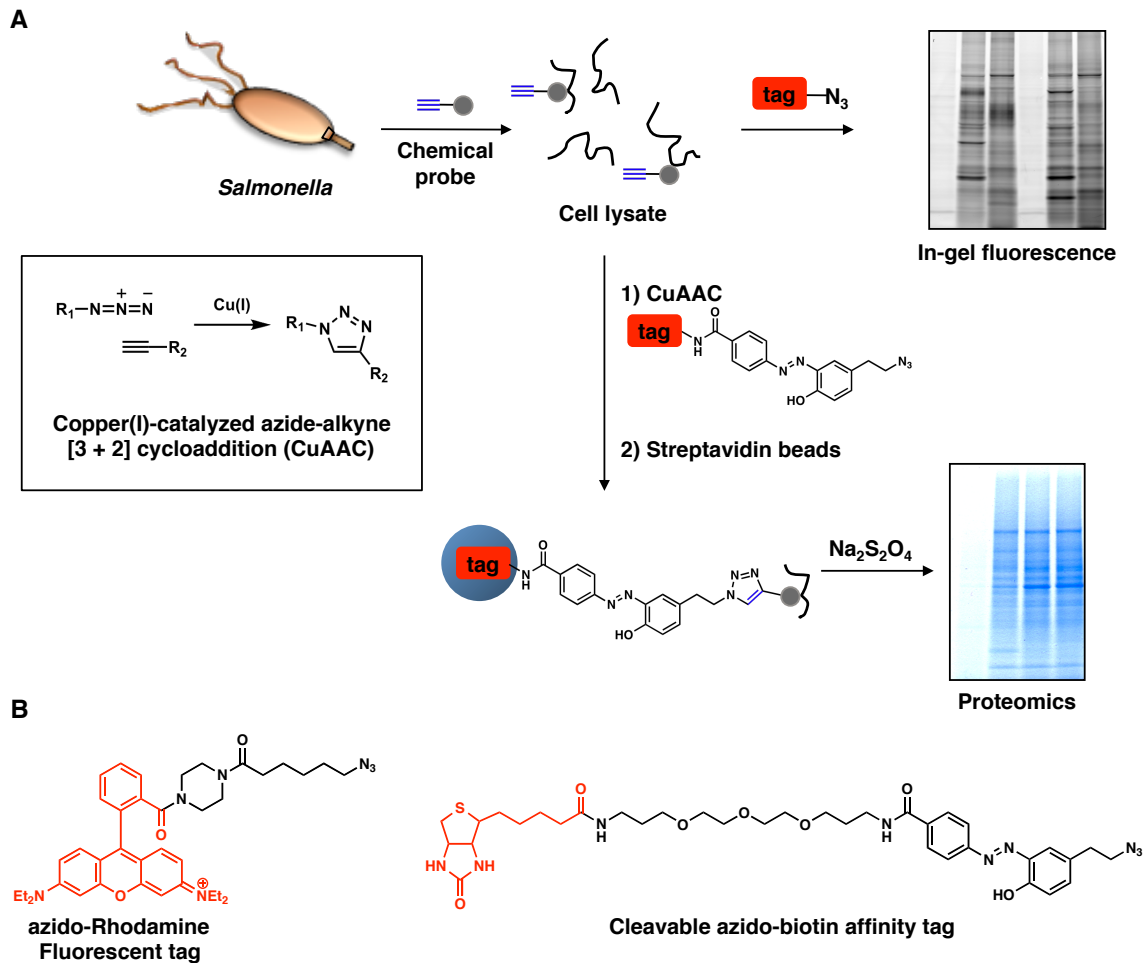


Figure 1.6 Bioorthogonal labeling strategy. **A)** An alkyne chemical probe can be incubated with cells and incorporated onto proteins. After lysis, the probe can be reacted with an azide via the copper(I)-catalyzed azide-alkyne [3+2] cycloaddition with a fluorescent tag for imaging and in-gel fluorescence or a biotin tag for retrieval and subsequent proteomic identification. **B)** Structures of the azido-Rhodamine dye (az-Rho) for imaging and the cleavable azido-biotin affinity tag for retrieval.

New strategies for antibacterial development are necessary to combat the emerging resistance among bacterial pathogens. Targeting bacterial virulence to treat infection provides an opportunity to circumvent resistance mechanisms while leaving the beneficial microbiota intact. There are several classes of small molecule inhibitors that target various steps necessary for many bacterial pathogens to establish infection. The SAHs are an interesting class of compounds that show significant promise as inhibitors of T3SSs and bacterial virulence, but no clear mechanism of action hampers their development. A bioorthogonal labeling strategy is a fitting approach for answering an important question in the development of new antibacterials and validating an anti-virulence approach.

CHAPTER 2 – Efforts Towards Target Identification of the Salicylidene

Acylhydrazides

Abstract

The salicylidene acylhydrazides are a class of anti-virulence compounds that block secretion of bacterial effector proteins through the T3SS and attenuate infection in various species of Gram-negative bacteria; however, the molecular target(s) of these compounds remains unknown, and the potency of these compounds is not optimal. To discover the molecular targets of SAHs and their mechanism of action, I synthesized alkynyl analogs and employed bioorthogonal labeling techniques for proteomic analysis of their protein-binding partners. Through SAR analysis of alkynyl analogs, I discovered important features for inhibitory activity of the SAHs and observed that they covalently modify many proteins; however, the functional protein targets responsible for SAH activity remain to be determined.

Introduction

Type III secretion is an essential process for many bacterial pathogens to establish infection [30]. It involves secreting effector proteins from the bacterial cytosol through a molecular syringe called the type III secretion system (T3SS) into the host cell, whereupon these effectors alter host cell signaling to establish and propagate infection [30,99]. Due to the increasing rate of emerging antibiotic resistant bacteria, targeting type III secretion has recently become an alternative “anti-virulence” approach for combating infection [1,2].

A large-scale screen for inhibitors of type III secretion in *Yersinia* discovered a class of compounds called the salicylidene acylhydrazides (SAHs) that were then found to block type III secretion in various pathogens [48] (**Table 1.1**); however, the precise target and mechanism of action of these compounds remains unknown. There are reports characterizing their activity in *Chlamydia* [65-69], *E. coli* [62,63], *Salmonella* [50,70-72], *Shigella* [73], and *Yersinia* [61], with studies suggesting the mechanism is through transcriptional effects [62,66,68,72], iron restriction [68,72], or disrupting the needle complex assembly [73]. Negative controls are lacking in some of these studies and species to species variation renders the mechanism unclear. To find the direct target of the SAHs, one study linked a compound to a solid support to pull down the non-covalent protein-binding partners in *E. coli* [63]. No single target could explain the observed phenotype for this class of compounds, and the authors concluded that the mechanism was likely a polypharmacological effect disrupting the normal metabolism of the bacteria, thus affecting their virulence. Since there is no clear consensus as to the mechanism of

action for the SAH's, we have taken a bioorthogonal approach to identify their protein targets and elucidate their mechanism of action.

Results

2.1 Synthesis and biological activity of photocrosslinking alkynyl SAH

The initial parent compound (INP-0007) discovered from the screen in *Yersinia* [48] contains a dibromophenol motif on one end of the molecule, which is important for its inhibitory activity. Based on preliminary SAR analysis, the other end of the molecule, however, appeared to be more tolerant to modification. We envisioned creating a trifunctional probe that could be used to identify the protein targets of these compounds [119]. By modifying the more tolerant side of the molecule with a photocrosslinker and an alkyne, we could covalently bind the small molecule to its protein targets with UV irradiation [120] and use the alkyne as a chemical handle to pull out the protein-binding partners (**Fig. 2.1**). The alkyne can be selectively reacted with an azide via the copper(I)-catalyzed azide-alkyne cycloaddition (CuAAC), or “click chemistry”, for visualization of protein-binding partners using an azido-fluorophore or selective retrieval with an azido-biotin tag for proteomic identification [111,112] (**Fig. 1.6**).

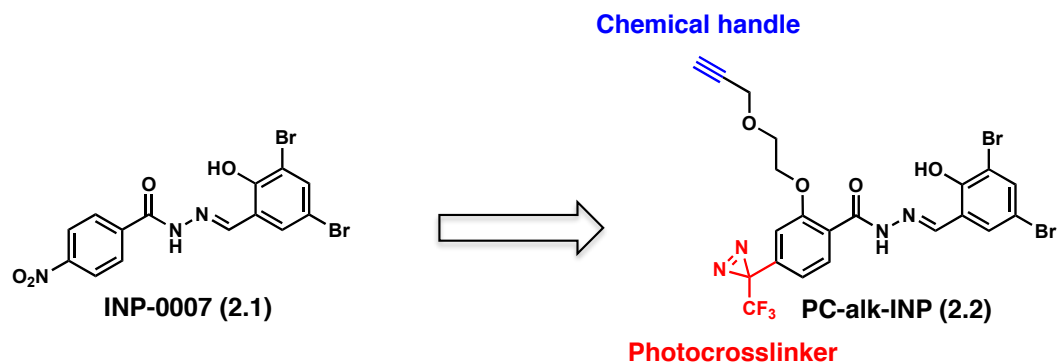


Figure 2.1 Structure of a type III secretion inhibitor and a bioorthogonal photocrosslinking analog. INP-0007 (2.1) can be modified to yield PC-alk-INP (2.2), an analog containing a photocrosslinker and a chemical handle for target identification studies.

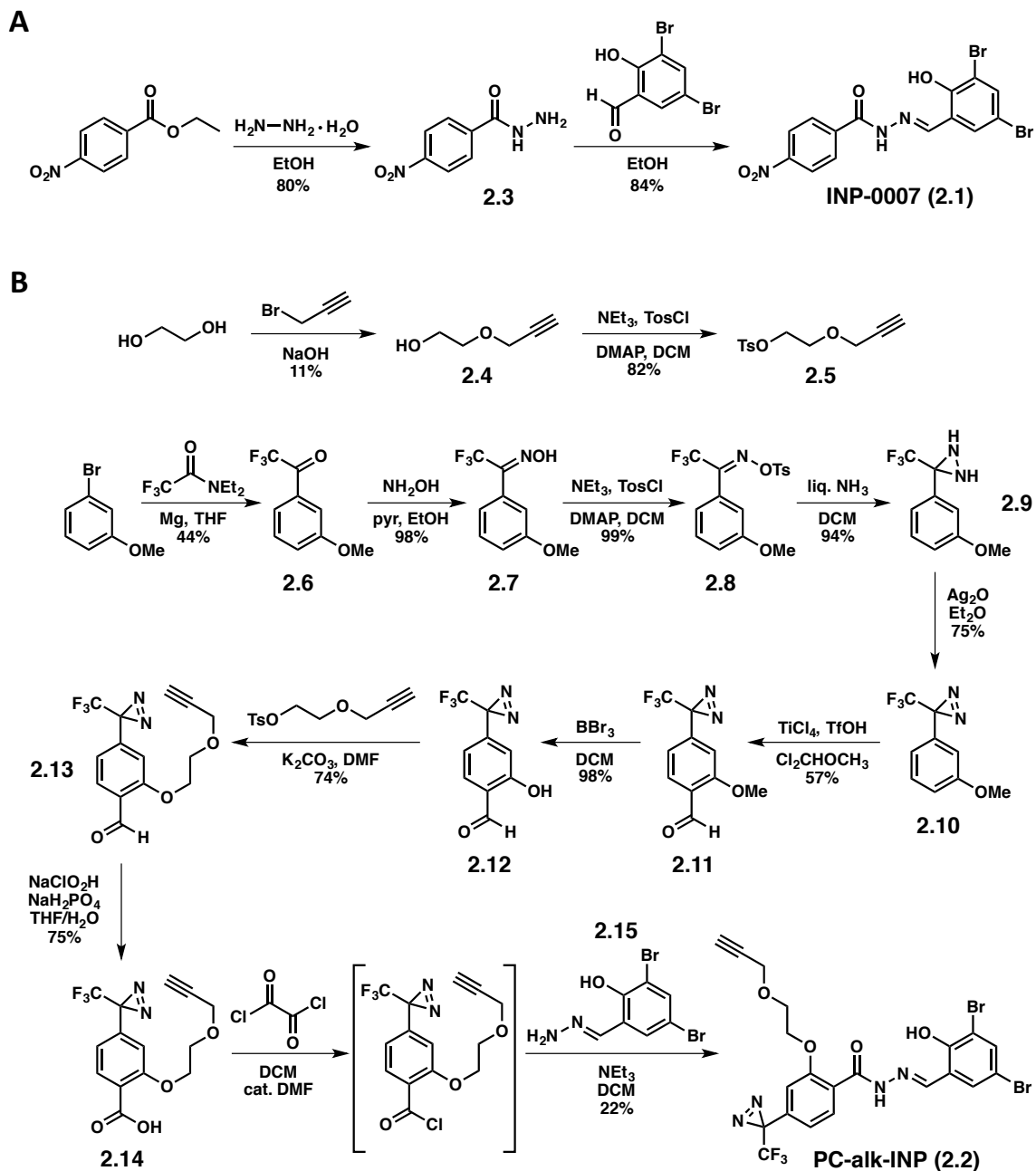


Figure 2.2 Synthesis of T3SS inhibitor INP-0007 (A) and photocrosslinking alkynyl INP probe PC-alk-INP (B).

INP-0007 was synthesized in two facile steps as previously reported [121], and PC-alk-INP (**2.2**) was synthesized by coupling the dibromophenol fragment with the alkynyl photocrosslinking component as depicted in **Figure 2.2**. The alkynyl photocrosslinking carboxylic acid (**2.14**) was synthesized according to published procedure [122], and the dibromophenol fragment (**2.15**) was synthesized by reacting hydrazine with 3,5-dibromosalicylaldehyde.

I first evaluated the activity of INP-0007 using a type III secretion assay in *Salmonella typhimurium*. Bacteria were incubated in the presence of compound or control for 4 hours. At the end of the incubation, the bacteria are spun down, and the proteins secreted into the culture supernatant are precipitated, separated by SDS-PAGE, and stained with Coomassie blue [71]. The majority of the secreted proteins are SPI-1 effectors, whose identities were confirmed by proteomic analysis of the Coomassie-stained gels from wild type and a SPI-1 T3SS-deficient strain ($\Delta invA$) of *S. typhimurium* (**Fig. 2.3** and **Table 2.1**).

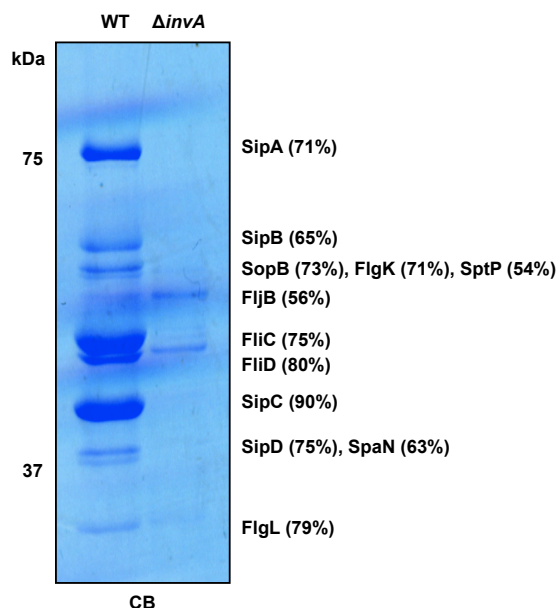


Figure 2.3 Proteomic analysis of secreted SPI-1 effectors. Secreted proteins were separated by SDS-PAGE and stained with Coomassie blue (CB). Bands were excised from the gel, trypsinized, and analyzed by LC-MS/MS. Percent coverage is shown in parentheses.

Table 2.1 Proteomic identification of secreted *Salmonella* proteins. A minimum of 2 unique tryptic peptides were used to assign protein bands. Accession numbers are from the UniProtKB database.

WT	Protein Name	Gene Name	Accession Number	Molecular Weight (kDa)	% Coverage	Peptide Spectral Counts
	Cell invasion protein sipA	sipA	Q56027	74	71	716
	Cell invasion protein sipB	sipB	Q56019	62	65	382
	Inositol phosphate phosphatase sopB	sopB	O30916	62	73	217
	Flagellar hook-associated protein 1	flgK	P0A1J5	59	71	214
	Secreted effector protein sptP	sptP	P74873	60	54	55
	Phase 2 flagellin	fliB	P52616	53	56	23
	Flagellin	fliC	P06179	52	75	322
	Flagellar hook-associated protein 2	fliD	P16328	50	80	366
	Cell invasion protein sipC	sipC	Q56020	43	90	605
	Cell invasion protein sipD	sipD	Q56026	37	75	118
	Surface presentation of antigens protein spaN	spaN	P40613	36	63	110
	Flagellar hook-associated protein 3	flgL	P16326	34	79	136
ΔinvA	Phase 2 flagellin	fliB	P52616	53	65	95
	Flagellin	fliC	P06179	52	73	404

After confirming the activity of INP-0007 in this secretion assay, PC-alk-INP (2.2) was tested. Unfortunately, PC-alk-INP was inactive likely due to the structural modifications introduced (Fig. 2.4A). When the bacteria treated with PC-alk-INP were lysed and reacted with azido-Rhodamine to evaluate the labeling profile, I observed an unexpected result; even without UV irradiation of the photocrosslinker, this compound covalently reacted with many proteins, suggesting something inherent in the structure of PC-alk-INP was capable of forming covalent bonds without photo-activation (Fig. 2.4B).

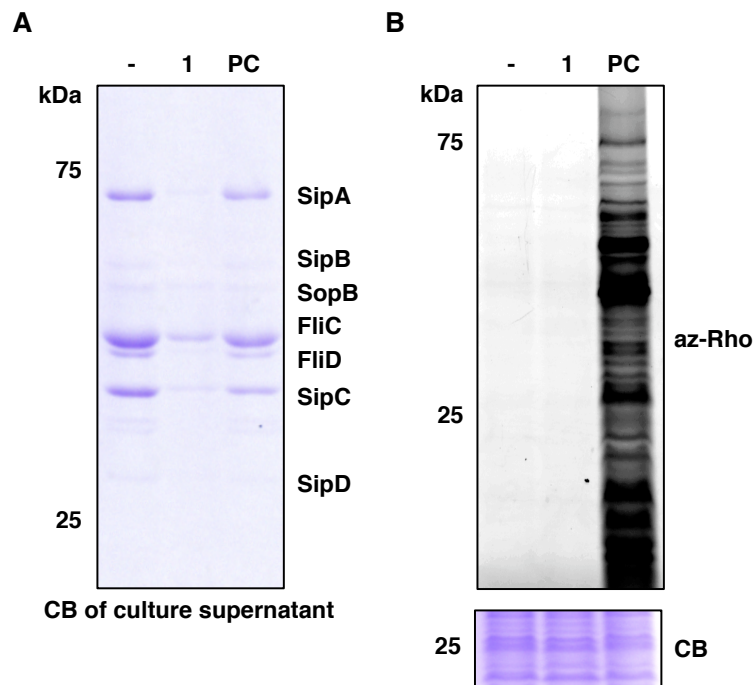


Figure 2.4 Secretion profile and protein labeling of T3SS inhibitor and PC-alk-INP probe. A) INP-0007 (1) and PC-alk-INP (PC) were incubated with *Salmonella* for 4 hours at a concentration of 50 μ M before the secreted proteins were precipitated, separated by SDS-PAGE, and stained with Coomassie blue (CB). B) The bacterial pellet was lysed, reacted with az-Rho, separated by SDS-PAGE, and analyzed by in-gel fluorescence imaging.

2.2 Synthesis and biological activity of alkynyl SAHs

Although the alkynyl photocrosslinking moiety rendered PC-alk-INP inactive, it appeared that a photocrosslinker was unnecessary to label proteins covalently. This led me to synthesize simpler alkynyl derivatives that did not contain the photocrosslinking group. With just a small structural modification, perhaps the compound could still be active and covalently bind its targets with a chemical handle intact. The larger alkynyl photocrosslinking fragment could be replaced with one containing just a small alkynyl group. As a negative control, the dibromophenol motif could be removed, and the corresponding alkynyl negative control could be synthesized to rule out nonspecific binding (**Fig. 2.5**).

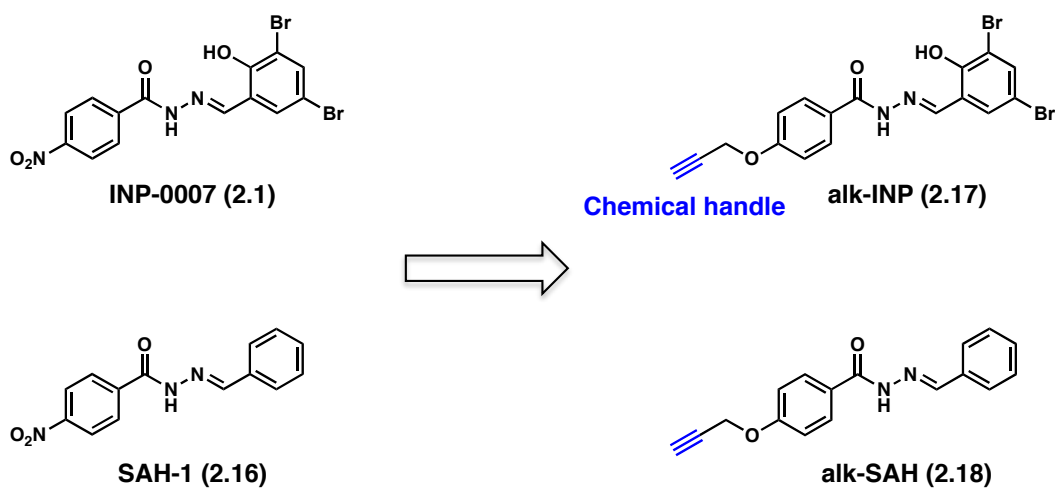


Figure 2.5 Structures of T3SS inhibitor INP-0007, a negative control (SAH-1), and their corresponding alkynyl analogs for protein labeling studies.

Initially, I synthesized three analogs of INP-0007 (**Fig. 2.6**): one without the dibromophenol motif (**2.16**), which was shown to be the ‘business end’ of the molecule, and an alkynyl analog for these two molecules (**2.17** and **2.18**). By precipitating the proteins secreted into the supernatant of cultures incubated with compound, I confirmed that the dibromophenol motif was essential for inhibiting type III secretion in *S. typhimurium* and that appending an alkyne did not significantly affect activity (**Fig. 2.7**); however, upon lysing the bacteria and performing the CuACC with azido-Rhodamine and separating the proteins by SDS-PAGE, in-gel fluorescence analysis showed that the active alkynyl analog **2.17** covalently modifies a large number of proteins while the inactive analog **2.18** does not (**Fig. 2.7D**).

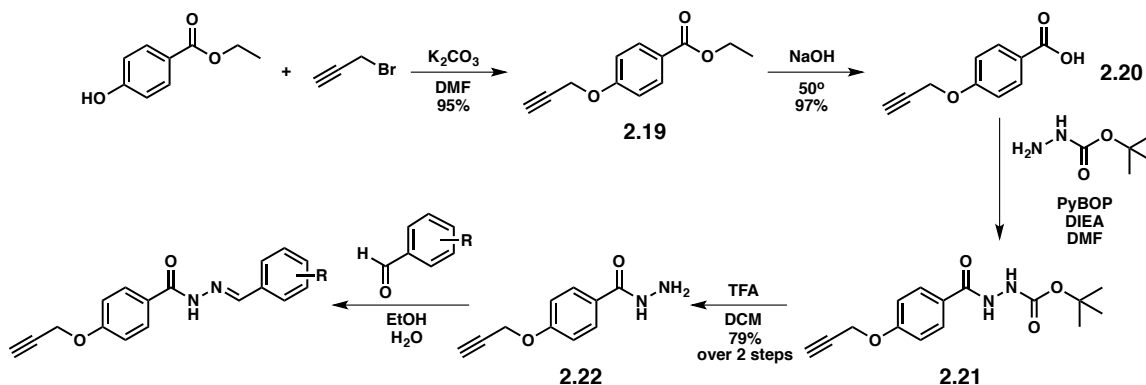


Figure 2.6 Synthesis of alkynyl salicylidene acylhydrazide analogs.

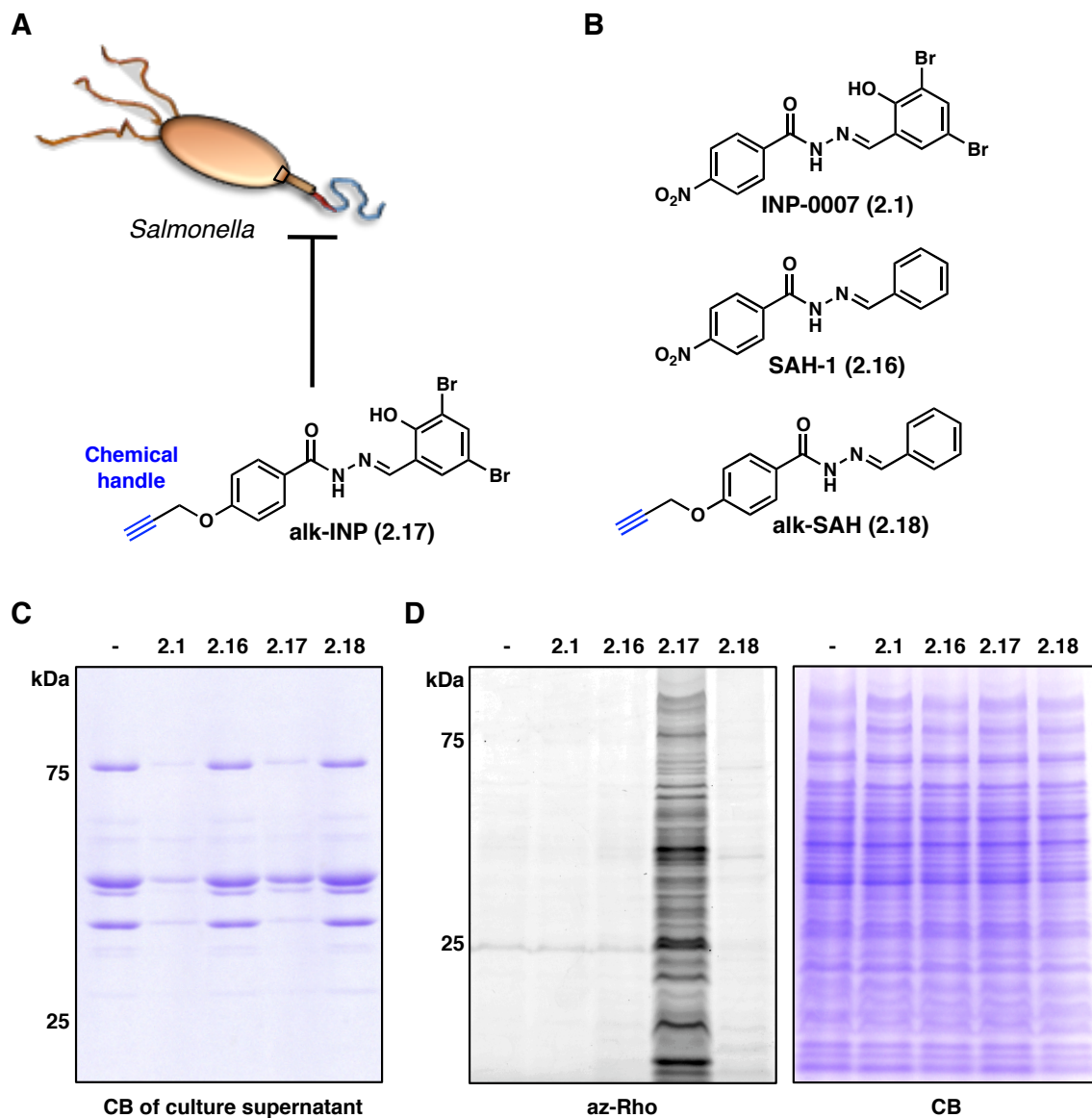


Figure 2.7 Activity of SAHs in *S. typhimurium*. **A)** Scheme of alkynyl SAH **2.17** blocking type III secretion in *Salmonella typhimurium*. **B)** Structures of INP-0007 (**2.1**), a negative control (**2.16**), and its corresponding alkynyl analog (**2.18**). SDS-PAGE gel of precipitated proteins secreted into the supernatant from cultures incubated with compound (**C**), and the corresponding labeled proteins analyzed by in-gel fluorescence after lysis (**D**). CB, Coomassie blue; az-Rho, azido-Rhodamine.

2.3 SAR analysis of alkynyl SAHs for inhibitory activity and covalent labeling

To determine the relevance of the covalent modification by the SAHs, I synthesized a panel of alkynyl analogs (2.23-2.28, Fig. 2.8) to systematically address the SAR of these compounds and correlate the covalent modification of proteins with inhibition of secretion. The analogs were synthesized in the same manner as alk-INP, using a different aldehyde in the final coupling step (Fig. 2.6). The panel of analogs displayed a range of both inhibitory activity (Fig. 2.9) and covalent modification of proteins (Fig. 2.10), but no correlation between the two was observed (Fig. 2.11). It is interesting to note that having just a single bromine atom on the phenolic ring at either the 3' or 4' position retains activity, while having no bromine at all decreases potency to some extent, but one at the 5' position completely abolishes activity. The phenol and the hydrazone are both crucial to activity since capping the phenol with a methyl group or reducing the hydrazone results in a loss of activity; however, the effects on inhibitory activity do not correlate with the extent of covalent modification.

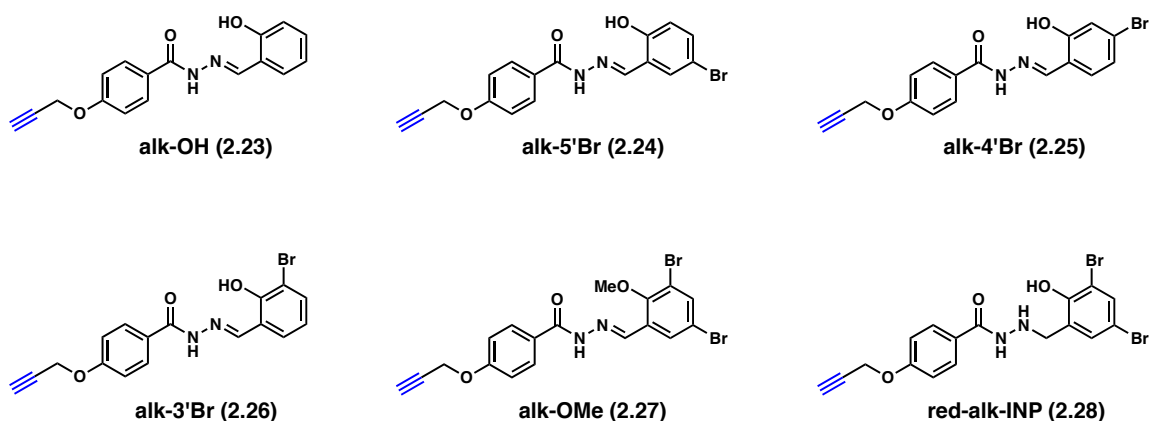


Figure 2.8 Panel of alkynyl salicylidene acylhydrazide analogs synthesized.

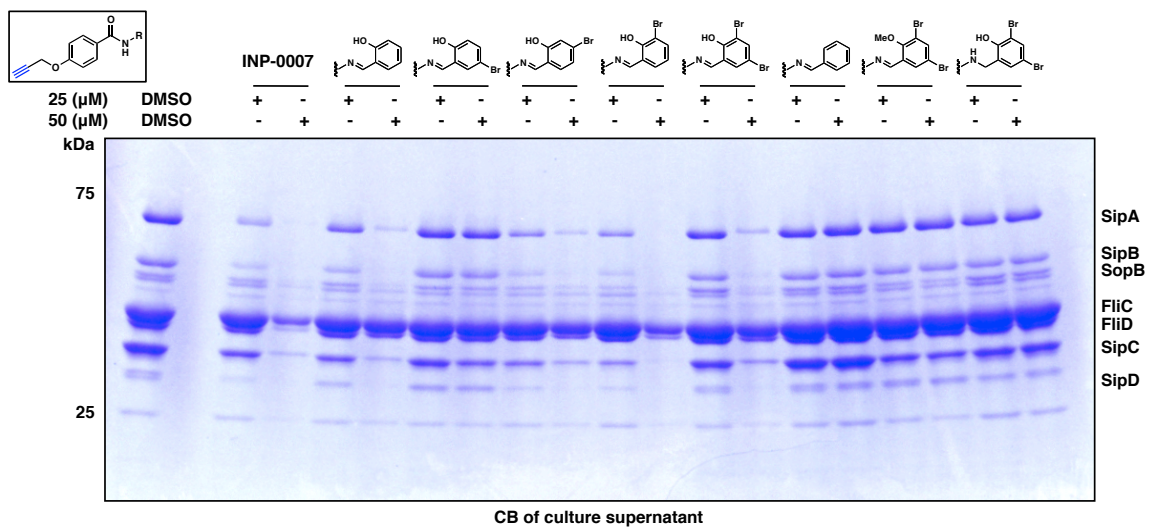


Figure 2.9 Effect of T3SS inhibitors and probes on SPI-1 effector secretion. Secreted proteins in the culture supernatant of bacteria incubated with compound were precipitated and separated by SDS-PAGE before staining with Coomassie blue (CB).

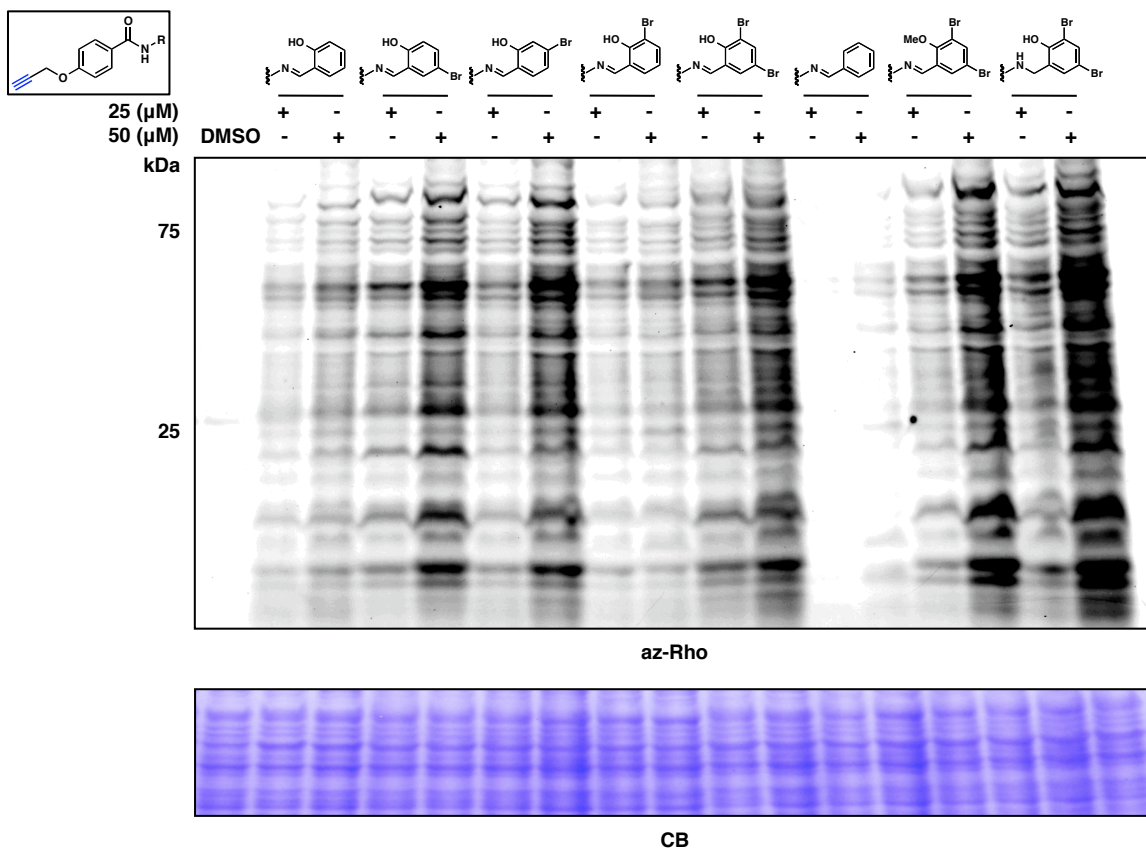


Figure 2.10 In-gel fluorescence analysis of proteins labeled by alkynyl SAHs. Bacteria were incubated with small molecule for 4 hours before the lysate was reacted with azido-Rhodamine (az-Rho) and separated by SDS-PAGE. CB, Coomassie blue.

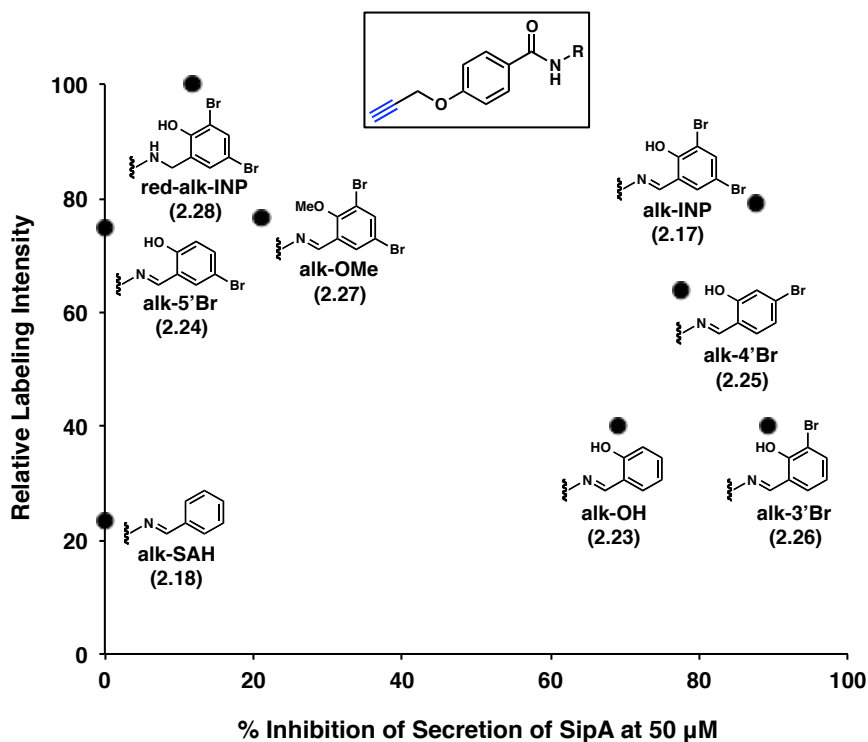


Figure 2.11 Plot comparing relative total lysate labeling fluorescence intensity vs T3SS inhibitory activity for alkynyl SAH analogs.

The formation of a covalent adduct with a protein proceeds by at least two steps and can be modeled using Michaelis-Menten kinetics. The general reaction scheme is shown in **Fig. 2.12**, where the first step is a reversible noncovalent binding step that forms an intermediate complex that allows for the subsequent covalent modification. The initial rate of product formation V_0 , can be described as

$$V_0 = \frac{v_{\max}[I]}{K_m + [I]} \quad (\text{Eq. 2.1})$$

This is analogous to the Michaelis-Menten equation where using a steady-state assumption, V_{\max} is the maximum rate of EI formation, $[I]$ is the inhibitor concentration, and K_m equals $(k_2 + k_{-1})/k_1$. K_m is the concentration of inhibitor when V_0 is one half V_{\max}

and can be described as a lumped rate constant that relates product formation (k_2) and dissociation (k_{-1}) of the intermediate EI* to its formation (k_1).

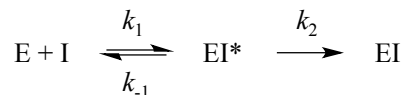


Figure 2.12 Reaction scheme for small molecule binding to proteins. An enzyme or protein, E, and an inhibitor, I, form an intermediate, EI*, that can then go on to form the covalent adduct, EI.

Given that we do not observe a significant difference in the profile of proteins labeled by the alkynyl SAHs but only in the extent of modification (**Fig. 2.10**), there are a few parameters that could explain these differences [123]. The relationship between the rate constants k_1 , k_{-1} , and k_2 controls the level of covalent labeling observed for the small molecule inhibitors. Only when the noncovalent complex EI* forms for a sufficient amount of time can the chemical covalent modification occur. The noncovalent affinity of an inhibitor for its target proteins is controlled by k_1 and k_{-1} , and it must be high enough to allow for the k_2 -dependent covalent modification step to occur. Compounds with high fluorescence labeling must have some combination of a high affinity for the target proteins with a k_2 large enough to permit covalent labeling during the residence time of the noncovalent complex. Compounds with low labeling may have minimal affinity for the target proteins, are less reactive, or a combination of the two. It is the interplay between affinity and reactivity that dictates the extent of covalent modification. It is also possible that the formation of the covalent adduct EI is reversible, and this would also play a role in the observed labeling intensity.

2.4 Effect of SAHs on *Salmonella* transcription

Since the SAHs react with many proteins, and there were previous reports of the SAHs affecting transcription [62,66,68] in *Salmonella* [72], we performed transcriptional profiling of virulence-related genes in cultures incubated with active (INP-0007 (**2.1**), alk-INP (**2.17**), and alk-3'Br (**2.26**)) or inactive compounds (alk-SAH (**2.18**) and alk-5'Br (**2.24**)). Genes involved in redox chemistry, iron homeostasis, SPI-1, and SPI-2 were analyzed, but no correlation between activity and transcriptional responses was observed (**Fig. 2.13A**). Using an effector-enzyme fusion protein assay developed in our laboratory [50], an enzymatic readout can be used to determine the amount of fusion protein present. While the parent compound **2.1** inhibits secretion of this fusion protein into the supernatant, it does not affect its levels in the lysate (**Fig. 2.13B**). These results demonstrate that transcriptional effects on virulence on a more global level and on a single effector level are not correlated with inhibition of secretion.

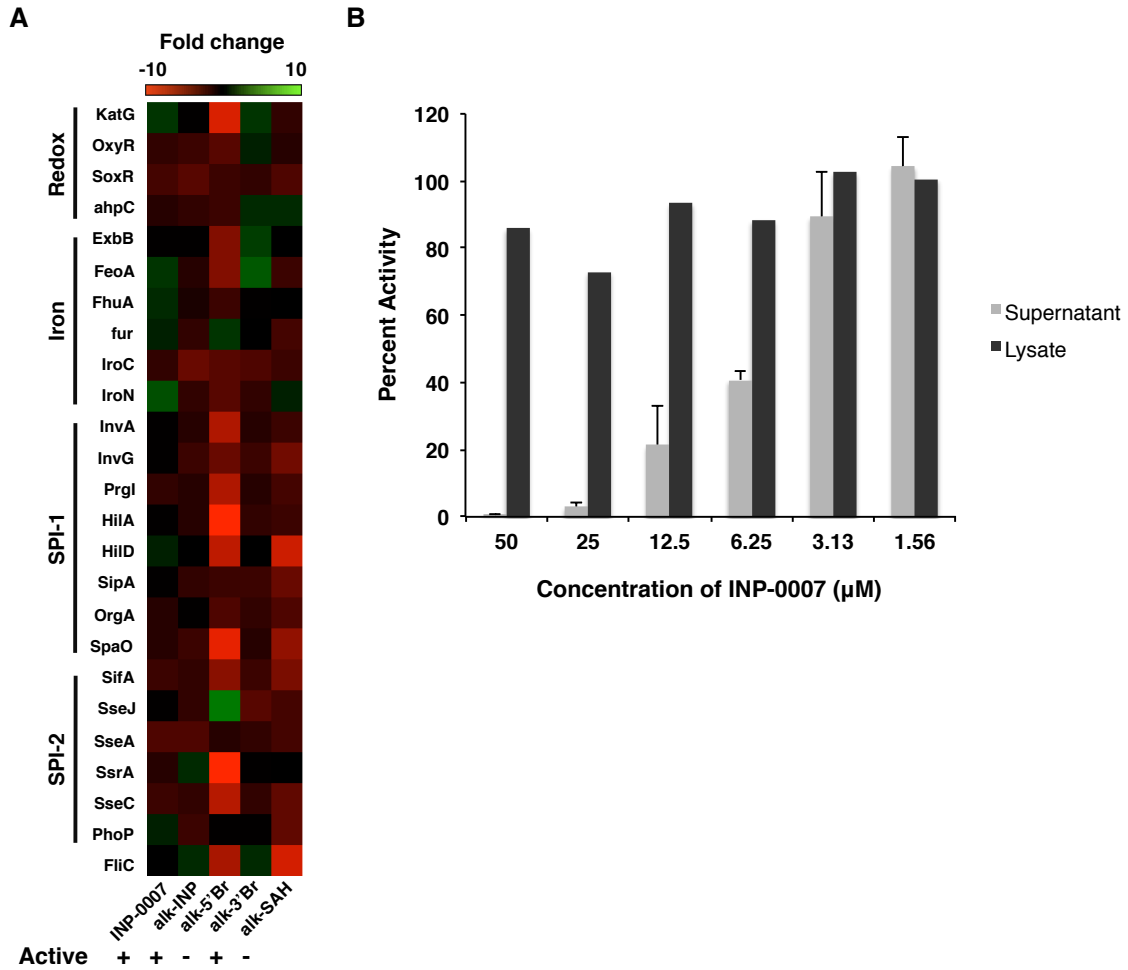


Figure 2.13 Effects of SAHs on expression of *Salmonella* virulence-related genes. **A)** RT-PCR analysis from cultures incubated with active or inactive compounds (performed by Angelica Ferguson). **B)** Percent CPG activity from SopE2-CPG2-HA effector-fusion protein secretion and expression after incubation with INP-0007 as compared to DMSO-treated control.

2.5 Proteomic identification of SAH protein-binding partners

Since the SAHs contain an inherent covalent reactivity, we wanted to identify the protein target(s) that are responsible for the observed phenotype. Although there was no

correlation between overall levels of protein labeling and inhibitory activity, it is possible, however, that it is not the overall extent of covalent modification that is important for inhibitory activity, but instead modification of specific proteins. In order to identify which proteins the small molecules modify, I performed a labeling and enrichment assay followed by mass spectrometry for proteomic identification of the alkynyl SAH targets (**Fig. 1.6**). Bacteria were incubated with compound before click chemistry was performed on the lysate with an azido-azo-biotin tag [111,112]. Streptavidin resin was used to capture the biotinylated proteins, and the azobenzene linker was cleaved using sodium dithionite to elute only the tagged proteins, leaving behind any nonspecifically bound proteins. The eluted proteins were separated by SDS-PAGE before trypsinization and analysis by liquid chromatography coupled with tandem mass spectrometry.

We chose to identify alk-3'Br's (**2.26**) protein targets because it showed the highest inhibitory activity compared to its covalent reactivity, thus potentially simplifying the results. In addition to a DMSO control, two inactive analogs that were at the extremes of covalent labeling, alk-SAH and alk-5'Br (compounds **2.18** and **2.24**), were also chosen to rule out irrelevant hits (**Fig. 2.11**). The identification of the high-confidence hits (10x DMSO sample and at least 10 spectral counts) for each sample is displayed in **Table 2.2**. The majority of the protein hits were metabolic proteins that had no obvious link to the observed phenotype. There were also no major differences in the protein-binding partners for the active (alk-3'Br, **2.26**) and inactive (alk-5'Br, **2.24**) compounds, suggesting the most abundant subset of covalently modified proteins is not responsible for inhibitory activity.

Table 2.2 High-confidence proteins pulled down by small molecule probes. Proteins were identified with at least two unique peptide spectra, 10 spectral counts, and 10 times the background.

Identified Proteins	Accession #	MW	Number of assigned spectra			
			DMSO	alk-5'Br	alk-3'Br	alk-SAH
30S ribosomal protein S2	P66541 RS2_SALTY	27 kDa	6	36	60	45
Cell invasion protein sipA	Q56027 SIPA_SALTY	74 kDa	0	16	27	23
3-oxoacyl-[acyl-carrier-protein] synthase I	Q7CQ97 Q7CQ97_SALTY	38 kDa	0	20	21	15
Glutathione S-transferase	Q8ZPM7 Q8ZPM7_SALTY	22 kDa	2	14	24	10
Transcription elongation factor greA	P64281 GREA_SALTY	18 kDa	0	10	15	11
Protein csID	Q9FA43 CSID_SALTY	37 kDa	0	14	18	8
Dihydrodipicolinate synthase	Q8ZN71 DAPA_SALTY	31 kDa	0	15	13	9
2-dehydro-3-deoxyphosphooctonate aldolase	P65215 KDSA_SALTY	31 kDa	0	14	17	6
Glyoxylate/hydroxypyruvate reductase A	Q8ZQ30 GHRA_SALTY	35 kDa	0	13	8	10
Glutamate/aspartate transporter	Q7CQY9 Q7CQY9_SALTY	27 kDa	0	10	9	8
Response regulator	Q7CP63 Q7CP63_SALTY	27 kDa	0	8	11	11
2,3-bisphosphoglycerate-dependent phosphoglyce	Q8ZQS2 GPMA_SALTY	28 kDa	0	10	11	7
Probable thiol peroxidase	Q8ZP65 TPX_SALTY	18 kDa	0	8	8	11
Inositol phosphate phosphatase sopB	O30916 SOPB_SALTY	62 kDa	0	6	15	6
Putative oxoacyl-(Acyl carrier protein) reduct	Q7CQG2 Q7CQG2_SALTY	28 kDa	0	7	9	13
Ribose-phosphate pyrophosphokinase	P0A1V6 KPRS_SALTY	34 kDa	0	11	12	5
D-ribulose-5-phosphate 3-epimerase	Q8ZLK4 Q8ZLK4_SALTY	24 kDa	0	13	15	0
Putative alcohol dehydrogenase	Q8ZM07 Q8ZM07_SALTY	42 kDa	0	8	12	0
S-ribosylhomocysteine lyase	Q9L4T0 LUXS_SALTY	19 kDa	0	7	10	8
Cell division inhibitor	Q8ZP10 Q8ZP10_SALTY	30 kDa	0	4	11	10
Putative intracellular proteinase	Q7CPQ5 Q7CPQ5_SALTY	19 kDa	0	6	10	11
Phosphoserine aminotransferase	P55900 SERC_SALTY	40 kDa	0	12	9	3
Flagellin	P06179 FLIC_SALTY	52 kDa	0	5	10	6
Sigma cross-reacting protein 27A	Q8ZLR6 Q8ZLR6_SALTY	23 kDa	0	10	12	0
Putative oxidoreductase	Q8ZKX9 Q8ZKX9_SALTY	21 kDa	0	10	8	4
L-threonine 3-dehydrogenase	Q8ZL52 TDH_SALTY	37 kDa	0	8	11	0
30S ribosomal protein S5	P0A7W4 RS5_SALTY	18 kDa	0	4	10	6
Oxygen-insensitive NADPH nitroreductase	Q9Z5Z2 NFSA_SALTY	27 kDa	0	7	11	6
Peptidyl-prolyl cis-trans isomerase	Q8ZLL4 Q8ZLL4_SALTY	21 kDa	0	9	11	0
ATP synthase subunit delta	Q7CPE5 ATPD_SALTY	19 kDa	0	7	10	5
ATP synthase subunit b	Q7CPE4 ATPF_SALTY	17 kDa	0	4	10	4
Amidophosphoribosyltransferase	Q8ZNC2 Q8ZNC2_SALTY	57 kDa	0	12	6	0
Putative periplasmic protein	Q7CQV7 Q7CQV7_SALTY	33 kDa	0	12	9	0
UDP-glucose 4-epimerase	P22715 GALE_SALTY	37 kDa	0	6	11	2
1,4-alpha-glucan-branching enzyme	Q8ZLG5 GLGB_SALTY	84 kDa	0	7	11	0
Protein hfq	P0A1R0 HFQ_SALTY	11 kDa	0	4	4	10
Universal stress protein E	Q8ZP84 JUSPE_SALTY	36 kDa	0	3	10	0
Putative diadenosine tetraphosphate	Q8ZM04 Q8ZM04_SALTY	17 kDa	0	6	10	0
Cell invasion protein sipD	Q56026 SIPD_SALTY	37 kDa	0	0	9	3

2.6 SAH inhibition of *Salmonella* invasion of HeLa cells

While the functional targets of the SAHs remains to be determined, I tested whether the inhibitory activity of these compounds against protein secretion correlated with preventing *Salmonella* invasion of host cells. HeLa cells were infected for 30 minutes at a multiplicity of infection (MOI) of 10 with *Salmonella* grown in the presence of compound or DMSO, and the extent of invasion was determined using flow cytometry.

The inhibition of effector secretion into the culture supernatant correlates well with preventing *Salmonella* from invading HeLa cells, and by systematically investigating the SAR of these compounds, I discovered an analog (alk-3'Br, compound **2.26**) with greater potency in an infection setting than the parent compound (**Fig. 2.14**).

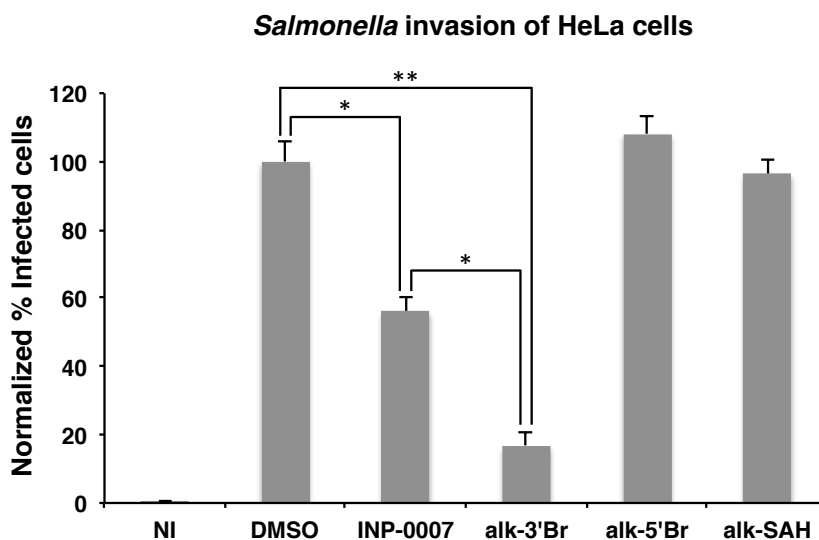


Fig 2.14 Effects of SAHs on *Salmonella* invasion of HeLa cells. Bacteria grown in the presence of 50 μ M compound or DMSO were used to infect HeLa cells for 30 min at an MOI of 10. The percentage of infected HeLa cells was determined by staining with an anti-*Salmonella* antibody followed by analysis with flow cytometry. The statistical values from a two-sided Student's t-test are as follows: *, $P < 0.001$; **, $P < 0.0001$.

Discussion

The salicylidene acylhydrazides are a well-studied class of anti-virulence compounds that inhibit type III secretion in several bacterial pathogens; however, their precise mechanism of action is unknown. By synthesizing a panel of SAH analogs

displaying a range of inhibitory activity (**Fig. 2.9**), I identified key chemical features important for activity. The analysis of these compounds in *Salmonella* suggests their effects on transcription are not linked to their inhibition of type III secretion (**Fig. 2.13**). The SAHs also covalently label *Salmonella* proteins, but the functional consequences of these findings on their mechanism of action are still unclear (**Fig. 2.10** and **Table 2.2**). Nonetheless, my studies of the SAHs have stressed the importance of negative controls and revealed a more potent compound at preventing *Salmonella* invasion of HeLa cells (**Fig. 2.14**).

CHAPTER 3 – The Repurposed Kinase Inhibitor H-89 Targets Bacterial Virulence Pathways to Limit Infection

Abstract

The emergence of antibiotic-resistant bacterial pathogens has motivated new approaches for antibacterial drug discovery that target virulence pathways or host enzymes important for infection [1,2]. The isoquinolinesulfonamide H-89 was discovered in a screen for host kinase inhibitors that blocked *Salmonella* replication in macrophages [124]. The authors claimed that H-89 prevented bacterial replication through inhibition of Akt, a host kinase activated during infection. H-89 did not affect the growth of the bacteria in culture, and inhibition of Akt did not fully explain H-89's effects, so we hypothesized it could be acting as an anti-virulence compound. We discovered that H-89 inhibits the expression of *S. typhimurium* genes associated with bacterial virulence including both SPI-1 and SPI-2 T3SSs. Since H-89 had a much larger effect on bacterial replication than a potent and specific Akt inhibitor, my results suggest the effect of H-89 on bacterial virulence is the more relevant mechanism of action.

Introduction

While several groups have specifically screened for compounds that inhibit type III secretion system activity in liquid culture (**Tables 1.1-1.3**), screens for inhibitors in an infection setting may reveal new lead compounds. Although this requires a more complex screen, it bypasses several follow-up experiments that are necessary from evaluating strictly bacterial systems. Hits from this type of screen are already known to be effective in at least a cell culture system and not to be toxic to mammalian cells. In addition, since many bacterial proteins are known to interact with host proteins, screening compounds in an infection setting allows for discovering compounds that disrupt these important pathogenic protein-protein interactions that would otherwise not be present in a screen with only bacteria. Compounds that disrupt the host pathways hijacked by the bacteria could also be effective for treating infection.

With more knowledge of host-pathogen interactions and the increasing need for new antibacterial compounds, specifically targeting host pathways required for pathogenesis is an alternative strategy. Chemical libraries previously developed for mammalian targets are beginning to be repurposed for anti-infectives [125-127]. Notably, Kuijl et al. conducted a whole-cell screen to identify host kinase inhibitors that could block replication of *Salmonella typhimurium* in macrophages [124]. This study showed that the isoquinolinesulfonamide H-89 could effectively inhibit *Salmonella* replication during infection without affecting bacterial growth in culture. A parallel siRNA screen against host kinases on bacterial replication suggested the Akt1 network was crucial for intracellular growth of *Salmonella* and *Mycobacteria* [124]. From these observations, the antibacterial activity of H-89 was attributed to inhibition of Akt [124], a host kinase that

is activated during *Salmonella* infection. However, a more potent and specific Akt inhibitor failed to recapitulate the inhibition of bacterial replication in the same study [124], suggesting an alternative mechanism of action for H-89 on intracellular bacterial replication (**Fig. 3.1**).

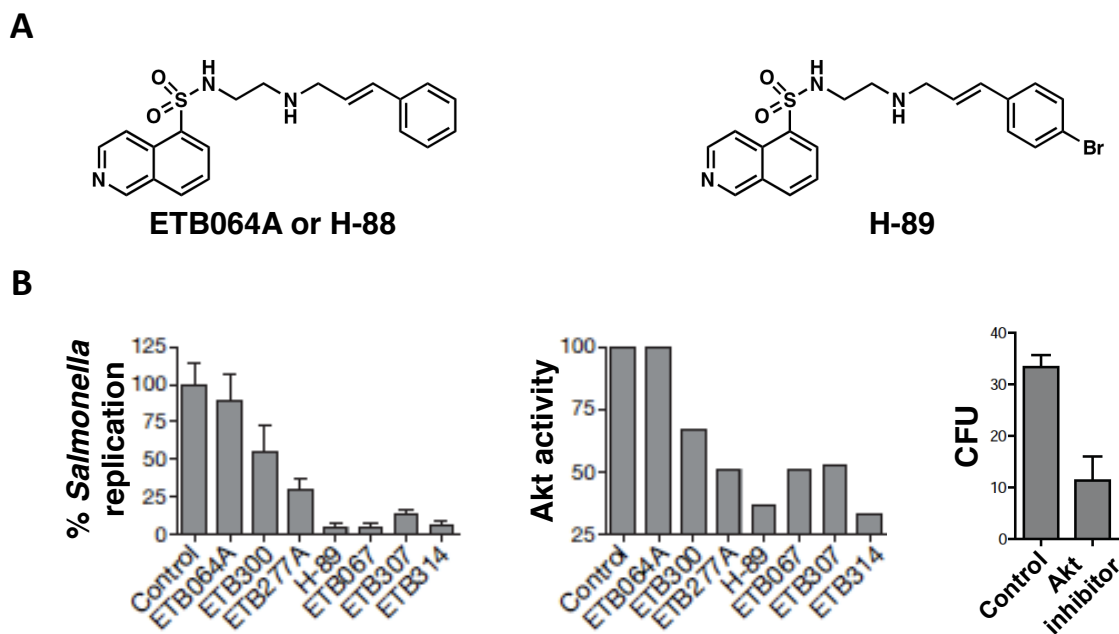


Figure 3.1 Structures and activity of isoquinolinesulfonamides on *Salmonella* and Akt. **A)** Structures of inactive isoquinolinesulfonamide H-88 and active compound H-89. **B)** Authors claimed isoquinolinesulfonamides prevented bacterial replication through inhibition of host kinase Akt. Taken from [124].

Since H-89 did not affect the growth of *Salmonella*, and inhibition of Akt could not fully explain its effect on bacterial replication, we hypothesized that it could be inhibiting the virulence functions of the bacteria and represent a new scaffold for anti-

virulence compounds. I therefore investigated its effects on bacterial virulence and type III secretion function.

Results

3.1 H-89 inhibits bacterial replication through Akt-independent mechanism

To begin investigating the mechanism of action for H-89 on *Salmonella* replication in mammalian cells, I compared the activity of H-89 and a more potent Akt inhibitor on *S. typhimurium* replication in murine RAW264.7 macrophages. Following entry into host cells, *Salmonella* replicates in a *Salmonella*-containing vacuole (SCV) [99] and the extent of replication can be monitored by a standard gentamicin protection assay. Briefly, RAW264.7 macrophages were infected with *S. typhimurium* for one hour, at which point gentamicin was added to kill any remaining extracellular bacteria. H-89 or other compounds were then added to infected macrophages and colony forming units (CFUs) were determined 16 hours post-infection (pi) to determine the number of viable intracellular bacteria. H-89, but not H-88, an analog that differs by one bromine atom (**Fig. 3.2A**), significantly decreased the number of bacterial CFUs at 20 μ M (**Fig. 3.2B**), which is consistent with published data [124]. However, a more potent and specific Akt-inhibitor (Akti1/2) [128] displayed minimal inhibitory activity against *Salmonella* replication compared to H-89 (**Fig. 3.2B**) even though the majority of active Akt in these infected macrophages was depleted, as judged by Akt phosphorylation at Ser⁴⁷³ (**Fig. 3.2C**). Phosphorylation at this site is required for full activation of Akt and its downstream signaling events [128]. These results demonstrate that pharmacological inhibition of Akt is not sufficient for preventing bacterial replication. In addition, as

reported by Kuijl et al., H-89 did not have any major effect on *Salmonella* growth in liquid culture (**Fig. 3.2D**) [124], demonstrating this compound does not kill the bacteria directly. These experiments suggest an alternative mechanism of action for H-89 on *Salmonella* replication in host cells that is independent of Akt inhibition.

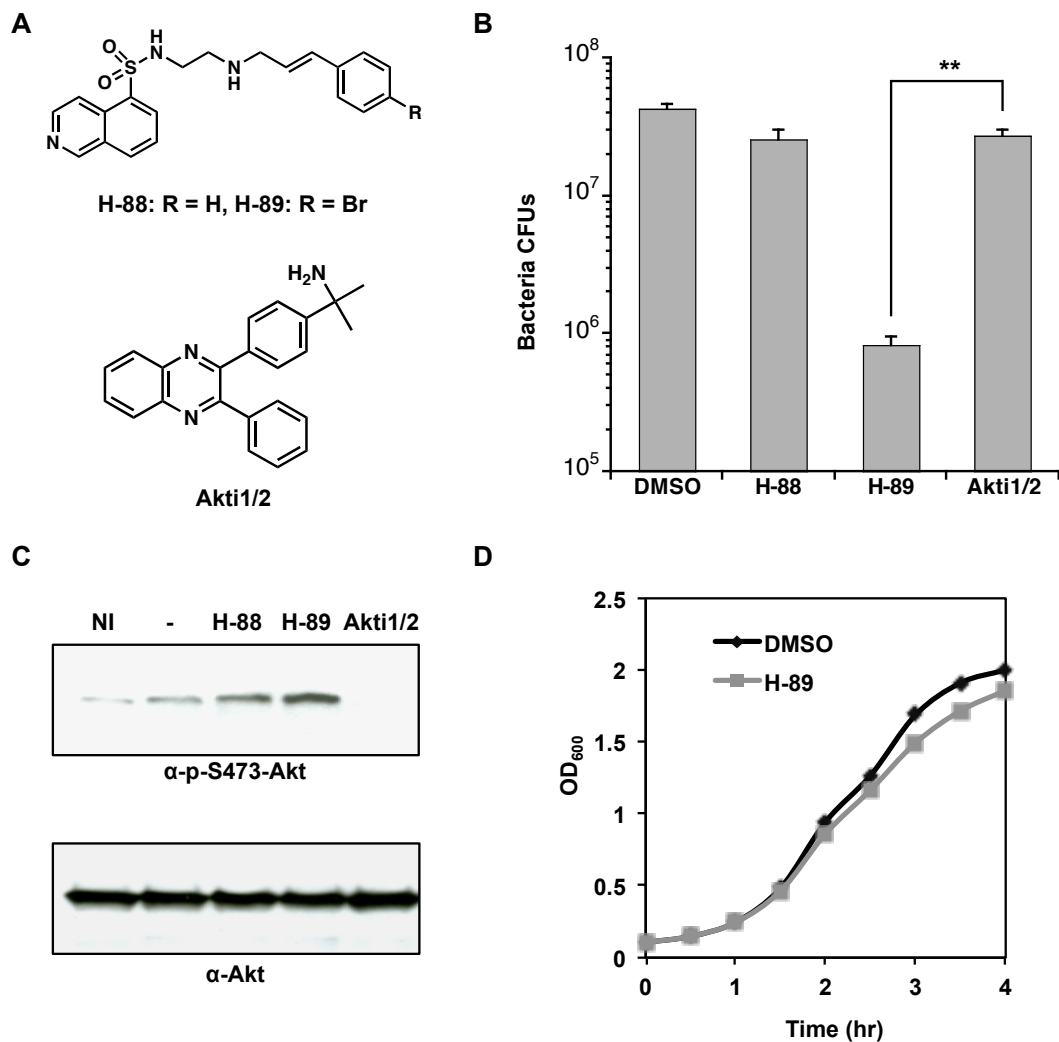


Figure 3.2 H-89 inhibits bacterial replication through Akt-independent mechanism.

A) Structures of isoquinolinesulfonamides H-88 and H-89 and Akt inhibitor Akti1/2. **B)** CFU numbers of intracellular *Salmonella* 16 hours pi. Compounds were added at 20 μ M after 1 hour of infection at an MOI of 5. The statistical value from a two-sided Student's t-test is as follows: **, $P < 0.001$. **C)** Western blots of phospho-Akt (Ser473) and total Akt levels 8 hours pi in infected macrophages with 20 μ M compound treatment. NI, not infected; WB, Western blot. **D)** Growth curves of *Salmonella* grown in the presence of compound. Bacteria were incubated with H-89 (20 μ M) or DMSO and OD₆₀₀ readings were taken every 30 minutes.

3.2 H-89 inhibits expression of *Salmonella* virulence genes required for bacterial infection

Since genetic and biochemical studies have shown that T3SSs are essential for infection but do not affect bacterial viability in culture [30,99], we performed targeted transcriptional profiling of *S. typhimurium* virulence factors to identify the potential mode of action for H-89. For genes involved in redox chemistry or iron transport/acquisition, no significant effect was observed for either H-88 or H-89 (**Fig. 3.3A**). In contrast, H-89 selectively decreased the expression of key *S. typhimurium* virulence factors required for bacterial replication in macrophages. SPI-2 effector genes: *sifA*, *sseJ*, and *sseC* were down-regulated along with SPI-1 T3SS components: regulator *hilA*, effector protein *sipA*, and needle complex components *invA*, *invG*, and *prgI* (**Fig. 3.3A**). To determine if the decreased levels of SPI-2 effector genes indeed affected protein levels, we evaluated the expression of an HA-tagged SPI-2 effector (SseJ-HA) under the control of its native promoter. Consistent with the transcriptional profiling data, SseJ-HA levels by Western blot analysis were decreased when incubated with H-89 compared to the inactive H-88 control and DMSO (**Fig. 3.3B**). These results suggest that H-89 selectively down-regulates several virulence genes involved in *S. typhimurium* T3SS-dependent invasion and replication.

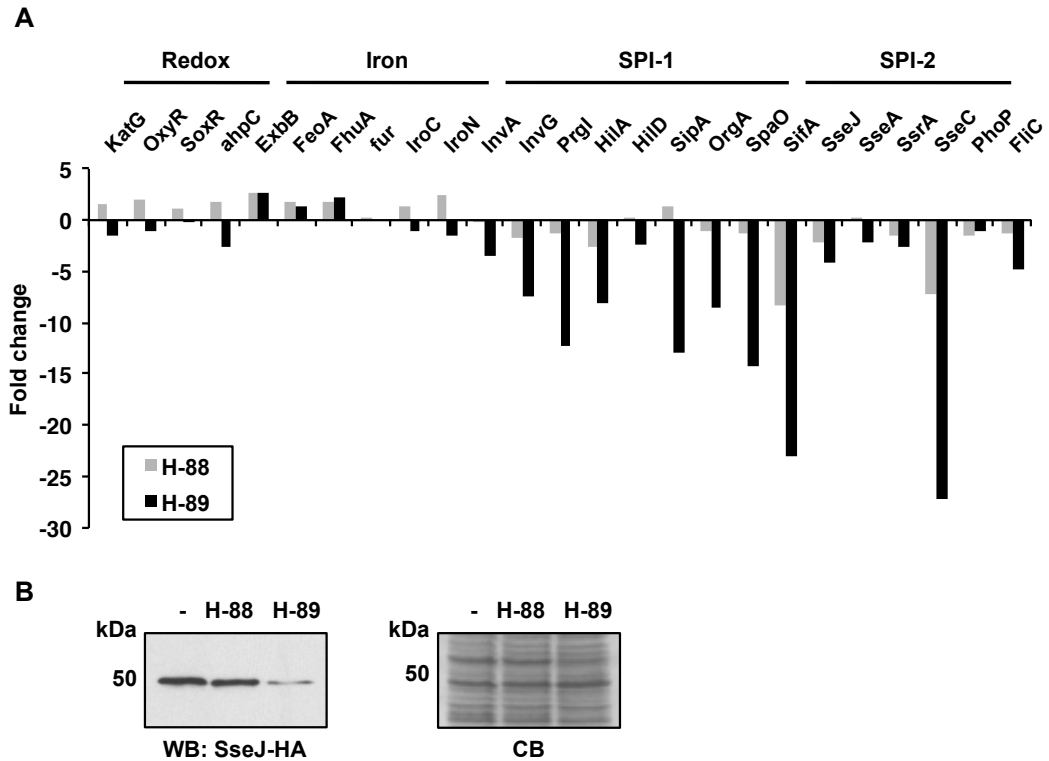


Figure 3.3 Compound effects on gene expression. **A)** RT-PCR analysis of bacterial cultures treated with 20 μ M of compound (performed by Angelica Ferguson). **B)** Western blot of SseJ-HA in the lysate of compound-treated cultures. WB, Western blot; CB, Coomassie blue.

3.3 H-89 decreases the levels of bacterial effectors secreted during *S. typhimurium* replication in host cells

Given the inhibition of bacterial replication and down-regulation of SPI-2 virulence genes *in vitro*, I investigated the effect of H-89 on intracellular levels of SseJ, a SPI-2 effector that is secreted during *Salmonella* replication in macrophages. SseJ is a key SPI-2 effector that exhibits phospholipase A and acyltransferase activity and opposes the function of SifA, another SPI-2 effector responsible for establishing and maintaining

the SCV in host cells [129,130]. To monitor the amount of SseJ secreted into the host cytosol during infection, I used an *S. typhimurium* strain expressing SseJ-HA. By immunofluorescence confocal microscopy, SseJ-HA was not observable in the host cytosol until about 4-5 hours pi and became robustly seen 7 hours pi. I therefore administered the compounds at 5 hours pi, and after a 2-hour incubation with compounds, *S. typhimurium*-infected macrophages were permeabilized, fixed, and stained to examine the amount of intracellular *S. typhimurium* and SseJ-HA. The H-89-treated samples showed a marked reduction in the amount of SseJ-HA staining, while no apparent effect on SseJ-HA expression or distribution was observed with 20 μ M of the H-88 control (**Fig. 3.4**). These results demonstrate that H-89 inhibition of SPI-2-associated virulence factor expression also results in reduced levels of SPI-2 protein effectors such as SseJ during *S. typhimurium* infection of host cells.

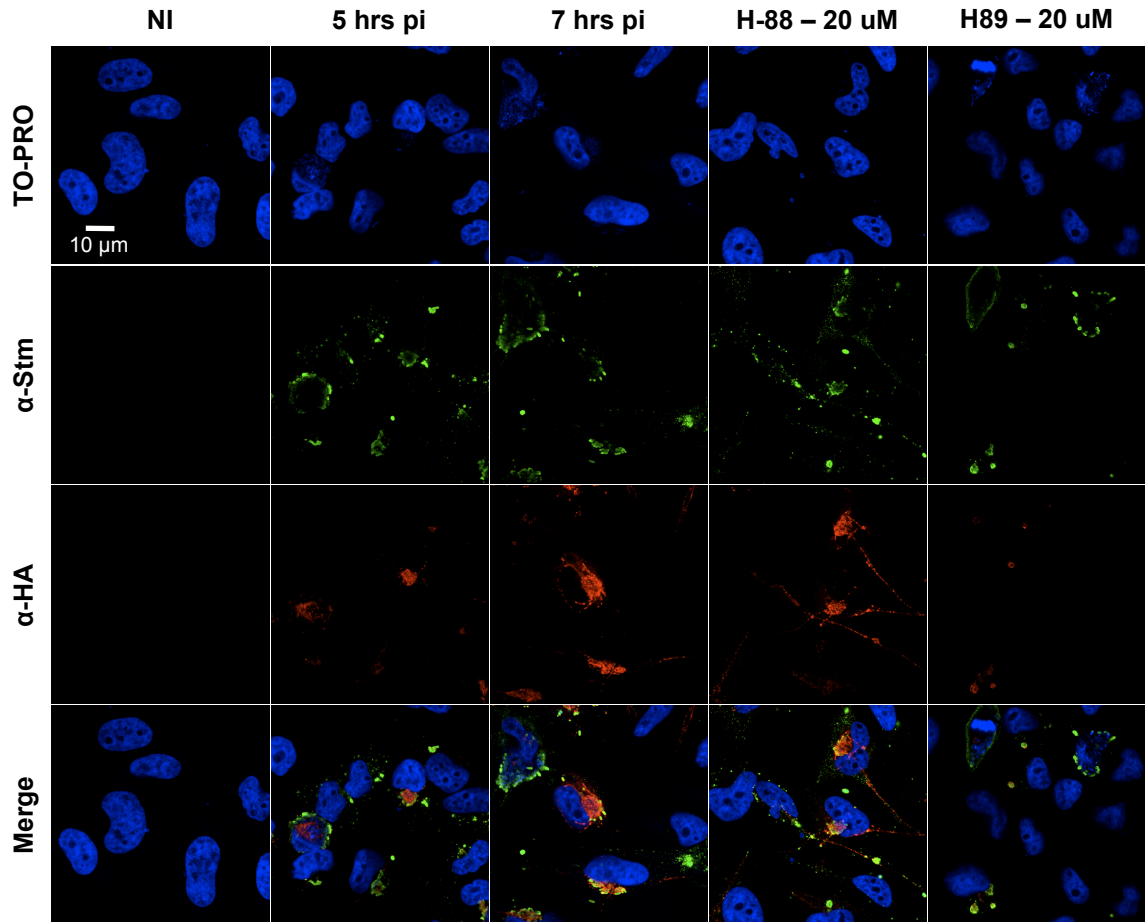


Figure 3.4 Imaging of SseJ-HA during *Salmonella* infection. RAW264.7 macrophages were infected for one hour (MOI = 1), and compound was added 5 hours pi. At 7 hours pi, cells were fixed and stained with TO-PRO (blue), anti-*Salmonella* (green), and anti-HA (red). Shown are representative images from three independent experiments.

3.4 H-89 also antagonizes the SPI-1 T3SS and inhibits *Salmonella* invasion of epithelial cells

As the transcriptional profiling data suggests H-89 also inhibits expression of *S. typhimurium* genes associated with the SPI-1-dependent invasion of host cells (Fig. 3.3A), I tested whether H-89 also impairs SPI-1 T3SS-associated functions. To validate

our SPI-1 gene expression data, I employed an effector-enzyme fusion reporter system, SopE2-CPG2-HA, for sensitive detection of type III protein expression and secretion in *S. typhimurium* previously developed by our laboratory [50]. For this effector reporter system, carboxypeptidase G2 (CPG2) is translationally fused to the *S. typhimurium* effector SopE2 under control of its native promoter. By monitoring the enzymatic activity of CPG2 with a fluorogenic substrate, this assay provides a visible and quantitative method for determining effector protein expression and secretion [50]. Using this assay, H-89 decreased the levels of SopE2-CPG2-HA in *S. typhimurium* cell lysates and in the supernatant in a dose-dependent manner (**Fig. 3.5A**). The decreased level of secretion correlates with the inhibition of protein expression observed in the cell lysate. The inhibitory activity of H-89 can also be readily observed visually with the SopE2-CPG2-HA system (**Fig. 3.5B**).

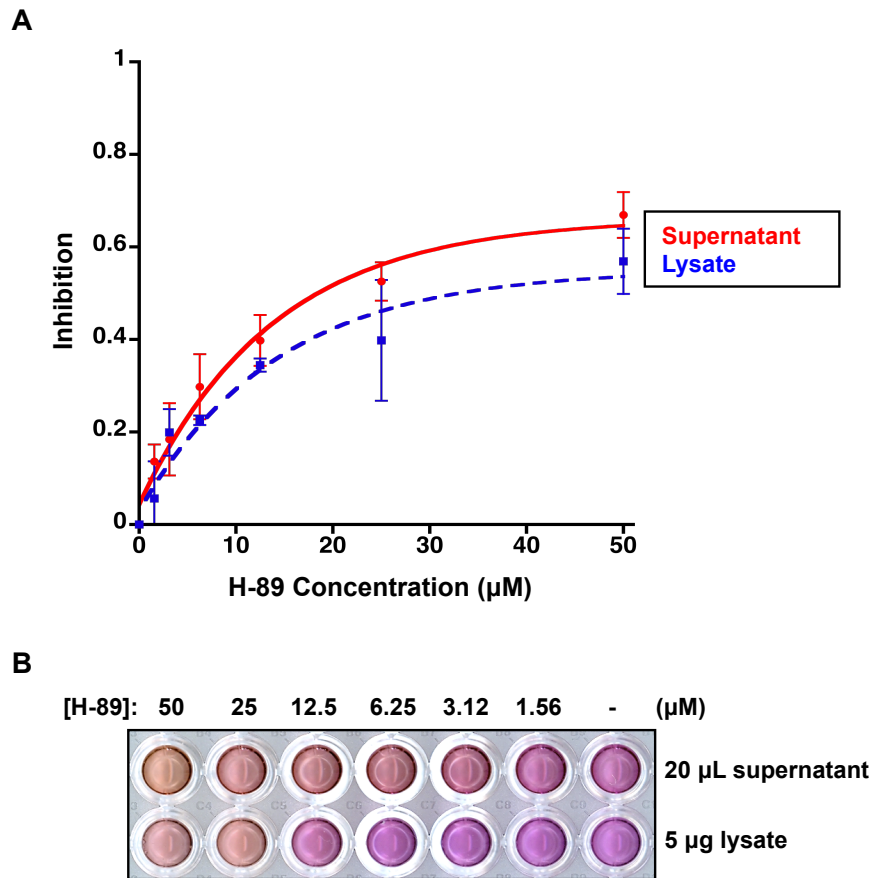


Figure 3.5 H-89's decrease of secreted effectors correlates with inhibition of expression. **A)** SopE2-CPG2-HA secretion and expression were monitored using a fluorescent readout from the supernatant and lysate, respectively. Samples incubated with H-89 were compared to a DMSO control. **B)** Visual color change in the supernatant and lysate samples from bacteria incubated with H-89.

I then evaluated the effect of H-89 on endogenously expressed SPI-1 effectors that are secreted in *S. typhimurium* growth media. Coomassie staining of *S. typhimurium* effector proteins secreted into the culture supernatant demonstrated that H-89 reduced the amount of secreted SPI-1 effector proteins while the inactive analog H-88 had no effect

(**Fig. 3.6A**). Other Akt-selective inhibitors (MK2206 and Akti1/2) [128,131,132] and another compound reported to prevent bacterial replication and inhibit Akt (AR-12) [133] had no activity towards inhibiting SPI-1 effector protein secretion (**Fig. 3.6A**). Additional broad-spectrum host kinase inhibitors (rottlerin and Sutent) [132,134] likewise did not affect secretion of SPI-1 effector proteins (**Fig. 3.6B**). The inhibitory activity of H-89 was dose-dependent up to a concentration that had no effect on bacterial growth and was more potent than the previously reported T3SS inhibitor INP-0007 [48,71] (**Fig. 3.7**).

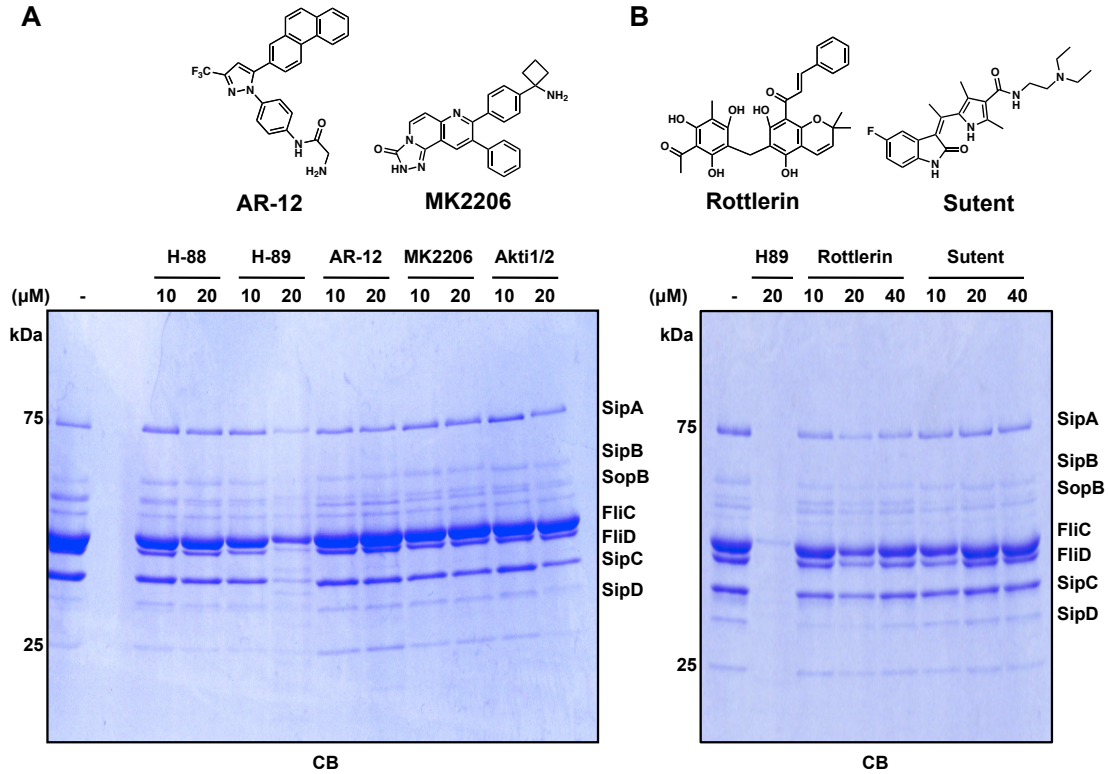


Figure 3.6 Levels of secreted SPI-1 effectors in bacterial culture supernatants. A, B) Bacteria were incubated with compound for 4 hours before secreted proteins were precipitated, separated by SDS-PAGE, and analyzed by Coomassie blue (CB) staining.

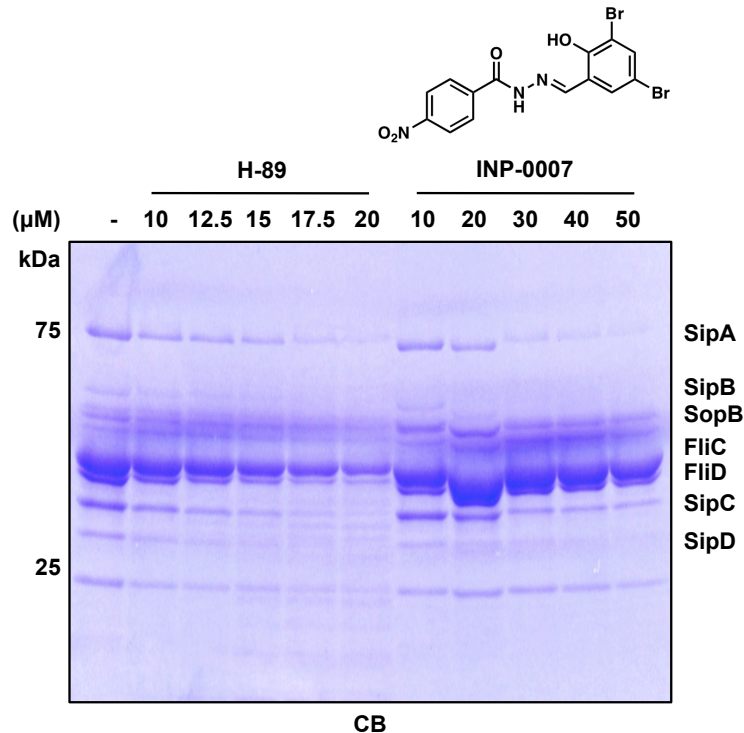


Figure 3.7 Dose-dependent decrease of secreted SPI-1 effectors. Bacteria were grown for four hours in the presence of compound before proteins precipitated from the culture supernatant were separated by SDS-PAGE and analyzed by Coomassie blue (CB) staining. H-89's potency was compared to the previously reported T3SS inhibitor INP-0007.

To determine whether this pharmacological reduction of secreted SPI-1 effectors could attenuate infection, I evaluated the effect of H-89 on *S. typhimurium* invasion of an epithelial cell line. Flow cytometry with anti-*Salmonella* antibody staining was used to quantify the number of *S. typhimurium*-infected cells (**Fig. 3.8**). Consistent with the reduction of SPI-1 effector data (**Fig. 3.3A** and **3.6A**), incubation of *S. typhimurium* with H-89 also inhibited *S. typhimurium* invasion of HeLa cells, whereas H-88 had no

significant effect (**Fig. 3.8**). These results demonstrate that H-89 can also inhibit SPI-1 T3SS function and attenuate *S. typhimurium* entry into epithelial cell lines.

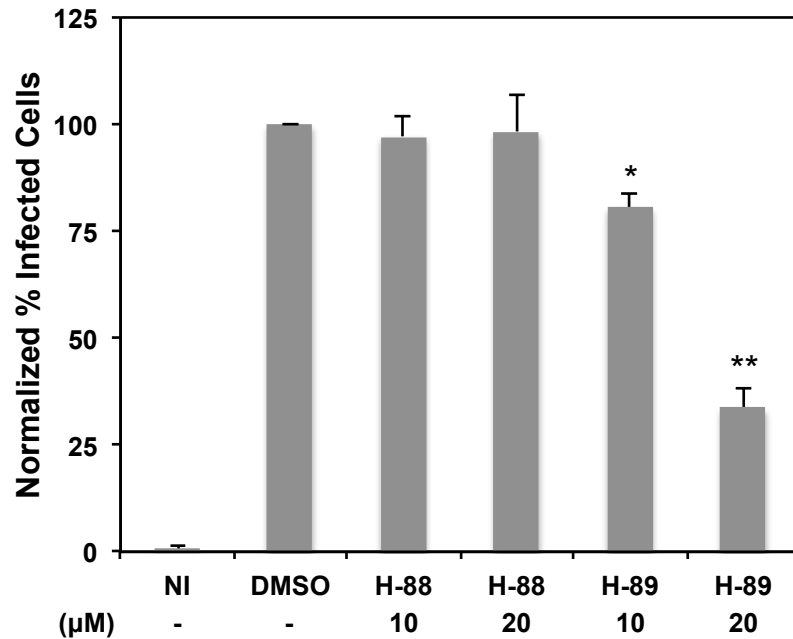


Figure 3.8 H-89 blocks *S. typhimurium* invasion of HeLa cells. HeLa cells were infected at an MOI of 10 for 30 minutes with *Salmonella* that was grown in the presence of compound. Experiments were done in triplicate and the number of infected cells was measured using flow cytometry. NI, not infected. The statistical values from a two-sided Student's t-test are as follows: *, $P < 0.01$; **, $P < 0.0001$.

Discussion

Bacterial pathogens continue to be a global health problem, which necessitates new strategies and antibacterials to combat infections. With the emergence of more antibiotic-resistant bacterial strains, targeting host pathways and bacterial virulence

mechanisms have become attractive strategies for counteracting and limiting drug resistance [1,2]. As host kinases are often hijacked for bacterial infection, the repurposing of kinase inhibitors may be an effective starting point for identifying new antibacterials [135,136]. Indeed, a chemical and siRNA screen against host kinases by Kuijl et al. has suggested the Akt kinase network may provide viable targets for limiting bacterial replication in host cells and even demonstrated that H-89, a reported PKA-inhibitor can block *Salmonella* and *Mycobacteria* replication in macrophages [124,137]. However, this study also reported that a more potent and specific Akt-inhibitor had less of an effect on bacterial replication [124]. Additionally, other H-89 analogs significantly inhibited *Salmonella* replication with only a small effect on Akt activity [124], suggesting Akt is not the primary target of H-89 to inhibit bacterial replication. Consistent with these observations, I found that H-89 is about 30-40 times more effective than an Akt-specific inhibitor (Akti1/2) at preventing *Salmonella* replication in macrophages (**Fig. 3.2B**) even though Akti1/2 completely depletes the active population of Akt (**Fig. 3.2C**). This demonstrates that pharmacological inhibition of Akt does not account for H-89's activity on bacterial replication. Taken together, these data suggest an alternative mechanism of action for H-89 on inhibition of bacterial replication.

As bacterial pathogens like *Salmonella* turn on specific virulence pathways for infection that are not required for growth *in vitro*, we evaluated whether H-89 impairs *Salmonella* virulence mechanisms. We initially focused on T3SSs since these protein secretion systems are essential for establishing and propagating *Salmonella* infection [99]. Our targeted transcriptional profiling data demonstrated that H-89 decreased the expression of genes associated with *Salmonella* virulence, including T3SS factors

responsible for bacterial invasion and replication, while genes involved in redox or iron homeostasis were not significantly affected (**Fig. 3.3A**). I further validated the impact of H-89 on *S. typhimurium* virulence factors by demonstrating this brominated isoquinolinesulfonamide impairs the expression (**Fig. 3.3B**) and consequently the secretion of a SPI-2 effector (SseJ) during bacterial infection of macrophages (**Fig. 3.4**).

In addition to SPI-2 components responsible for *Salmonella* replication in host cells, H-89 reduced the expression of SPI-1 T3SS components associated with bacterial invasion (**Fig. 3.3A**). Notably, H-89 also diminished the secreted levels of SPI-1 effectors into the bacterial culture media, whereas the inactive analog H-88, Akt-specific inhibitors, and other promiscuous kinase inhibitors had no effect (**Fig. 3.6A** and **3.6B**). H-89 was also slightly more potent than the previously described T3SS inhibitor INP-0007 (**Fig. 3.7**) and effectively blocked *S. typhimurium* invasion of epithelial cells (**Fig. 3.8**). Taken together, our results demonstrate that while H-89 does not affect bacterial growth, it inhibits key virulence pathways in *Salmonella*. By inhibiting the expression of virulence factors involved in both the initial and later stages of infection, H-89 can prevent the T3SS-dependent invasion and replication of *S. typhimurium*. Disrupting bacterial virulence rather than inhibiting Akt more likely explains the activity of H-89 on bacterial replication.

CHAPTER 4 – Discussion and Future Outlook

Developing anti-virulence compounds as an alternative to traditional antibiotics is an attractive and promising strategy to combat the emerging antibiotic resistance we are experiencing today [1,2]. The rate at which new antibiotic resistance is observed is alarming compared to development of new antibiotics. If we were to continue on this path, we would be at risk of reverting to a pre-antibiotic era, which would be devastating to human health. Therefore, it is necessary to develop alternative approaches to circumvent this pressing issue. An anti-virulence strategy that specifically targets pathogenic bacteria falls into this category and also has the added benefit of leaving the normal commensal microbiota largely intact. As we learn more about the relationship between commensal bacteria and humans, we are realizing their importance in preventing infection and stimulating the immune response [5,7]. It is also hypothesized that anti-virulence compounds would apply less selective pressure for developing resistance, so this could be a longer-term solution for battling bacterial pathogens. Support for this claim comes from the fact that resistance is often transferred from commensals to pathogens via horizontal gene transfer [3]. Resistance mechanisms develop due to random mutations that yield a competitive advantage and are thus selected for, but since the commensals would be generally unaffected by virulence inhibitors, they would be less likely to aid the pathogenic bacteria in evolving resistance. The current state of antibiotics emphasizes the need for alternative approaches to keep bacterial pathogens at bay, and the advantages of targeting virulence mechanisms make it a promising strategy moving forward.

The discovery of T3SSs as essential mechanisms of bacterial virulence has provided important and exciting targets for antibacterial development to address the shrinking arsenal of antibiotics. Consequently, many new classes of small molecules have been reported with inhibitory activity against T3SSs (**Tables 1.1-1.3**). Despite the attractiveness of these potential anti-virulence compounds, none of the currently reported T3SS inhibitors have advanced into the clinic. Major challenges still need to be addressed before these compounds can be effective therapeutics. Notably, nearly all of the T3SS inhibitors discovered from HTS cell-based assays have limited potency and lack clear targets and mechanisms of action. For example, the preliminary studies of previously described salicylidene acylhydrazides and thiazolidinones yielded structural features for blocking the activity of T3SSs, but none of ~120 new analogs yielded more potent inhibitors. Even though tethered thiazolidinone derivatives [78] and peptide-functionalized analogs [77] have yielded improved inhibitory activity towards T3SS-mediated invasion *in vitro*, the activity of more potent second generation thiazolidinones (~56) in cell culture or animal models of bacterial infection have not been reported.

Anti-virulence compounds present a unique problem for identifying the targets of these antibacterial compounds. Since they do not kill bacteria directly, the standard antibiotic resistance selection strategy does not apply; bacterial viability needs to be dependent on resistance. A potential alternative for target identification of anti-virulence compounds is an infection-based selection strategy. Mutagenizing the bacteria and infecting cells in the presence of compound could be a way to tie bacterial viability to some level of resistance. If the compound is used at a high enough concentration where only a small percent of bacteria survive, those bacteria can be plated and used to re-infect

another batch of cells. Over several rounds of serial infections, any competitive advantage that exists will be selected for, and a decrease in the compound's efficacy would be observed. Repeating the infections and increasing the compound's concentration will apply more pressure to develop resistance, and should resistant colonies arise, they could be sequenced to uncover the mutation(s) that confer resistance. This strategy is unlikely to work with compounds that have multiple targets, so compounds exhibiting polypharmacological effects might not be suitable for such an approach.

The salicylidene acylhydrazides were the first class of compounds discovered to inhibit type III secretion [48]. Being active against several Gram-negative pathogens made them an appealing class of anti-virulence compounds, and though several groups have studied them, no clear mechanism exists for how they exert their inhibition. We took a bioorthogonal approach to identify their target(s) and mechanism of action. By inserting an alkyne onto the part of the molecule tolerant to modification, we made a panel of bioorthogonal derivatives that taught us about the SAR of this class and provided us with several negative controls for follow-up assays. Similar to the study by Wang et al. [63], we pulled down many metabolic enzymes (**Table 2.2**) using our labeling and enrichment strategy, which could suggest that the mechanism is due to a polypharmacological effect that disrupts metabolism and dis-regulates virulence without affecting growth. We learned that the SAHs have an inherent covalent reactivity, but subsequent experiments cast doubt on the relevance of the covalent-binding partners' role in inhibiting type III secretion. This is important to keep in mind when thinking about their potential clinical application and possible side effects.

In general, I believe bioorthogonal labeling is a powerful method and can be an effective strategy for target ID, but there are several things to keep in mind when using this approach (**Fig. 1.6**). First, it is very useful for identifying the covalent-binding partners of a small molecule – non-covalent interactions require a different workflow. Ideally, the compound of interest would have a small number of protein-binding partners to simplify the analysis and limit the number of potential targets. Another important aspect is the necessity for negative controls. Though this is not exclusive to bioorthogonal labeling strategies, they are essential for ruling out non-specific interactions and were a key component of my studies with the SAHs.

Another issue that arises for inhibitors of T3SSs is that they need to be effective at several stages of infection and be able to reach the relevant compartments. For example, *Salmonella typhimurium* has two stages of infection, the initial invasion stage and the subsequent replication stage, and both require a T3SS [99]. Once the bacteria successfully invade host cells, they reside in the SCV while replicating and spreading. It is quite possible that compounds can antagonize T3S activity in culture but are unable to reach the bacteria during infection or only inhibit the initial stage of infection. Many of the compounds discovered thus far are from HTSs that specifically look for inhibitors of this first stage of T3S. While setting up a HTS of this nature is easier, in a clinical setting, this would not be the relevant phase to be targeting. For example, the SAHs inhibit only the initial stage of infection and for the most part require pre-incubation to see an inhibitory effect, so from a clinical perspective, they might not be as useful. While T3SS inhibitors present promising leads for antibacterial development, significant improvements in their potency are needed for clinical studies.

Beyond *in vitro* screening of T3SS inhibitors, the analysis of small molecules that inhibit bacterial virulence in more complex cell culture systems or animals could reveal new classes of compounds and also begin to address their activity on host cells. For enteric pathogens, it will be interesting to assay compounds targeting the bacterial replication cycles in mammalian cells. These compounds may serve as better drug candidates to treat systemic infection rather than anti-virulence compounds that may only be used to prevent infection. Alternatively, analysis of compounds in small animal models such as worms [138-140] and zebrafish [141] are already beginning to reveal potential anti-virulence inhibitors as well as potential mechanisms of drug tolerance. While this approach may yield compounds that activate host immunity [142], this strategy may already select for compounds that can access the appropriate sites and tissues relevant for bacterial infection *in vivo* and provide promising leads for clinical development in humans.

The isoquinolinesulfonamide H-89 is an example of a compound that was discovered in a screen using an infection setting [124]. The goal of the study was to find compounds that block *Salmonella* replication during infection. The authors attributed the activity of H-89 on bacterial replication to inhibition of the host kinase Akt. In agreement with our findings, they also reported that a more potent and specific Akt inhibitor did not have the same inhibitory effect as H-89, but they believed it was because H-89 targeted other host kinases. Since they had only shown H-89 does not affect the growth of the bacteria in culture, we examined whether H-89 affects the virulence properties of the bacteria. Our data show that H-89 down-regulates genes involved in bacterial virulence and impairs the T3SS-dependent invasion and subsequent replication stages of infection.

We believe this is responsible for the increased potency of H-89 compared to Akt-specific inhibitors and is the relevant mechanism for its antibacterial effects. In conclusion, the isoquinolinesulfonamide H-89 primarily acts on bacterial virulence pathways rather than host kinases to inhibit infection and represents a new chemical scaffold for the development of anti-virulence compounds.

Future avenues for H-89 are to synthesize analogs that have limited Akt inhibition while retaining their antibacterial effects, find its targets in *Salmonella*, and investigate its effects on bacterial transcription. Since Akt is part of a major host kinase network, it would be desirable to find effective analogs that do not affect host cell signaling. Based on structural and SAR studies, it was shown that the nitrogen in the isoquinoline ring is essential for kinase binding and inhibition of Akt [143,144]. Analogues with modifications here should display decreased Akt inhibition while perhaps maintaining antibacterial activity. The obvious potential pitfall is that H-89's activity in the bacteria could be due to kinase inhibition, so modifying the isoquinoline ring could render the compound inactive. Discovering the bacterial targets of H-89 by non-covalent pull-downs would shed light on its mechanism and potentially uncover a kinase or kinase network involved in virulence regulation. My studies have laid the groundwork for using H-89 as a tool compound for studying bacterial virulence mechanisms in *Salmonella*. By impairing the T3SS-dependent stages of infection without affecting growth, H-89 represents a new chemical scaffold for the development of more potent and selective anti-infectives. Gaining a better understanding of what H-89 targets, how it affects bacterial transcription, and the broader effects it has on gene expression could provide an additional point of intervention for inhibiting bacterial virulence.

Classically, antimicrobials are small molecules that act as antibiotics to kill bacteria directly. Due to the increased frequency of antibiotic-resistant strains and with more knowledge of bacterial pathogenesis, targeting virulence pathways required for bacterial infection has become an alternative strategy for antimicrobial development. Two potential benefits are that targeting bacterial pathogenesis as opposed to viability could make it more difficult for bacteria to develop resistance while preserving the normal host microbiota. Key virulence mechanisms of many bacterial pathogens like T3SSs have now been uncovered and are prime targets for chemical intervention. Potent and specific T3SS inhibitors with validated mechanisms of action are still needed to establish whether this conserved virulence pathway is indeed a druggable target and viable approach towards disarming clinically relevant bacterial pathogens. Many of the virulence factors are essential for causing human diseases but are dispensable for the growth of pathogens, complicating efforts towards identifying the targets of virulence inhibitors. It remains to be determined whether the use of anti-virulence compounds would exert less selective pressure on bacterial pathogens to develop drug resistance as well as preserve beneficial microbiota *in vivo*; however, given the current state of antibacterials, the potential benefits are worth the effort. It is possible that inhibitors of bacterial virulence could slow the spread of infection and be used in conjunction with traditional antibiotics [145]. A focused effort on inhibitors of bacterial virulence could address these major challenges in antibacterial drug discovery and help combat microbial infections that impact human health.

CHAPTER 5 – Materials and Methods

Compounds

Most commercially available compounds were purchased from Sigma Aldrich, Fisher Scientific, Alfa Aesar, or Fluka. All final compounds were stored in 20 mM stock solutions in DMSO. Reactions were monitored by thin layer chromatography (TLC). Products were purified by flash column chromatography (FCC). Nuclear magnetic resonance (NMR) spectra were recorded on either a 400 or 600 MHz Bruker spectrometer. Chemical shifts are reported in ppm from tetramethylsilane. Coupling constants are reported as *J* values in Hertz (Hz). Mass spectra were obtained on a MALDI-TOF spectrometer or by LC-MS, performed by The Rockefeller University Proteomics Resource Center. Akti1/2 and MK2206 were gifts from N. Rosen (Memorial Sloan-Kettering Cancer Center).

5.1 Synthesis of T3SS inhibitor INP-0007 (2.1)

INP-0007 was synthesized according to published procedure [121].

4-nitrobenzohydrazide (2.3)

To 15 mL of EtOH was added p-nitrobenzoate (2 g, 10.2 mmol) and hydrazine monohydrate (2.5 mL, 41 mmol). The mixture was refluxed at 80 °C overnight. The

precipitate was collected and washed with water to yield **2.3** as a yellowish solid (1.5 g, 80%).

^1H NMR (600 MHz, CDCl_3): δ = 4.18 (s, 2H), 7.40 (s, 1H), 7.94 (d, 2H, J = 8.7 Hz), 8.34 (d, 2H, J = 8.7 Hz).

***N'*-(3,5-dibromo-2-hydroxybenzylidene)-4-nitrobenzohydrazide (INP-0007) (2.1)**

To a 1:2 mixture of EtOH and water (2 mL) was added **2.3** (50 mg, 0.28 mmol). In 2 mL of EtOH was dissolved 3,5-dibromosalicylaldehyde (85 mg, 0.30 mmol). This mixture was added to **2.3** and stirred at room temperature until the reaction was complete. The product was filtered and washed with water, EtOH, and ether before recrystallization in ether to give **INP-0007** as a yellow solid (100 mg, 82%).

^1H NMR (600 MHz, DMSO-d_6): δ = 7.86 (s, 2H), 8.19 (d, 2H, J = 8.6 Hz), 8.40 (d, 2H, J = 8.6 Hz), 8.57 (s, 1H). MALDI-TOF calcd for $\text{C}_{14}\text{H}_{10}\text{Br}_2\text{N}_3\text{O}_4$ $[\text{M}+\text{H}]^+$ 441.90, found 441.92.

5.2 Synthesis of photocrosslinking-alkynyl-INP (PC-alk-INP) (2.2)

The synthetic route up to the final coupling step was performed as previously described [122].

2-(prop-2-yn-1-yloxy)ethan-1-ol (2.4)

^1H NMR (600 MHz, CDCl_3): δ = 2.49 (t, 1H, J = 2.3 Hz), 3.68-3.69 (m, 2H), 3.79-3.80 (m, 2H), 4.24 (d, 2H, J = 2.3 Hz).

2-(prop-2-yn-1-yloxy)ethyl 4-methylbenzenesulfonate (2.5)

^1H NMR (600 MHz, CDCl_3): δ = 2.45 (t, 1H, J = 2.3 Hz), 2.47 (s, 3H), 3.75 (d, 2H, J = 4.7 Hz), 4.14 (d, 2H, J = 2.3 Hz), 4.21 (d, 2H, J = 4.7 Hz), 7.36 (d, 2H J = 8.2 Hz), 7.82 (d, 2H, J = 8.2 Hz).

2,2,2-trifluoro-1-(3-methoxyphenyl)ethan-1-one (2.6)

^1H NMR (600 MHz, CDCl_3): δ = 3.90 (s, 3H), 7.28 (m, 1H), 7.48 (t, 1H, J = 8.0 Hz), 7.68 (s, 1H), 7.69 (d, 1H, J = 7.8 Hz).

2,2,2-trifluoro-1-(3-methoxyphenyl)ethan-1-one oxime (2.7)

^1H NMR (600 MHz, CDCl_3): δ = 3.85 (s, 3H), 7.04-7.11 (m, 3H), 7.40 (t, 1H, J = 7.5 Hz), 8.85 (s, 1H).

2,2,2-trifluoro-1-(3-methoxyphenyl)ethan-1-one *O*-tosyl oxime (2.8)

^1H NMR (600 MHz, CDCl_3): δ = 2.48 (s, 3H), 3.83 (s, 3H), 6.94-7.07 (m, 3H), 7.34-7.40 (m, 3H), 7.89-7.93 (m, 2H).

3-(3-methoxyphenyl)-3-(trifluoromethyl)diaziridine (2.9)

^1H NMR (600 MHz, CDCl_3): δ = 2.25 (d, 1H, J = 8.4 Hz), 2.80 (d, 1H, J = 8.4 Hz), 3.85 (s, 3H), 6.99 (d, 1H, J = 8.3 Hz), 7.17 (s, 1H), 7.22 (d, 1H, J = 7.6 Hz), 7.36 (t, 1H, J = 8.0 Hz).

3-(3-methoxyphenyl)-3-(trifluoromethyl)-3*H*-diazirine (2.10)

¹H NMR (600 MHz, CDCl₃): δ = 3.83 (s, 3H), 6.71 (s, 1H), 6.79 (d, 1H, *J* = 7.7 Hz), 6.96 (d, 1H, *J* = 8.3 Hz), 7.33 (t, 1H, *J* = 8.0 Hz).

2-methoxy-4-(3-(trifluoromethyl)-3*H*-diazirin-3-yl)benzaldehyde (2.11)

¹H NMR (600 MHz, CDCl₃): δ = 3.94 (s, 3H), 6.70 (s, 1H), 6.84 (d, 1H, *J* = 8.2 Hz), 7.83 (d, 1H, *J* = 8.2 Hz), 10.4 (s, 1H).

2-hydroxy-4-(3-(trifluoromethyl)-3*H*-diazirin-3-yl)benzaldehyde (2.12)

¹H NMR (600 MHz, CDCl₃): δ = 6.80-6.82 (m, 2H), 7.62 (d, 1H, *J* = 8.1 Hz), 9.95 (s, 1H), 11.08 (s, 1H).

2-(2-(prop-2-yn-1-yloxy)ethoxy)-4-(3-(trifluoromethyl)-3*H*-diazirin-3-yl)benzaldehyde (2.13)

¹H NMR (600 MHz, CDCl₃): δ = 2.49 (t, 1H, *J* = 2.3 Hz), 3.97-3.99 (m, 2H), 4.26-4.29 (m, 4H), 6.77 (s, 1H), 6.86 (d, 1H, *J* = 12.3 Hz), 7.86 (d, 1H, *J* = 12.3 Hz), 10.51 (s, 1H).

2-(2-(prop-2-yn-1-yloxy)ethoxy)-4-(3-(trifluoromethyl)-3*H*-diazirin-3-yl)benzoic acid (2.14)

¹H NMR (600 MHz, CDCl₃): δ = 2.52 (t, 1H, *J* = 2.3 Hz), 4.01 (t, 2H, *J* = 4.4 Hz), 4.29 (d, 2H, *J* = 2.3 Hz), 4.43 (t, 2H, *J* = 4.4 Hz), 6.82 (s, 1H), 6.97 (d, 1H, *J* = 8.2 Hz), 8.22 (d, 1H, *J* = 8.2 Hz), 10.6 (br. s, 1H).

2,4-dibromo-6-(hydrazonomethyl)phenol (2.15)

To a mixture of 3,5-dibromosalicylaldehyde (2 g, 7.15 mmol) cooled to 0°C in 7.5 mL EtOH was added hydrazine monohydrate (1.8 mL, 28.6 mmol). The mixture was stirred for 1.5 hours as it was allowed to warm to room temperature. The solid was filtered, washed with EtOH, water, and ether and dried to yield crude **2.15** in quantitative yield.

¹H NMR (600 MHz, CDCl₃): δ = 5.64 (s, 2H), 7.20 (s, 1H), 7.60 (s, 1H), 7.76 (s, 1H).

***N'*-(3,5-dibromo-2-hydroxybenzylidene)-2-(2-(prop-2-yn-1-yloxy)ethoxy)-4-(3-(trifluoromethyl)-3*H*-diazirin-3-yl)benzohydrazide (PC-alk-INP) (2.2)**

In 1 mL dry DCM was added **2.14** (50 mg, 0.15 mmol), oxalyl chloride (262 μL, 3.0 mmol), and 1 drop of DMF. This solution was stirred at room temperature for 1 hour before being rotovapped. DCM was added and again rotovapped off. This was repeated 2 more times to remove all excess oxalyl chloride. In 1 mL of DCM was dissolved **2.15** (67.6, 0.23 mmol), and this was added to the acid chloride. To this mixture was slowly added 6 drops of triethylamine. The reaction was stirred at room temperature overnight and then washed with 10% HCl and brine before being dried over magnesium sulfate, filtered, and concentrated. The crude product was purified by FCC in 1:1 ethyl acetate:DCM to yield **PC-alk-INP** (20 mg, 22%).

¹H NMR (600 MHz, CDCl₃): δ = 3.42 (t, 1H, *J* = 2.5 Hz), 3.85 (t, 2H, *J* = 4.2 Hz), 4.25 (d, 2H, *J* = 2.5 Hz), 4.33 (t, 2H, *J* = 4.2 Hz), 6.92 (s, 1H), 7.79 (d, 1H, *J* = 2.4 Hz), 7.83 (s, 1H), 7.84 (s, 1H), 7.86 (d, 1H, *J* = 2.4 Hz), 8.38 (s, 1H). ¹³C NMR (100 MHz, DMSO-*d*₆): δ = 31.2, 58.1, 78.0, 80.6, 80.8, 110.9, 118.8, 121.3, 124.7, 132.5, 132.7, 133.9,

134.1, 138.3, 138.4, 147.6, 154.1, 157.0, 161.6. LC-MS calcd for $C_{21}H_{15}Br_2F_3N_4O_4$ $[M+H]^+$ 602.94, found 602.97.

5.3 Synthesis of inactive SAH analog

N'-benzylidene-4-nitrobenzohydrazide (SAH-1) (2.16)

To a solution of 4-nitrobenzoylhydrazide (**3**) (362 mg, 2 mmol) in 33% ethanol (4 mL) was added benzaldehyde (206 μ L, 2.04 mmol) dissolved in 0.5 mL ethanol. The mixture was stirred for one hour at room temperature before the yellow precipitate was filtered and washed with cold water, EtOH, and ether to yield the product as a yellow solid (442 mg, 82%).

1H NMR (600 MHz, DMSO- d_6): δ = 7.49 (m, 3H), 7.76 (d, 2H, J = 6.7 Hz), 8.16 (d, 2H, J = 8.6 Hz), 8.39 (d, 2H, J = 8.6 Hz), 8.48 (s, 1H). ^{13}C NMR (150 MHz, DMSO- d_6): δ = 124.1, 127.7, 129.4, 129.7, 130.8, 134.6, 139.7, 149.4, 149.7, 162.0. MALDI-TOF calcd for $C_{14}H_{12}N_3O_3$ $[M+H]^+$ 270.08, found 270.40.

5.4 Synthesis of alkynyl SAHs

ethyl 4-(prop-2-yn-1-yloxy)benzoate (2.19)

To p-Ethyl-hydroxy benzoate (1.5 g, 9 mmol) was added 50 mL of dry DMF. This solution was cooled to 0 $^{\circ}C$ before potassium carbonate (1.9 g, 13.5 mmol) was added. This mixture was stirred for 30 minutes before propargyl bromide (3.01 mL, 27 mmol)

was added. The solution was warmed to room temperature and stirred for 3 hours. Once the reaction was complete, ethyl acetate was added, and the solution was washed with 1 N HCl and brine before being dried over magnesium sulfate and concentrated. The product was purified by flash column chromatography (FCC) in hexanes:ethyl acetate to give **2.19** (1.7 g, 95 %) as a yellow oil.

^1H NMR (600 MHz, CDCl_3): δ = 1.40 (t, 3H, J = 7.1 Hz), 2.57 (t, 1H, J = 2.4 Hz), 4.37 (q, 2H, J = 7.1 Hz), 4.77 (d, 2H, J = 2.4 Hz), 7.01 (d, 2H, J = 8.8 Hz), 8.04 (d, 2H, J = 8.8 Hz).

4-(prop-2-yn-1-yloxy)benzoic acid (2.20)

2.19 (250 mg, 1.22 mmol) was dissolved in a 1:1 mixture of THF and water (3 mL: 3 mL). To this was added sodium hydroxide (122 mg, 3.05 mmol), and the solution was heated at 60 °C overnight. Upon completion, the THF was evaporated, ethyl acetate was added, and the mixture was washed with 10 % HCl. The solution was dried with magnesium sulfate and concentrated to give **2.20** (210 mg, 97 %) as a white solid.

^1H NMR (600 MHz, CDCl_3): δ = 2.57 (t, 1H, J = 2.4 Hz), 4.78 (d, 2H, J = 2.4 Hz), 7.04 (d, 2H, J = 13.3 Hz), 8.08 (d, 2H, J = 13.3 Hz).

***tert*-butyl 2-(4-(prop-2-yn-1-yloxy)benzoyl)hydrazine-1-carboxylate (2.21)**

PyBOP (162 mg, 0.31 mmol), BOC-hydrazine (41 mg, 0.31 mmol), and **2.20** (50 mg, 0.28 mmol) were dissolved in 3 mL of DMF. To this was added DIEA (98 μL , 0.56 mmol), and the reaction was stirred overnight at room temperature. Upon completion, ethyl acetate was added, and the solution was washed with 10 % HCl, sodium

bicarbonate, and brine before being dried over magnesium sulfate and concentrated to give the crude product **2.21**, which was carried through to the next step.

^1H NMR (600 MHz, CDCl_3): δ = 1.48 (s, 9H), 2.52 (t, 1H, J = 2.3 Hz), 4.72 (d, 2H, J = 2.3 Hz), 6.99 (d, 2H, J = 8.7 Hz), 7.76 (d, 2H, J = 8.7 Hz).

4-(prop-2-yn-1-yloxy)benzohydrazide (2.22)

Crude **2.21** (1g, ~3.4 mmol) was added to 18 mL of dry DCM. This mixture was cooled to 0 °C and to it was added 8 mL of TFA, at which point the reaction bubbled. As the solution warmed to room temperature, it turned from yellow to orange. The solvent was evaporated, and the product was resuspended in ethyl acetate, washed with sodium bicarbonate, dried over magnesium sulfate, and concentrated. The product was purified by FCC with hexanes:ethyl acetate to yield **2.22** (430 mg, 79 % over 2 steps).

^1H NMR (600 MHz, CDCl_3): δ = 2.52 (t, 1H, J = 2.4 Hz), 4.72 (d, 2H, J = 2.4 Hz), 7.01 (d, 2H, J = 8.8 Hz), 7.71 (d, 2H, J = 8.8 Hz).

The final coupling step for synthesizing INP-0007 was also used to synthesize the alkynyl SAH analogs. In general, **2.22** (25 mg, 0.13 mmol) was dissolved in a 2 mL mixture of 33% EtOH in water. The corresponding aldehyde (0.14 mmol) was dissolved in 1 mL of EtOH and added to the solution containing **2.22**. The solution was stirred at room temperature until compound crashed out of solution. The precipitate was collected and washed with water, cold EtOH, and ether before being dried and recrystallized from EtOH (81-92% yield).

***N'*-(3,5-dibromo-2-hydroxybenzylidene)-4-(prop-2-yn-1-yloxy)benzohydrazide**

(alk-INP) (2.17)

¹H NMR (400 MHz, DMSO-d₆): δ = 3.63 (t, 1H, *J* = 2.3 Hz), 4.91 (d, 2H, *J* = 2.3 Hz), 7.13 (d, 2H, *J* = 8.9 Hz), 7.81 (s, 1H), 7.81 (s, 1H), 7.94 (d, 2H, *J* = 8.9 Hz), 8.51 (s, 1H). ¹³C NMR (100 MHz, DMSO-d₆): δ = 56.1, 79.1, 79.2, 110.8, 111.6, 115.3, 121.5, 125.4, 130.1, 132.5, 132.7, 136.0, 147.1, 154.1, 160.8, 162.9. LC-MS: calcd for C₁₇H₁₂Br₂N₂O₃ [M+H]⁺ 450.92, found 451.00.

***N'*-benzylidene-4-(prop-2-yn-1-yloxy)benzohydrazide (alk-SAH) (2.18)**

¹H NMR (400 MHz, DMSO-d₆): δ = 3.58 (t, 1H, *J* = 2.3 Hz), 4.87 (d, 2H, *J* = 2.3 Hz), 7.07 (d, 2H, *J* = 8.6 Hz), 7.41 (m, 3H), 7.68 (d, 2H, *J* = 6.4 Hz), 7.87 (d, 2H, *J* = 8.6 Hz), 8.41 (s, 1H). ¹³C NMR (100 MHz, DMSO-d₆): δ = 55.9, 78.6, 79.2, 115.2, 125.9, 127.6, 127.9, 129.3, 129.9, 130.1, 131.0, 134.3, 148.9, 160.4, 164.1. LC-MS: calcd for C₁₇H₁₄N₂O₂ [M+H]⁺ 279.11, found 279.17.

***N'*-(2-hydroxybenzylidene)-4-(prop-2-yn-1-yloxy)benzohydrazide (alk-OH) (2.23)**

¹H NMR (400 MHz, DMSO-d₆): δ = 3.63 (t, 1H, *J* = 1.3 Hz), 4.91 (d, 2H, *J* = 2.3 Hz), 6.93 (m, 2H), 7.12 (d, 2H, *J* = 8.4 Hz), 7.29 (m, 1H), 7.52 (d, 1H, *J* = 7.6 Hz), 7.93 (d, 2H, *J* = 8.4 Hz), 8.62 (s, 1H). ¹³C NMR (100 MHz, DMSO-d₆): δ = 56.1, 79.1, 79.3, 115.1, 116.8, 119.2, 119.7, 126.0, 129.9, 130.1, 131.7, 148.3, 157.9, 160.5, 162.7. LC-MS: calcd for C₁₇H₁₄N₂O₃ [M+H]⁺ 295.10, found 295.17.

***N'*-(5-bromo-2-hydroxybenzylidene)-4-(prop-2-yn-1-yloxy)benzohydrazide**

(alk-5'Br) (2.24)

¹H NMR (400 MHz, DMSO-d₆): δ = 3.62 (t, 1H, *J* = 2.1 Hz), 4.90 (d, 2H, *J* = 2.1 Hz), 6.89 (d, 1H, *J* = 8.8 Hz), 7.11 (d, 2H, *J* = 8.7 Hz), 7.43 (d, 1H, *J* = 8.8 Hz), 7.78 (s, 1H), 7.93 (d, 2H, *J* = 8.7 Hz), 8.59 (s, 1H). ¹³C NMR (100 MHz, DMSO-d₆): δ = 56.1, 79.1, 79.3, 110.9, 115.2, 119.1, 121.8, 125.9, 130.1, 130.9, 131.1, 133.9, 145.8, 156.9, 160.6, 162.8. LC-MS: calcd for C₁₇H₁₃BrN₂O₃ [M+H]⁺ 373.01, found 373.08.

***N'*-(4-bromo-2-hydroxybenzylidene)-4-(prop-2-yn-1-yloxy)benzohydrazide**

(alk-4'Br) (2.25)

¹H NMR (400 MHz, DMSO-d₆): δ = 3.62 (t, 1H, *J* = 2.3 Hz), 4.90 (d, 2H, *J* = 2.3 Hz), 7.10-7.14 (m, 4H), 7.52 (d, 1H, *J* = 8.3 Hz), 7.92 (d, 2H, *J* = 8.4 Hz), 8.60 (s, 1H). ¹³C NMR (100 MHz, DMSO-d₆): δ = 56.1, 79.1, 79.2, 79.3, 115.2, 119.0, 119.5, 119.6, 122.9, 124.2, 126.0, 129.9, 130.1, 130.9, 131.0, 146.6, 158.5, 160.5, 162.7. LC-MS: calcd for C₁₇H₁₃BrN₂O₃ [M+H]⁺ 373.01, found 373.08.

***N'*-(3-bromo-2-hydroxybenzylidene)-4-(prop-2-yn-1-yloxy)benzohydrazide**

(alk-3'Br) (2.26)

¹H NMR (400 MHz, DMSO-d₆): δ = 3.58 (t, 1H, *J* = 1.3 Hz), 4.87 (d, 2H, *J* = 1.3 Hz), 6.87 (m, 1H), 7.11 (d, 2H, *J* = 8.3 Hz), 7.46 (d, 1H, *J* = 7.6 Hz), 7.58 (d, 2H, *J* = 7.9 Hz), 7.91 (d, 2H, *J* = 8.3 Hz), 8.52 (s, 1H). ¹³C NMR (100 MHz, DMSO-d₆): δ = 56.1, 79.1, 79.2, 79.2, 110.4, 115.3, 119.9, 121.0, 125.5, 130.0, 130.2, 130.8, 134.6, 134.8, 148.6, 154.7, 160.7, 162.8. LC-MS: calcd for C₁₇H₁₃BrN₂O₃ [M+H]⁺ 373.01, found 373.08.

***N'*-(3,5-dibromo-2-methoxybenzylidene)-4-(prop-2-yn-1-yloxy)benzohydrazide (alk-OMe) (2.27)**

¹H NMR (400 MHz, DMSO-d₆): δ = 3.63 (t, 1H, *J* = 2.4 Hz), 3.82 (s, 3H), 4.91 (d, 2H, *J* = 2.4 Hz), 7.12 (d, 2H, *J* = 8.8 Hz), 7.92-7.97 (m, 3H), 8.00 (s, 1H), 8.62 (s, 1H). ¹³C NMR (100 MHz, DMSO-d₆): δ = 56.1, 79.2, 79.3, 115.1, 117.8, 119.2, 126.2, 130.0, 130.2, 131.8, 136.5, 137.3, 140.8, 155.3, 160.6, 163.0. LC-MS: calcd for C₁₈H₁₄Br₂N₂O₃ [M+H]⁺ 464.94, found 465.00.

***N'*-(3,5-dibromo-2-hydroxybenzyl)-4-(prop-2-yn-1-yloxy)benzohydrazide (red-alk-INP) (2.28)**

To a solution of alk-INP (**17**) (50 mg, 0.111 mmol) in 3 mL of MeOH:THF (1:2 mL) was added sodium cyanoborohydride (21 mg, 0.332 mmol). The solution turned yellow. To this mixture was added 10% HCl in MeOH (2 mL). A whitish precipitate crashed out of solution. The precipitate was collected and dissolved in EtOAc, washed with water and sodium bicarbonate, dried over magnesium sulfate, filtered and concentrated to yield **2.28** (35 mg, 70%).

¹H NMR (400 MHz, DMSO-d₆): δ = 3.60 (t, 1H, *J* = 2.2 Hz), 4.02 (s, 2H), 4.87 (d, 2H, *J* = 2.2 Hz), 7.05 (d, 2H, *J* = 8.8 Hz), 7.39 (s, 1H), 7.63 (s, 1H), 7.80 (d, 2H, *J* = 8.8 Hz). ¹³C NMR (100 MHz, DMSO-d₆): δ = 52.5, 56.0, 79.1, 79.3, 110.5, 111.7, 115.0, 115.1, 125.9, 128.1, 129.4, 129.6, 131.7, 131.8, 133.5, 133.8, 153.6, 160.2, 166.3. LC-MS: calcd for C₁₇H₁₄Br₂N₂O₃ [M+H]⁺ 452.94, found 452.92.

5.5 Bacterial strains and eukaryotic cell lines for SAH experiments

Wild-type *S. typhimurium* strain IR715, which is a nalidixic acid-resistant strain of 14028, was used for all experiments unless otherwise noted. The SPI-1 T3SS-deficient mutant ($\Delta invA$) was taken from the *Salmonella* deletion library [36]. The SopE2-CPG2-HA strain was used as previously described [50]. HeLa cells were grown in DMEM supplemented with 10% FBS at 37°C in a 5% CO₂ incubator.

5.6 Isolation of secreted SPI-1 effector proteins

Overnight cultures of *S. typhimurium* grown in Luria-Bertani broth (LB) in a 37°C shaker were diluted 1:30 and grown for four hours in the presence of compound or DMSO. Bacteria were pelleted by centrifugation at 15,000 g for 10 minutes. The supernatant was removed and spun down again to remove any remaining bacteria. The secreted proteins in 1 mL of the remaining supernatant were precipitated overnight at 4°C with 10% trichloroacetic acid (TCA). The proteins were pelleted by centrifugation at 20,000 g for 30 minutes, and the supernatant was discarded. The pellet was washed with acetone to remove remaining TCA and pelleted again. The acetone washes were done a total of three times before the pellet was resuspended in 35 μ L 4% SDS buffer, 12.5 μ L loading buffer, and 2.5 μ L BME. The samples were vortexed, heated at 95°C, and run on an SDS-PAGE gel for 1 hour at 200 volts. The precipitated secreted proteins were visualized by staining the gel with Coomassie blue.

5.7 Characterization of secreted effector proteins

Once the secreted proteins were separated by SDS-PAGE, protein bands were visualized by Coomassie blue staining and identified by in-gel trypsinization followed by LC-MS/MS analysis. Briefly, each band in the gel was cut into small slices, which were subsequently washed for 15 minutes in 250 mM ammonium bicarbonate (ABC), twice in 1:1 ABC to acetonitrile (ACN), and once in ACN before drying. Once dry, 2 μ g of trypsin in 30 μ L ABC was added to each slice before overnight incubation at 37°C. The liquid was collected, and the gel slices were washed in 1:1 ABC:ACN + 0.1% trifluoroacetic acid (TFA) twice, collecting the liquid after each wash [112]. The combined supernatants were dried under vacuum before being resuspended in 0.1% TFA in water for LC-MS/MS analysis (performed by The Rockefeller University Proteomics Resource Center). Sequest and X!Tandem data was imported into Scaffold for Peptide Prophet filtering. Peptides with $\geq 95\%$ likelihood of correct assignment were accepted. Proteins matched with 2 or more tryptic peptides were accepted; for those proteins, non-tryptic peptides were also accepted.

5.8 Bacterial lysis

Overnight cultures were diluted 1:30 and grown for four hours in the presence of compound or DMSO. They were pelleted and washed with PBS before lysis. A lysis buffer cocktail was made by adding 100 μ L of 0.1% SDS buffer (0.1% SDS, 150 mM NaCl, 50 mM TEA, pH 7.4), 4 μ L PMSF (250 mM in ethanol), 2 μ L 250x protease inhibitor (Roche), and 0.1 μ L benzonase per sample. The cell pellets were resuspended in

100 μ L of the lysis buffer and sonicated 2x30 seconds before being put on ice for 10 minutes and sonicated again. Cell debris was removed by spinning at 1,000 g for 5 minutes and collecting the supernatant. Protein concentration was determined using a BCA assay.

5.9 Click chemistry protocol and in-gel fluorescence analysis

A click chemistry cocktail was made by mixing 1 μ L of copper sulfate (50 mM), 1 μ L of TCEP-HCl (50 mM), 2.5 μ L TBTA (2mM), and 0.5 μ L azido-Rhodamine (10mM) per sample [113]. To 50 μ g of lysate in 45 μ L of 4% SDS buffer was added 5 μ L of the click chemistry cocktail was added. The samples were vortexed, and the reaction was performed for one hour at room temperature in the dark before being precipitated with 200 μ L MeOH, 75 μ L chloroform, and 150 μ L water. The solution was vortexed then centrifuged for 2 minutes at 20,000 g. The top layer was removed, and again 200 μ L of MeOH was added before the pellet was spun down. This MeOH wash was repeated and the samples were left to dry. Once dry, 35 μ L of 4% SDS buffer, 12.5 μ L loading buffer, and 2.5 μ L BME were added to each sample. The tubes were heated at 95°C for 5 minutes and separated by SDS-PAGE. The proteins were visualized by scanning the gel with an Amersham Biosciences Typhoon 9400 imager (excitation 532 nm, 580 nm filter, 30 nm band-pass).

5.10 Transcriptional profiling of *S. typhimurium*

Performed by Angelica Ferguson. Overnight cultures were inoculated at 1:30 dilution and compound was added to a final concentration of 20 μ M. Cultures were grown for four hours and then harvested by centrifugation. RNA was extracted using the RNeasy Protect Bacteria Mini Kit (Qiagen) according to the manufacturer's protocol for bacterial cells. Equivalent masses of RNA from each sample (1-2.5 μ g) were reverse transcribed using Affinity Script RT enzyme (Stratagene) and oligo dT (Roche). cDNA was diluted 50-fold with water, and PCR reactions were performed in triplicate with specific primers using SYBR green (Roche) and Platinum *Taq* polymerase (Roche). Reactions were run on a 384-well plate using the Roche Lightcycler. Normalization was performed using *rrsH* and *rpoD* (rRNA and housekeeping gene, respectively) mRNA levels. Analysis was performed using the comparative C_t method and fold inductions of compound-treated samples were calculated over DMSO-treated values.

5.11 Secretion and expression of SopE2-CPG2-HA

Performed as previously described [50]. SopE2-CPG2-HA-expressing bacteria were grown in the presence of compound or DMSO for four hours. The bacteria were spun down to separate them from the supernatant. The pellet was washed once with PBS and lysed in 1% Brij buffer (1% Brij-97, 150 mM NaCl, 50 mM TEA, pH 7.4) by sonicating twice for 30 s each, separated by 10 min on ice. To 20 μ L of the supernatant and 5 μ g of the lysate in 20 μ L Brij buffer was added 80 μ L Glu-CyFur buffer (10 μ M Glu-CyFur, 50 mM Tris, 0.1 mM ZnCl₂, 0.1% Brij-97, pH 7.4). CyFur fluorescence was monitored on a

SpectraMax M2 multi-detection reader (Molecular Devices) for one hour at 610 nm with excitation at 563 nm as a readout of SopE2-CPG-HA secretion and expression, respectively.

5.12 Proteomic identification of modified proteins

5.12.1 Bacterial lysis

This protocol is described in [112]. Overnight cultures of bacteria were diluted 1:30 in LB and grown in the presence of 50 μ M compound or DMSO for four hours before being washed with PBS and flash-frozen. Typically 10-20 mL cultures were used to obtain larger amounts of protein. The bacteria were lysed by resuspending the pellet in 1 mL of 0.1% SDS buffer (0.1% SDS, 150 mM NaCl, 50 mM TEA, pH 7.4), 40 μ L PMSF (250 mM in ethanol), 20 μ L 250x protease inhibitor (Roche), 1 μ L benzonase, and 10 μ L of lysozyme (from 10 mg/mL solution in water) per sample and put on ice for 10 minutes. The solutions were sonicated 2 x 30 seconds and iced again for 10 minutes, at which point 500 μ L of 12% SDS buffer was added. The solution was sonicated again for 2 x 30 seconds. If the solution is not clear, more SDS buffer can be added and the sonication repeated. Once the solution is mostly clear, the cell debris can be removed by centrifuging at 1,000 g for 5 minutes and collecting the supernatant. Protein concentration was estimated by BCA assay.

5.12.2 Click chemistry reaction with azido-biotin

Equal amounts of protein (~5 mg) per sample were brought up to 7 mL in 1% Brij buffer with 2 mL of 10% SDS buffer being added to that. A click chemistry cocktail can be mixed before being added to each sample. The cocktail contained 100 μ L of azido-biotin (10 mM) (Fig 1.x), 200 μ L copper sulfate (50 mM), 200 μ L of TCEP-HCl (50 mM), and 500 μ L TBTA (2mM) per sample. To each sample was added 1 mL of the click chemistry cocktail. The samples were vortexed and placed in the dark at room temperature for 1.5 hours. In order to precipitate the protein, the samples were split into two 5 mL solutions in 50 mL Falcon tubes. To each sample was added 20 mL cold MeOH, 7.5 mL chloroform, and 15 mL water. The samples were vortexed and spun at 5,250 g for 30 minutes. Similar to the click reaction with azido-Rhodamine, the top layer was removed, 20 mL of MeOH was added, and the samples were spun at 5,250 g for 30 minutes again. This MeOH wash was repeated one more time before the samples were allowed to dry for several hours. Once dry, the pellets were resuspended in 1 mL of 4% SDS buffer containing 20 μ L of 0.5 M EDTA solution, and protein concentration was estimated by BCA assay.

5.12.3 Binding the protein to streptavidin beads

Streptavidin beads (100 μ L for 5 mg of protein) were washed in PBS, spun down at 4,000 g for 2 minutes, and resuspended in an equal volume of 1% Brij buffer. The beads were pipetted with chopped pipet tips. To 5 mg of protein in 3 mL of Brij buffer in a 15 mL Falcon tube was added 100 μ L of the pre-washed streptavidin beads. The mixture was rocked at room temperature for 1 hour. The beads were then extensively washed to

remove any non-specifically-bound proteins, spinning at 3,000 g for 2.5 minutes after each wash. They were first washed twice with 10 mL 0.2% SDS in PBS, followed by 3 washes with 10 mL of PBS, then 2 washes of 10 mL of ABC (250 mM in water). The beads were then incubated in 500 μ L urea (8 M in ABC), 25 μ L TCEP (200 mM in water), and 25 μ L iodoacetamide (390 mM in water) for 1 hour at room temperature to reduce and cap the cysteines. The beads were washed 2 more times with ABC, transferred to a dolphin tube, and spun down.

5.12.4 Eluting the protein from the beads and concentrating the sample

To each sample was added 250 μ L of an elution buffer consisting of 50 mL ABC (250 mM), 50 mg SDS, and 218 mg sodium dithionite ($\text{Na}_2\text{S}_2\text{O}_4$). The solution was gently mixed and incubated at room temperature for one hour. The beads were then spun down at 5,000 g for 1 minute, and the eluent was collected. The elution step was repeated with 200 μ L of elution buffer, with the beads being incubated for 30 minutes. The beads were again spun down, and the eluents were combined. To concentrate the eluent, centricons (10,000 kDa MW cutoff; Millipore) were first washed with water and spun at 14,000 g for 15 minutes. The eluent was then added to the centricons and spun at 14,000 g for 15 minutes. The centricons were inverted and placed into a new tube and spun at 1,000 g for 3 minutes to collect the concentrated sample. They were rinsed with 50 μ L of 1% SDS containing 75 mM BME. This solution was collected by spinning the centricon upside down at 1,000 g for 3 minutes. This rinsing step was repeated before the concentrated sample was dried on a speedvac.

5.12.5 Separating the sample by SDS-PAGE and preparing it for mass spec analysis

The dried powder was resuspended in 25 μL LDS buffer with 5% BME (per 100 μL of buffer needed: 25 μL 4x LDS buffer (Invitrogen), 5 μL BME, 70 μL water). The samples were vortexed and heated on a 95°C heating block before being loaded on an SDS-PAGE gel with blank lanes between each sample. The blank lanes contained 1x LDS buffer with 14% SDS and 5 % BME. The gel was run for 1 hour at 200 volts before being stained with Coomassie blue. Lanes were cut into slices and prepared as in 5.7. Identified proteins had 2 unique peptides with 95% confidence. High-confidence hits had 10x the spectral counts as the background.

5.13 *S. typhimurium* invasion of HeLa cells

HeLa cells were grown in 12-well plates containing DMEM with 10% FBS. Bacteria grown in the presence of compound or DMSO were added at an MOI of 10 in DMEM/10% FBS containing compound or DMSO before being centrifuged at room temperature for 5 min at 1000 x g. The plates were placed in a 37°C incubator for a 30-minute invasion period. Cells were then washed three times with room temperature PBS containing 100 $\mu\text{g}/\text{mL}$ gentamicin and then incubated with DMEM/10% FBS containing 100 $\mu\text{g}/\text{mL}$ gentamicin at 37°C for an additional 30 minutes to kill all extracellular bacteria. Cells were then washed an additional three times with PBS containing 100 $\mu\text{g}/\text{mL}$ gentamicin to remove any remaining extracellular bacteria. Cells were trypsinized then fixed with 3.7% paraformaldehyde in PBS for 10 minutes. They were then permeabilized with 0.2% saponin in PBS for 10 min and blocked with 2% FBS in PBS

for 10 min. All antibody stainings and washes were performed with ice-cold 0.2% saponin in PBS. Cells were stained with anti-*Salmonella* rabbit serum (Biodesign International) for one hour at room temperature before being washed three times. Goat anti-rabbit secondary antibody conjugated to AlexaFluor 488 (Invitrogen) was added for 30 minutes before cells were washed 3 times. Flow cytometry was performed using a Becton Dickinson LSRII machine and FlowJo software was used for analysis.

5.14 Bacterial strains, plasmids, and eukaryotic cell lines for H-89 experiments

Wild-type *S. typhimurium* strain IR715, which is a nalidixic acid-resistant strain of 14028, was used for all experiments unless otherwise noted. Overnight cultures grown in Luria-Bertani broth (LB) at 37°C were diluted 1:30 and grown for four hours in the presence of compound or DMSO. For construction of the SseJ-HA strain (provided by Markus Grammel), initially a pWSK29_HA plasmid was generated by annealing two primers (TCGAGTTATGCATAATCAGGAACATCATAAGGATAG and AATTCTATCCTTATGATGTTCCCTGATTATGCATAAC), digesting them with EcoRI and XhoI, and ligating them into pWSK29, which was also digested with EcoRI and XhoI. SseJ was amplified from *S. typhimurium* (IR715) by PCR (GAATTCTTCAGTGGAATAATGATGAGCTATAAAAC and TCTAGAGATAGCAGTCAGATAATATGTACCAGGC). The resulting PCR product was digested with EcoRI and XbaI and ligated into pWSK29-HA plasmid, also digested with EcoRI and XbaI. The SopE2-CPG2-HA strain was used as before (5.11). HeLa cells

and RAW264.7 macrophages were grown in DMEM supplemented with 10% FBS at 37°C in a 5% CO₂ incubator.

5.15 Bacterial replication in macrophages

Macrophages were grown in 12-well plates containing DMEM with 10% FBS. They were infected with *Salmonella typhimurium* for one hour in a 37°C incubator at a multiplicity of infection (MOI) of 5 before being washed three times with 100 µg/mL gentamicin in PBS. DMEM containing 10% FBS and 20 µM of compound or DMSO and 10 µg/mL gentamicin was added to the cells and incubated for 16 hours before CFU plating. From each sample were plated 3 dilutions (10⁻⁵-10⁻⁷) in triplicate for CFU counts.

5.16 Western blotting for Akt during macrophage infection

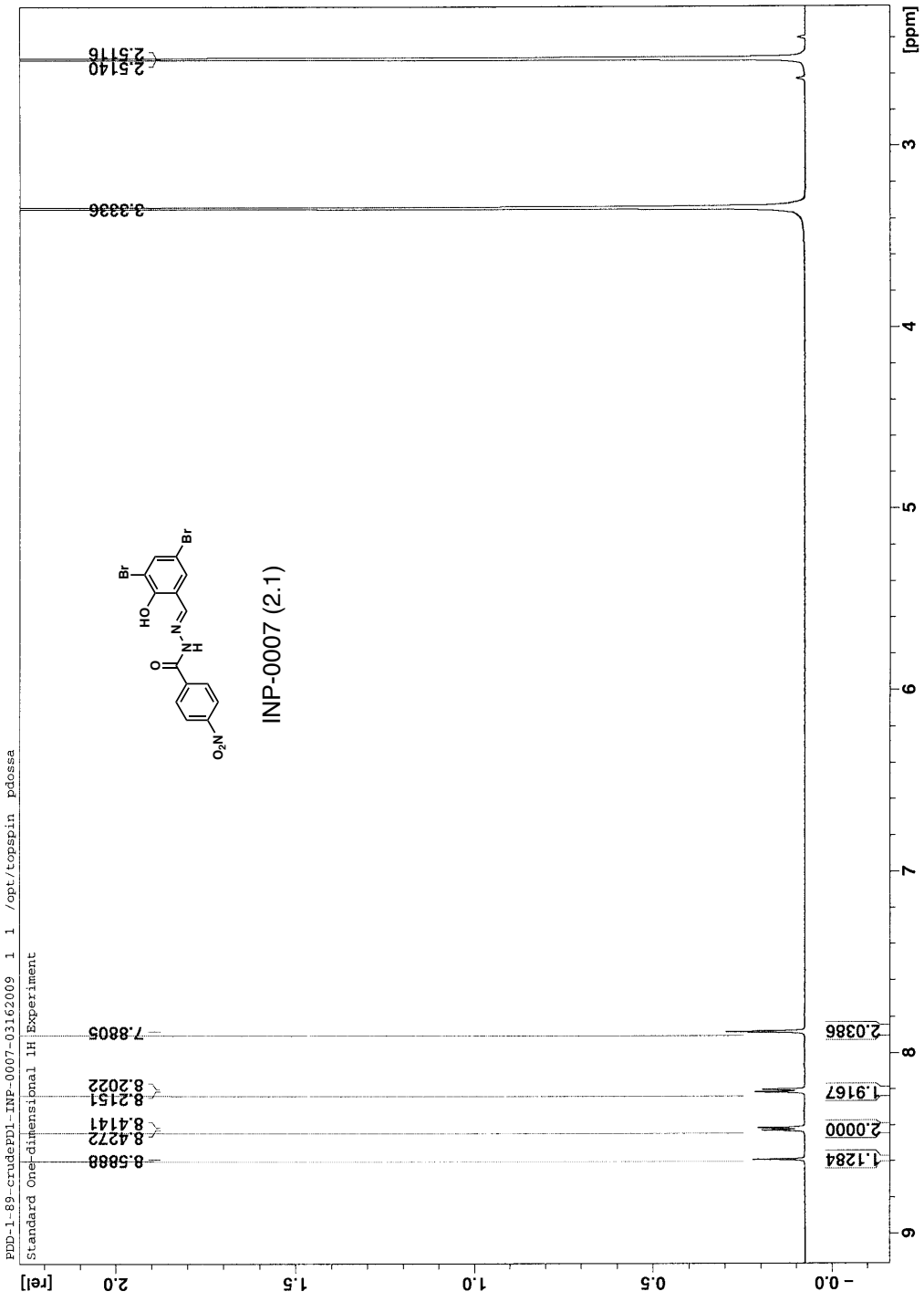
For Akt blots, macrophages in 6-well plates were infected in the same manner as for CFU plating, but instead they were harvested 8 hours pi, lysed in 30 mM Tris/HCl pH 7.5, 150 mM NaCl, 1% Triton X-100, Halt Phosphatase Inhibitor Cocktail (Thermo Scientific), and EDTA-free protease inhibitor cocktail (Roche). Protein concentration was estimated by BCA assay, and equal amounts of protein were separated on an SDS-PAGE gel before being transferred to a nitrocellulose membrane. The membrane was probed with antibodies (Cell Signaling Technology) for total Akt levels and phospho-Akt (Ser473).

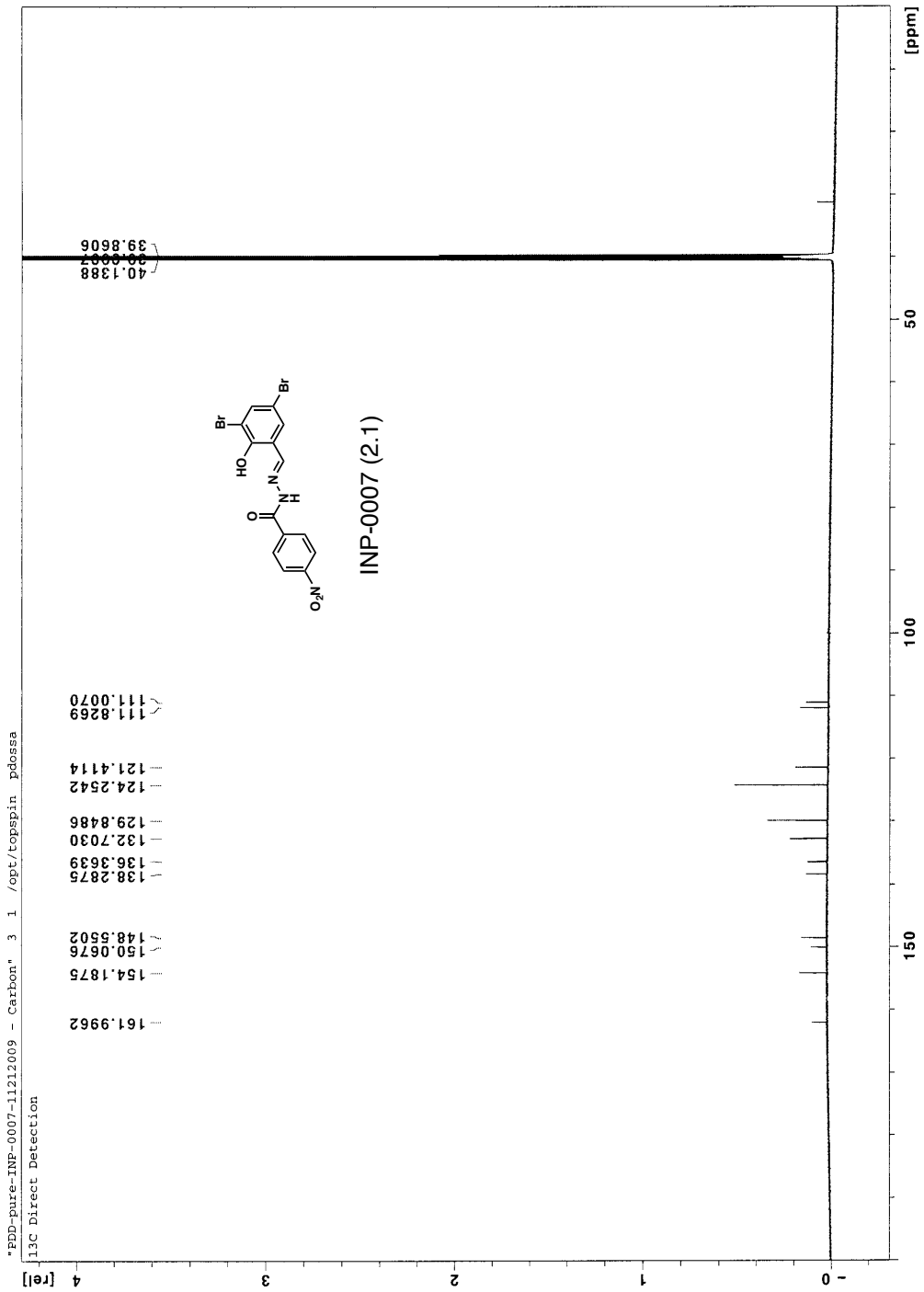
5.17 Imaging macrophages and secreted SseJ-HA during infection

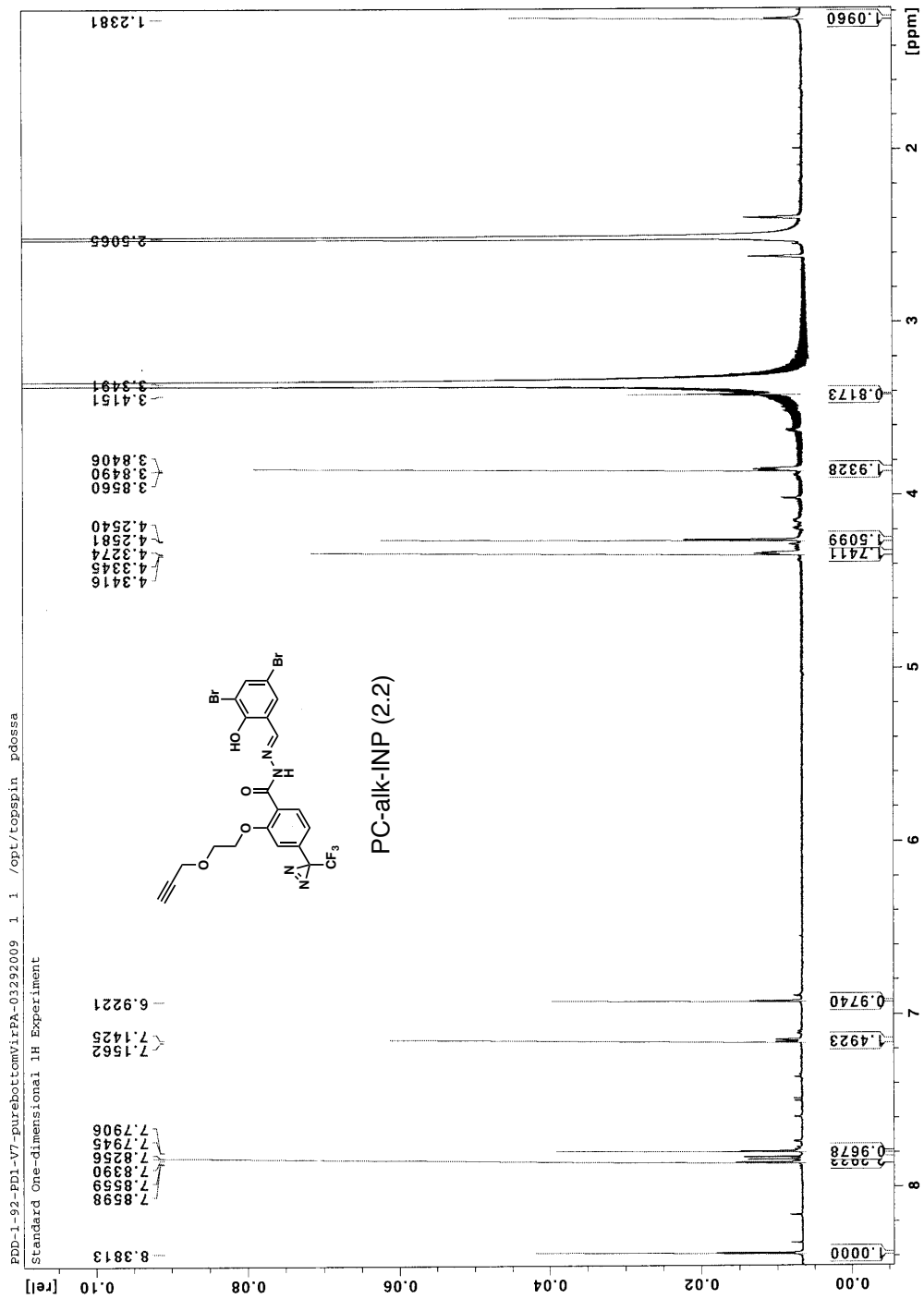
For imaging experiments, macrophages grown on cover slips in 12-well plates were infected for one hour at an MOI of 1. At this point, they were washed three times with 100 µg/mL gentamicin in PBS before being resuspended in DMEM containing 10% FBS and 10 µg/mL gentamicin. At 5 hours pi, compound was added, and cells were incubated for two more hours before being fixed and stained. All antibody stainings and washes were performed with ice-cold 0.2% saponin in PBS. Cells were stained with anti-*Salmonella* rabbit serum (Biodesign International) for one hour followed by goat anti-rabbit secondary antibody conjugated to AlexaFluor 488 (Invitrogen) for 30 minutes. Then cells were stained with mouse anti-HA (Sigma) antibody for one hour followed by goat anti-mouse secondary antibody conjugated to Rhodamine Red (Invitrogen) for 30 minutes. DNA was stained with TO-PRO-3 for five minutes before imaging. Cells were washed three times between each staining. All microscopy was performed on a Zeiss LSM 510 laser scanning confocal microscope.

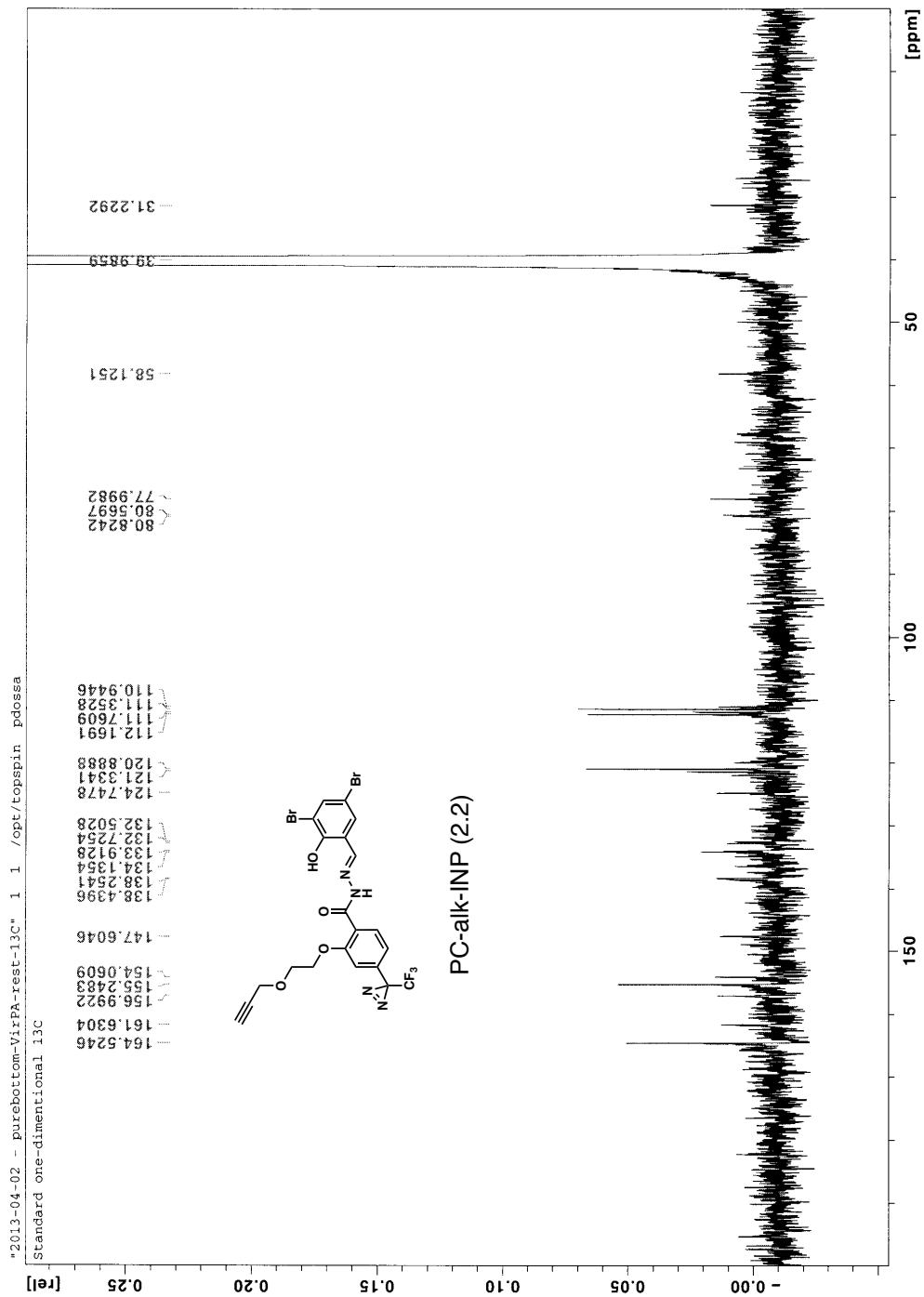
APPENDIX

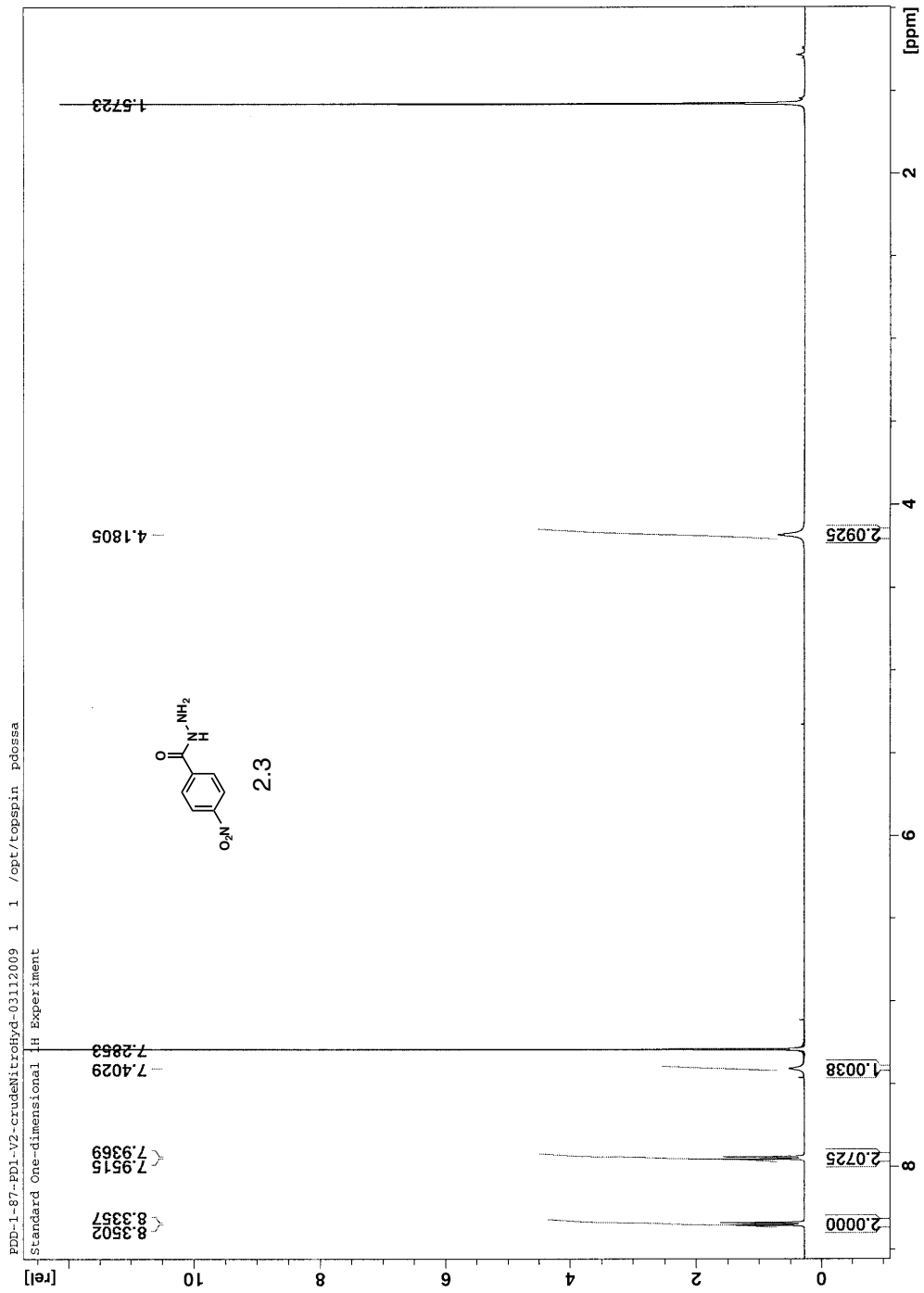
^1H and ^{13}C NMR spectra

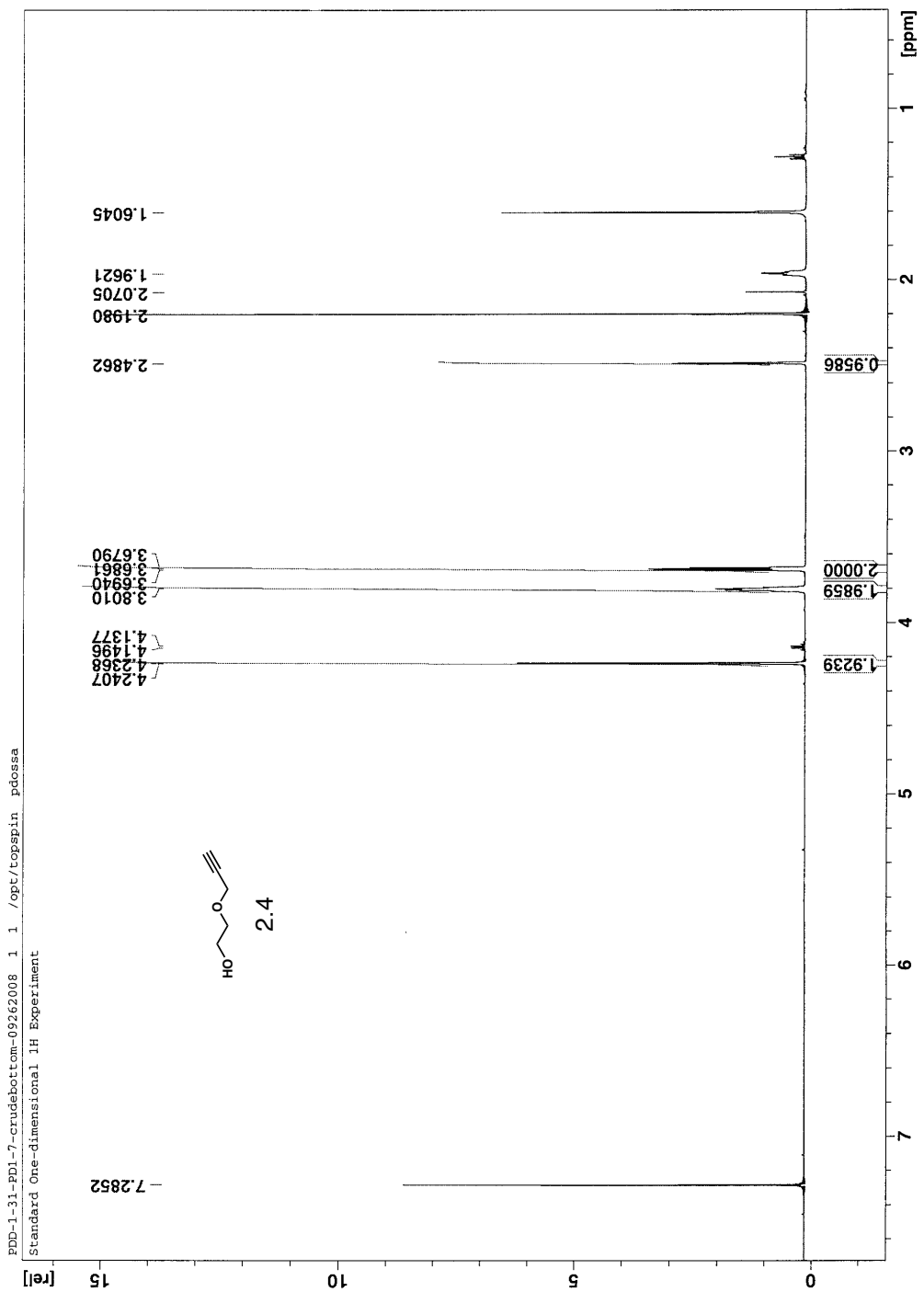


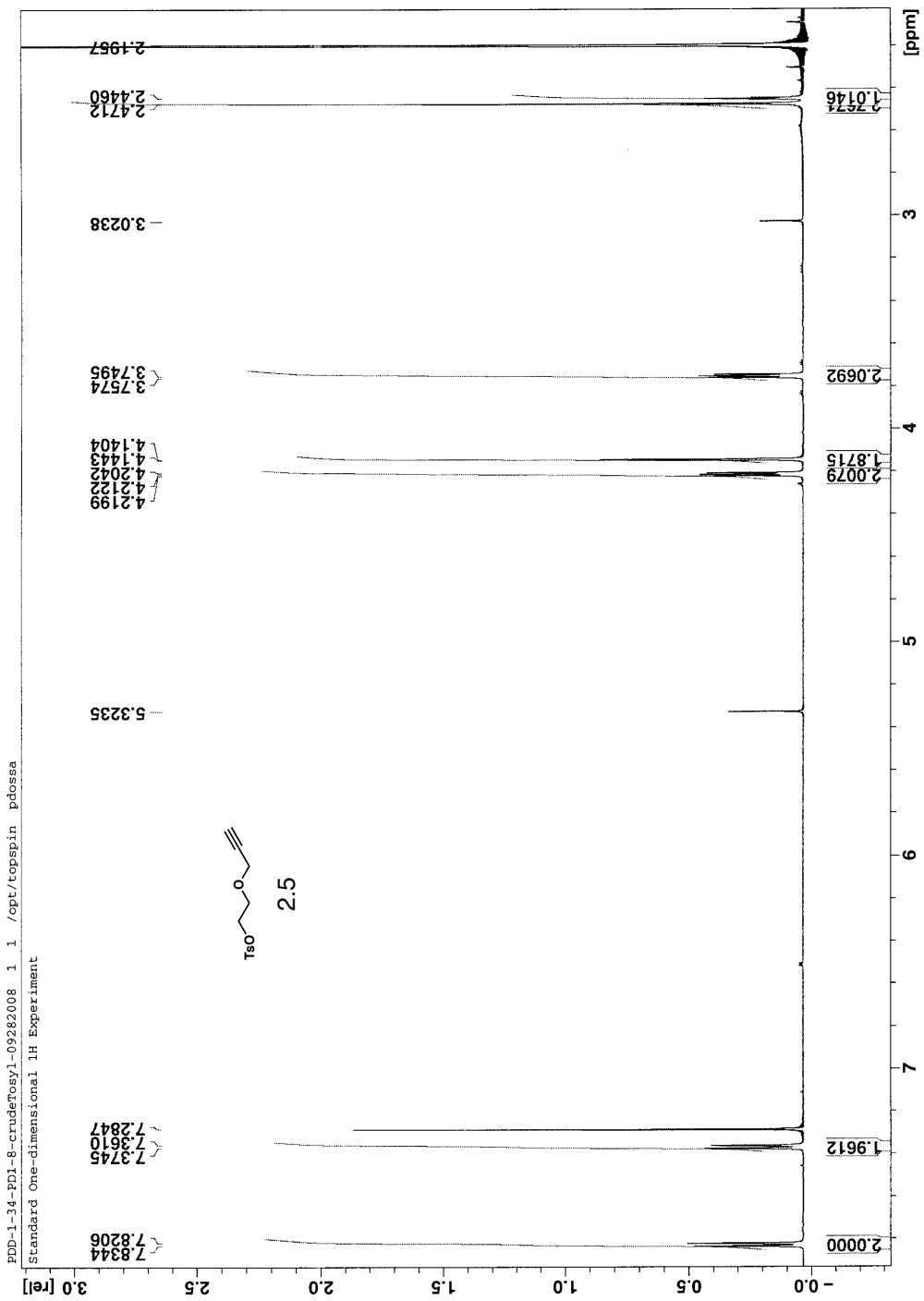


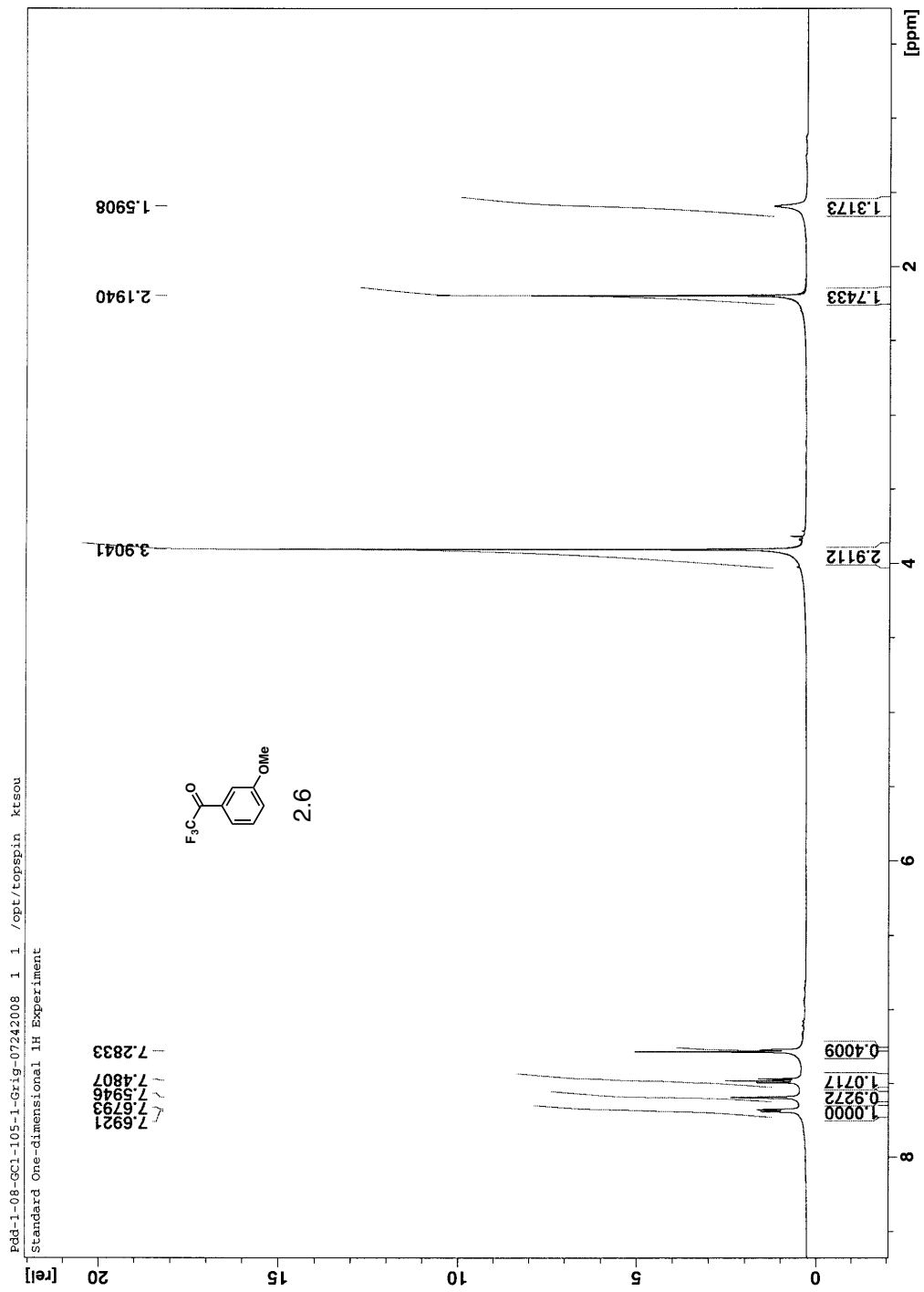


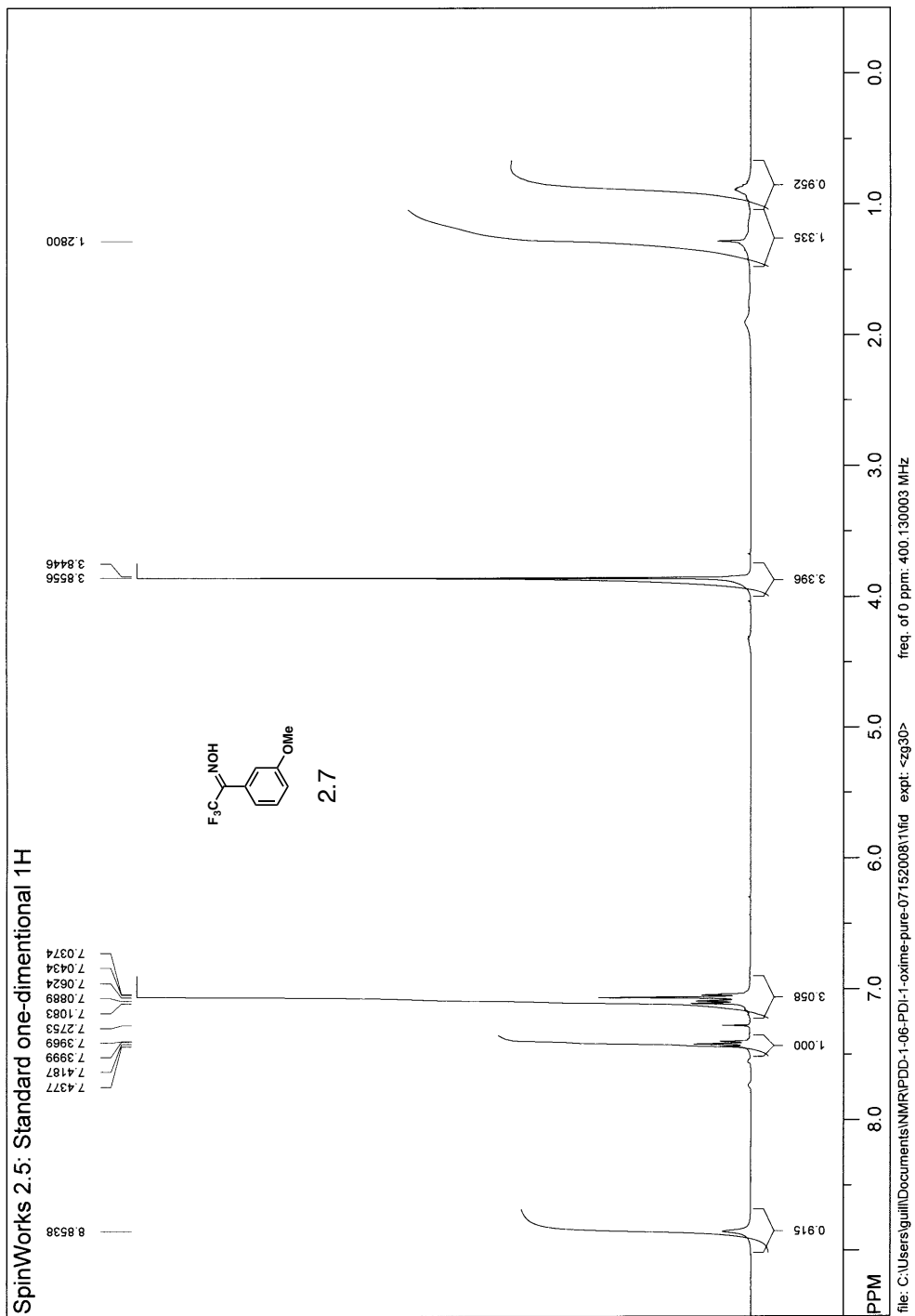


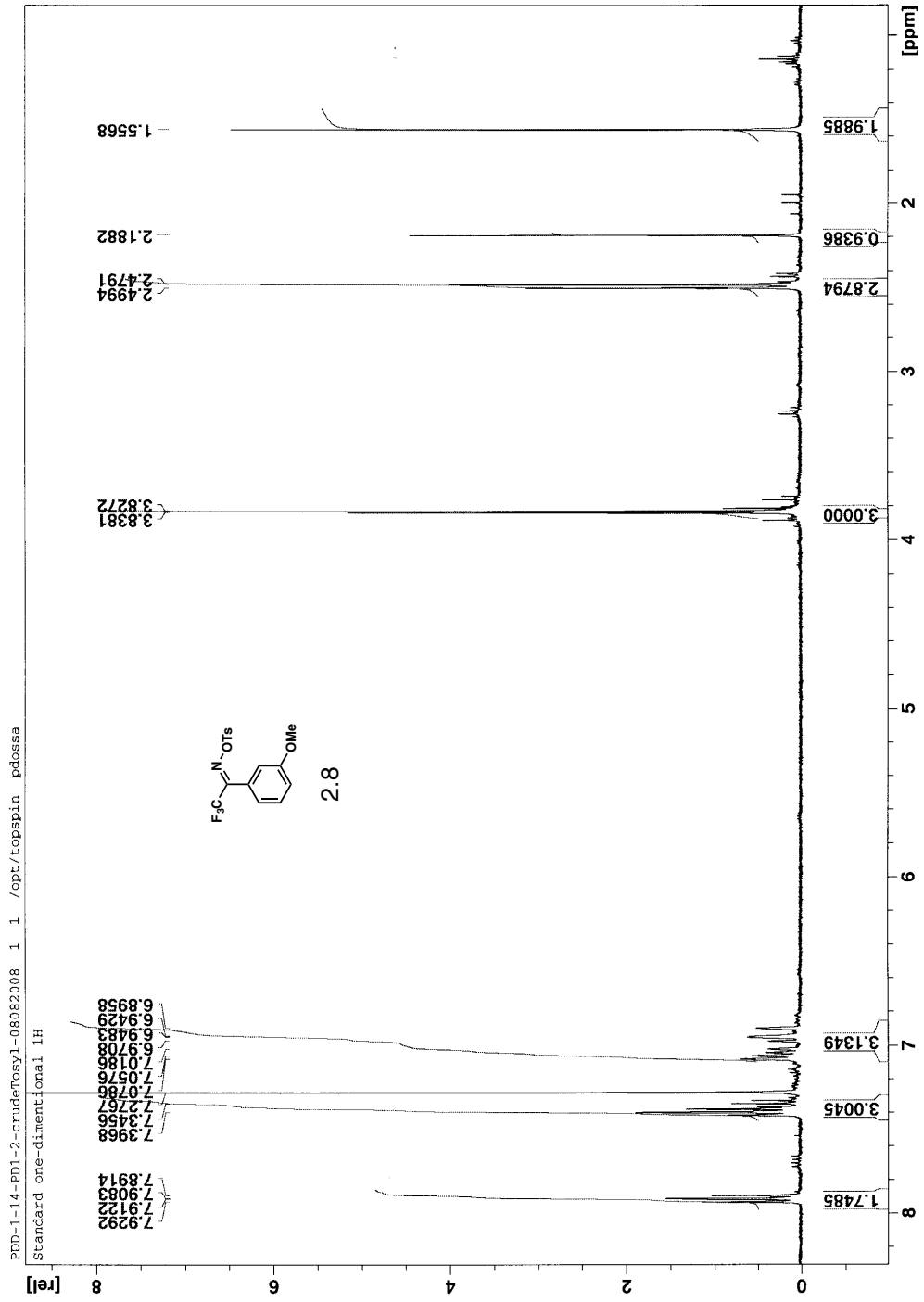


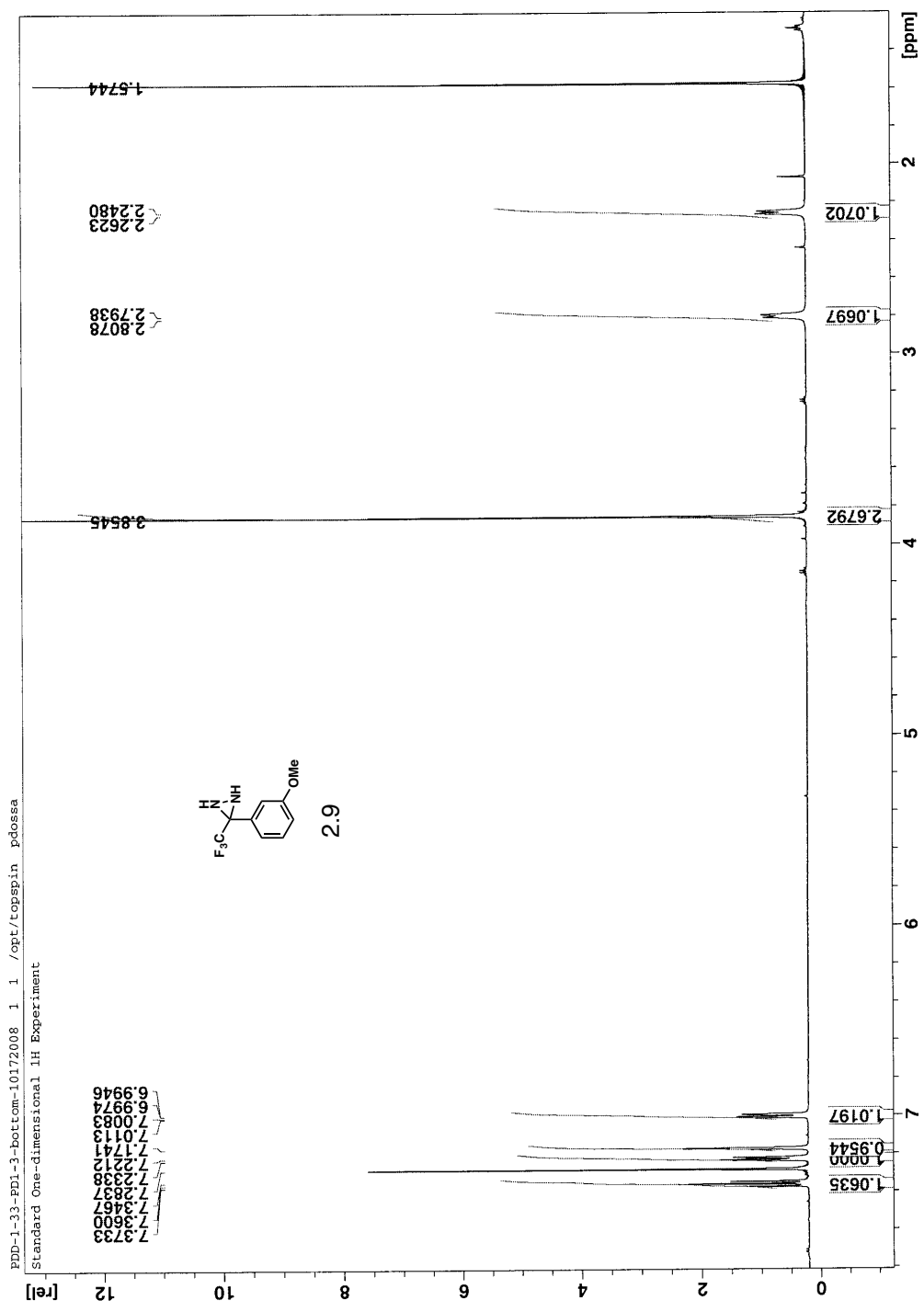


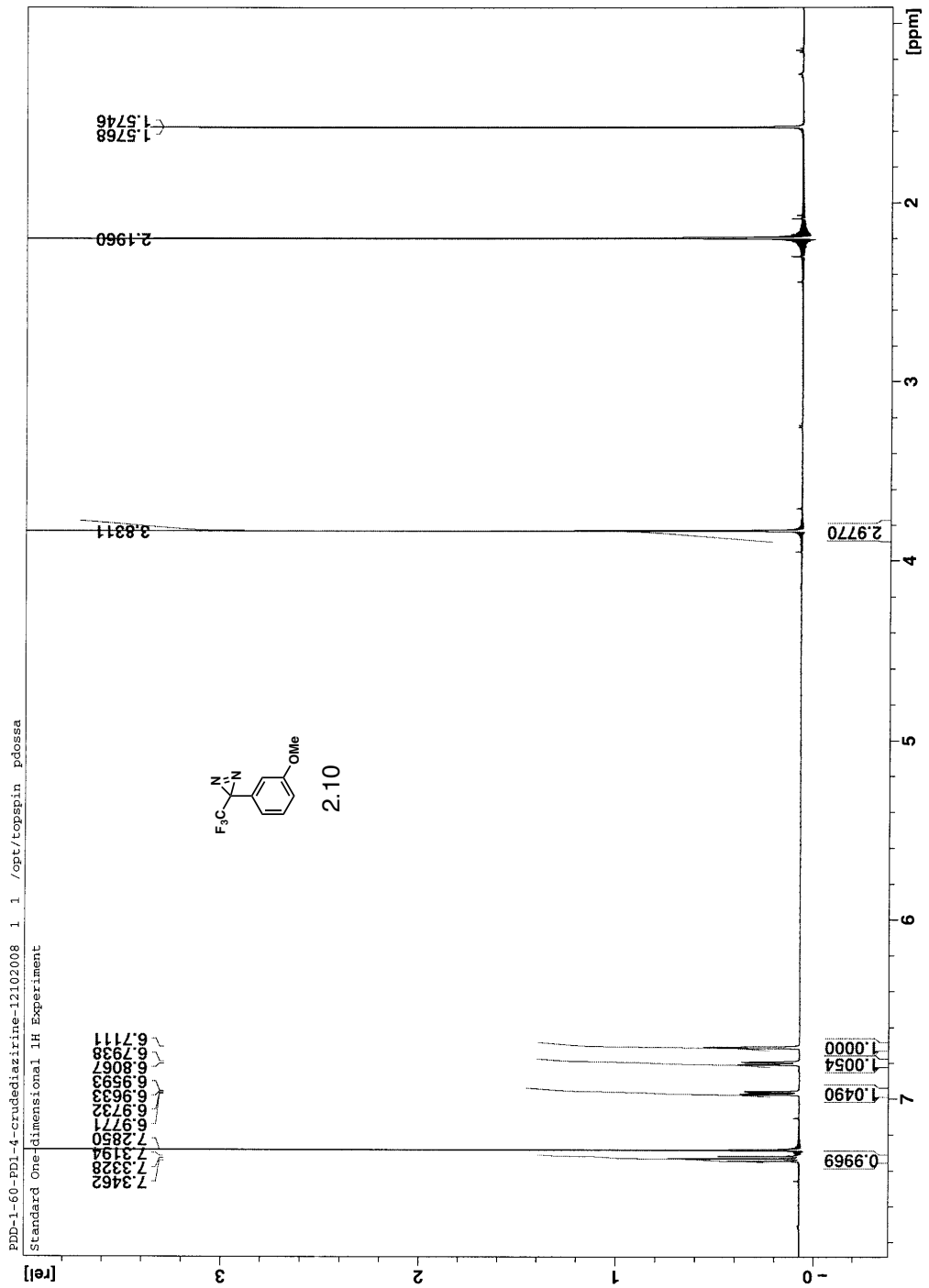


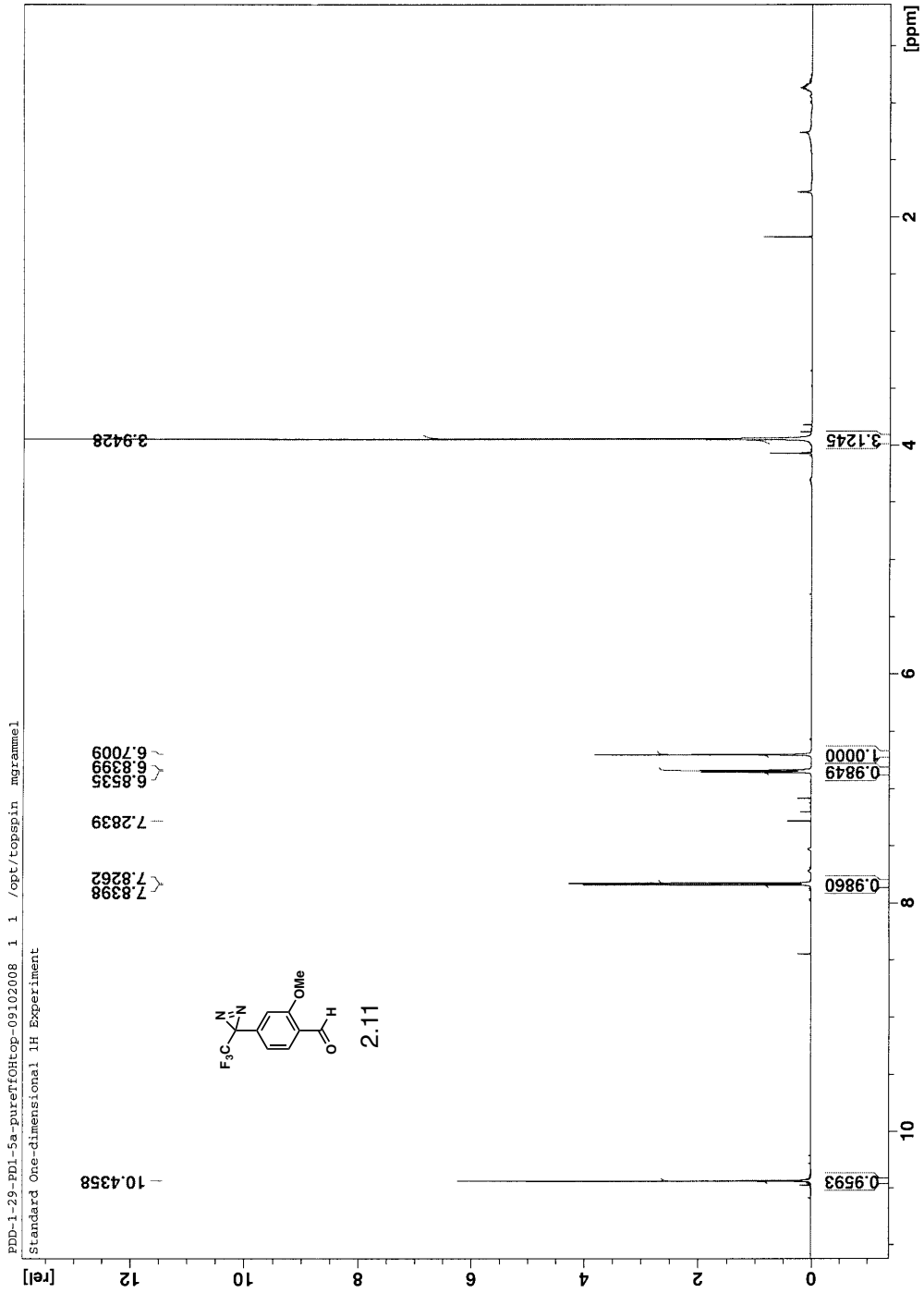


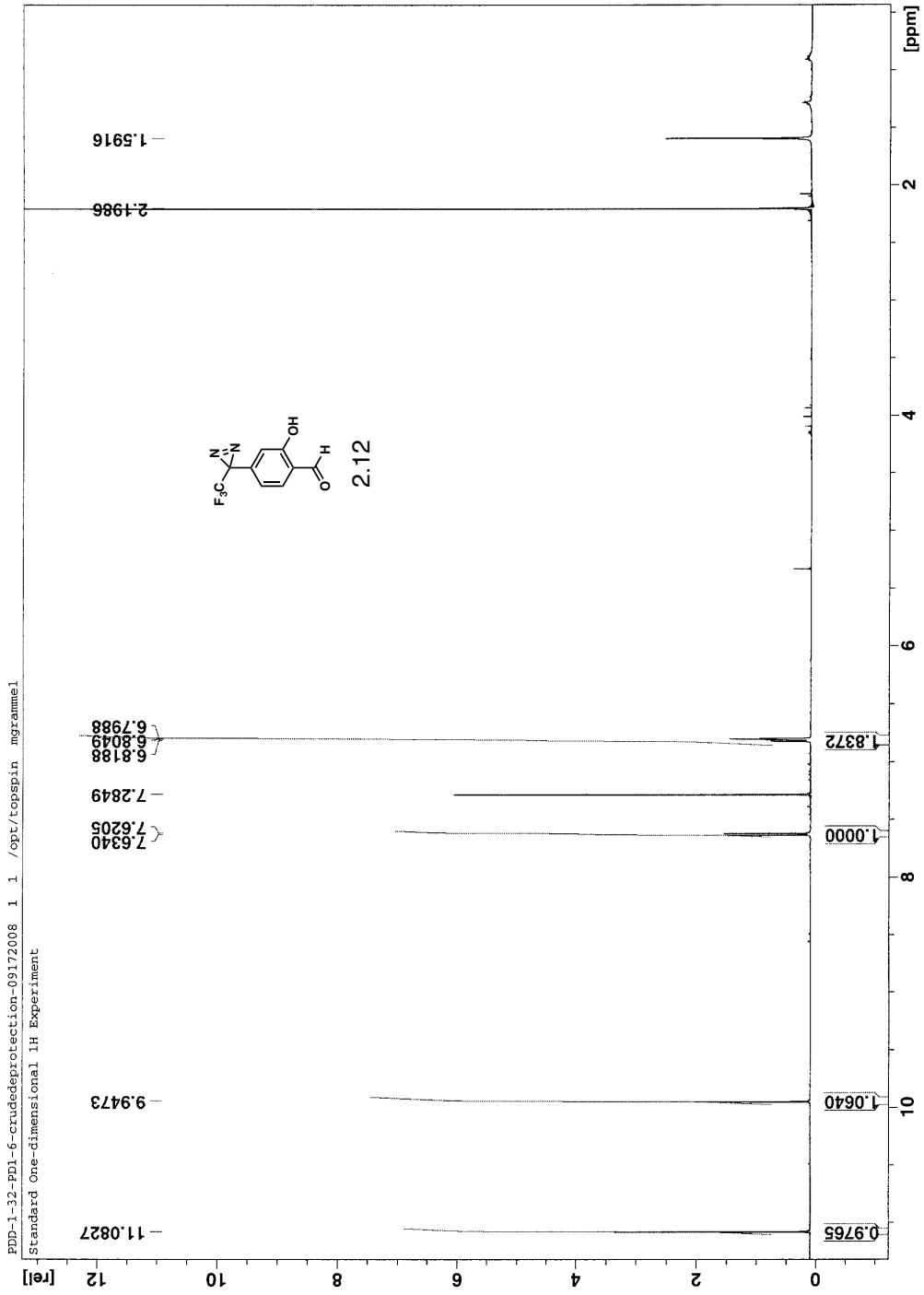


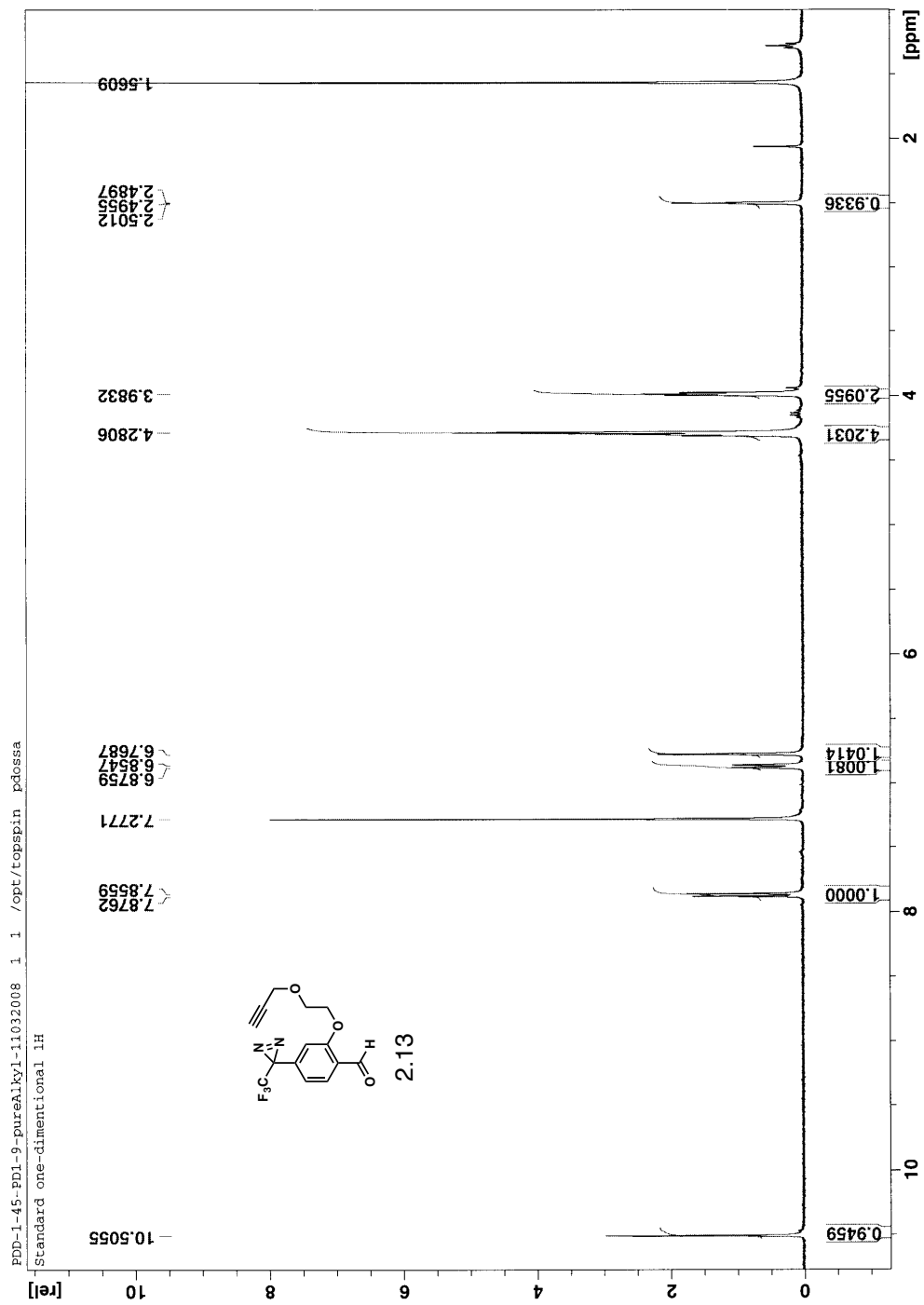


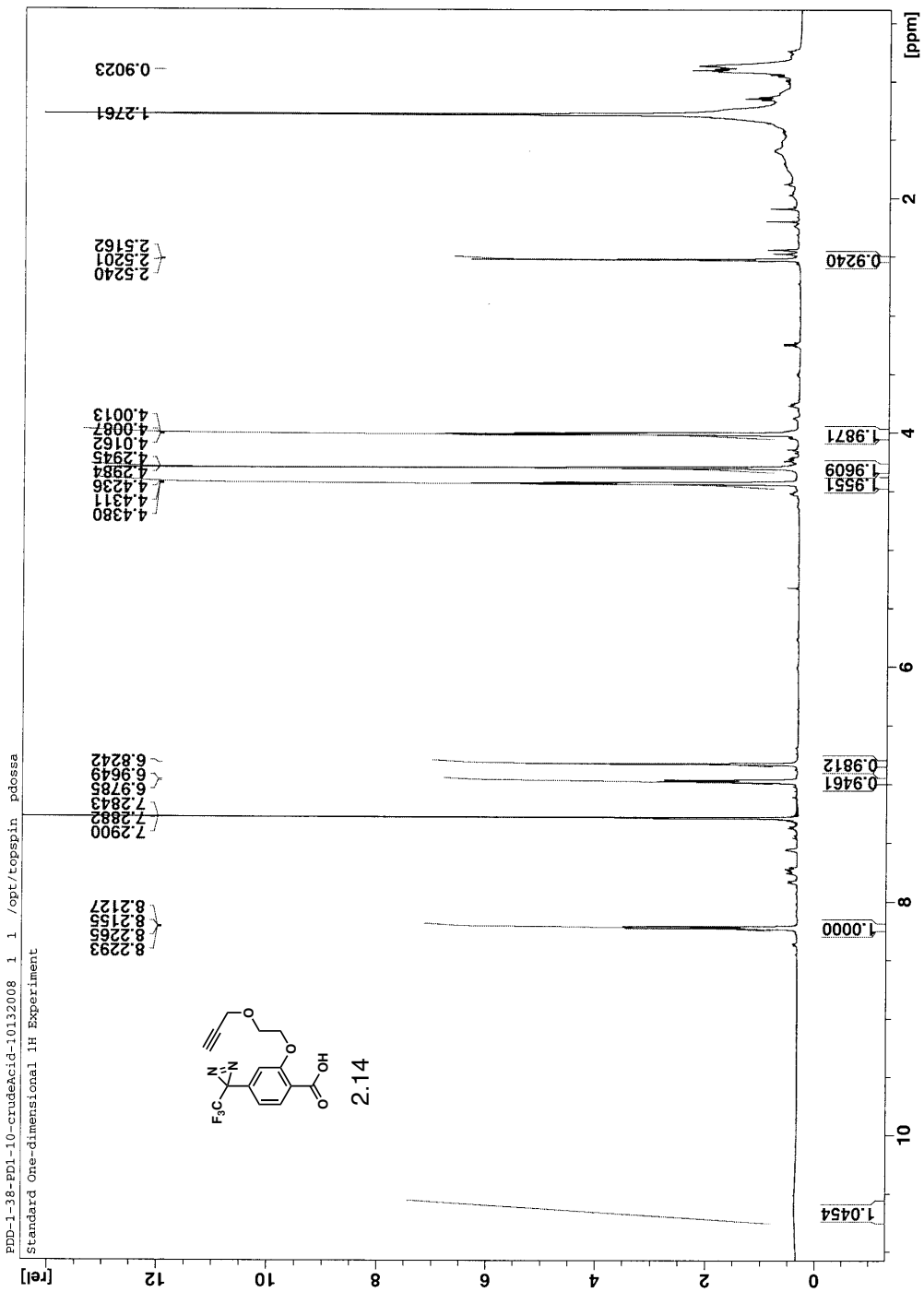


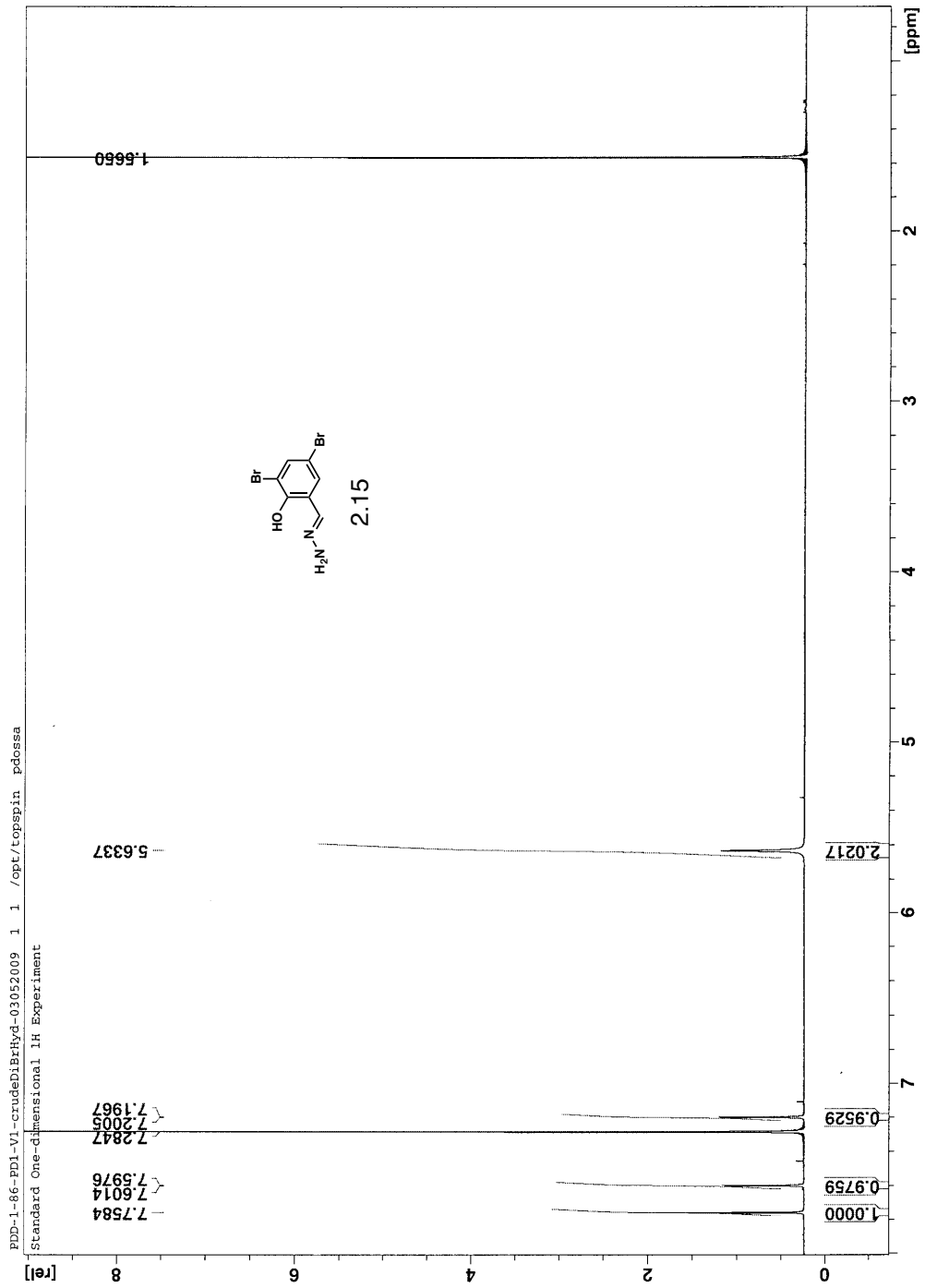


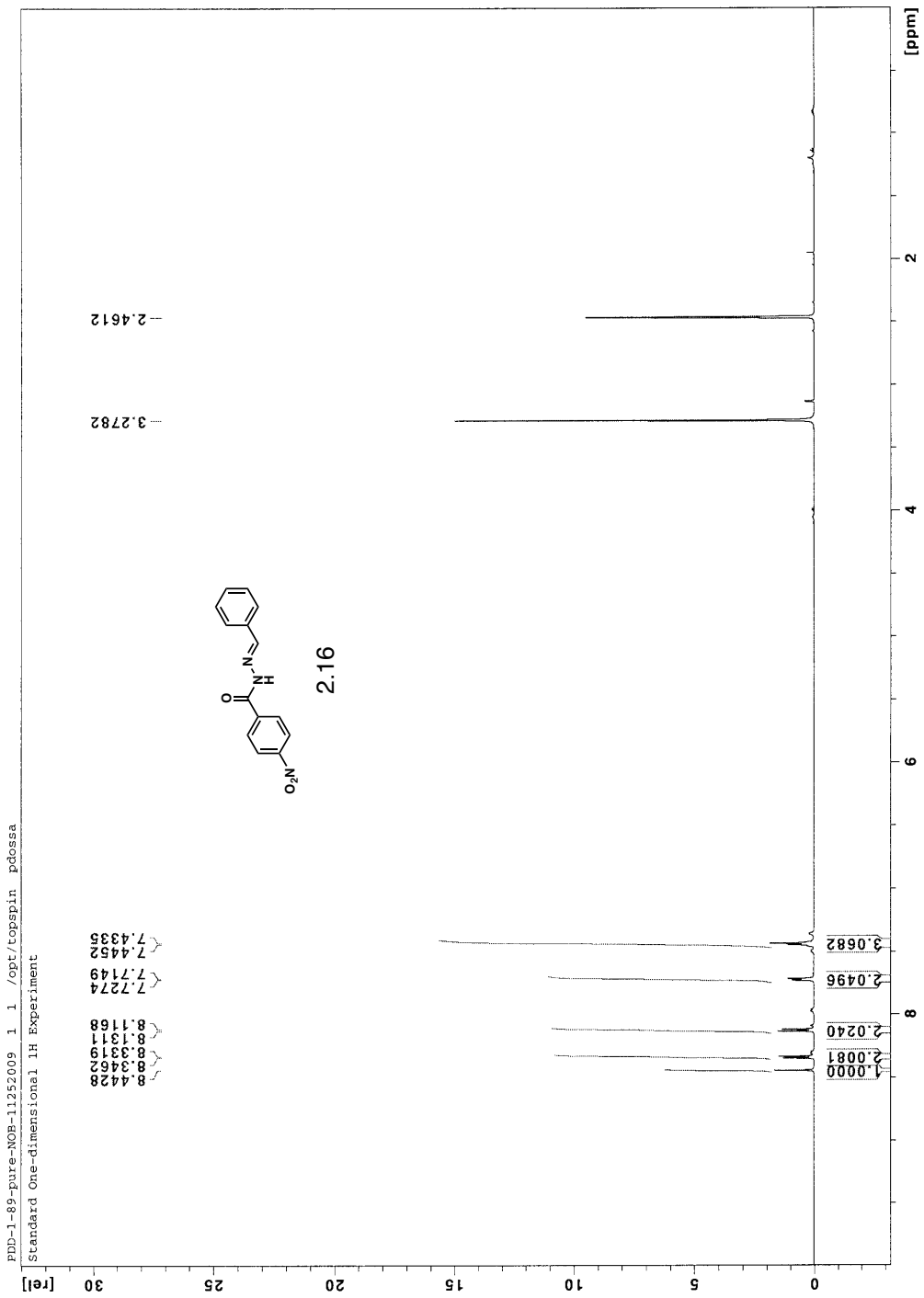


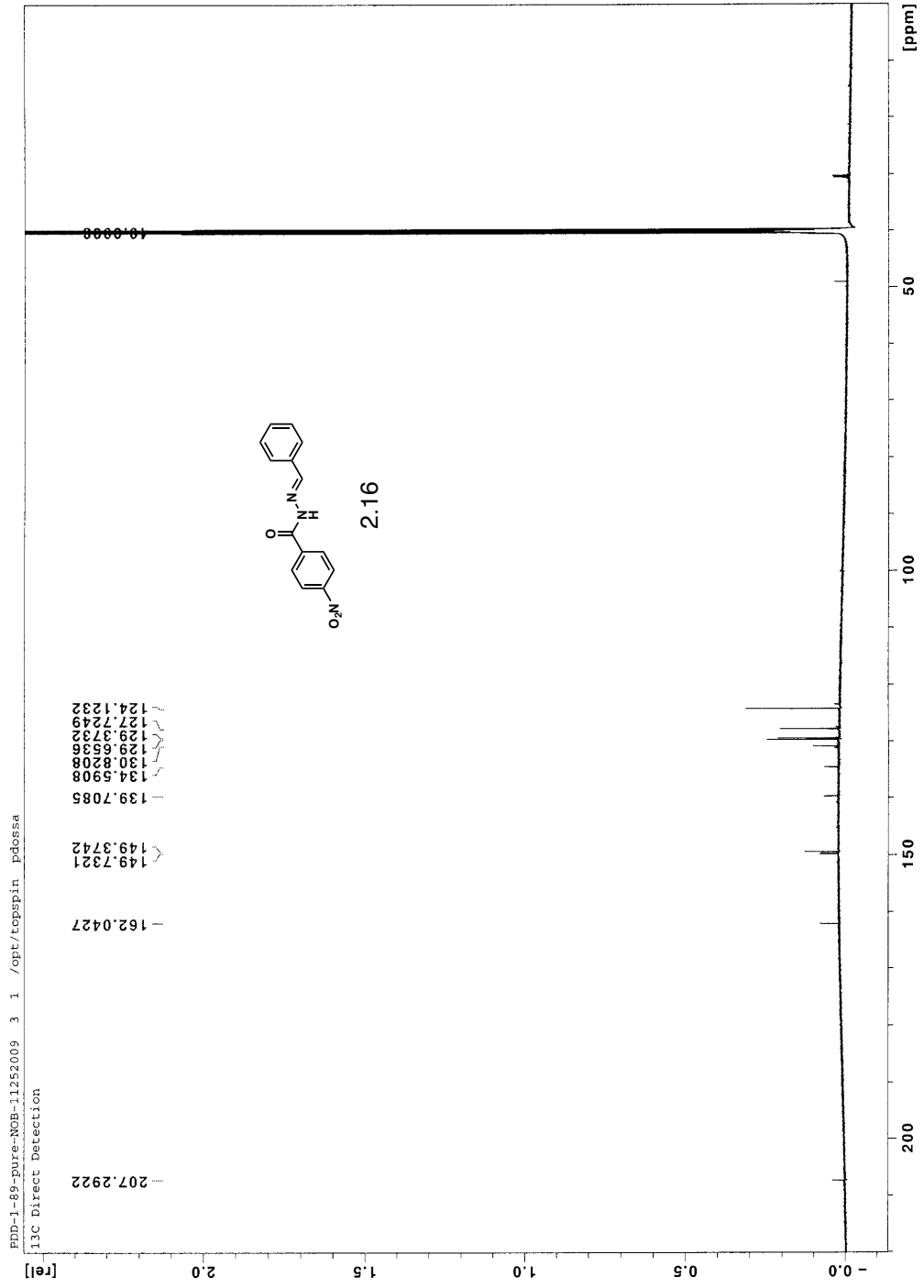


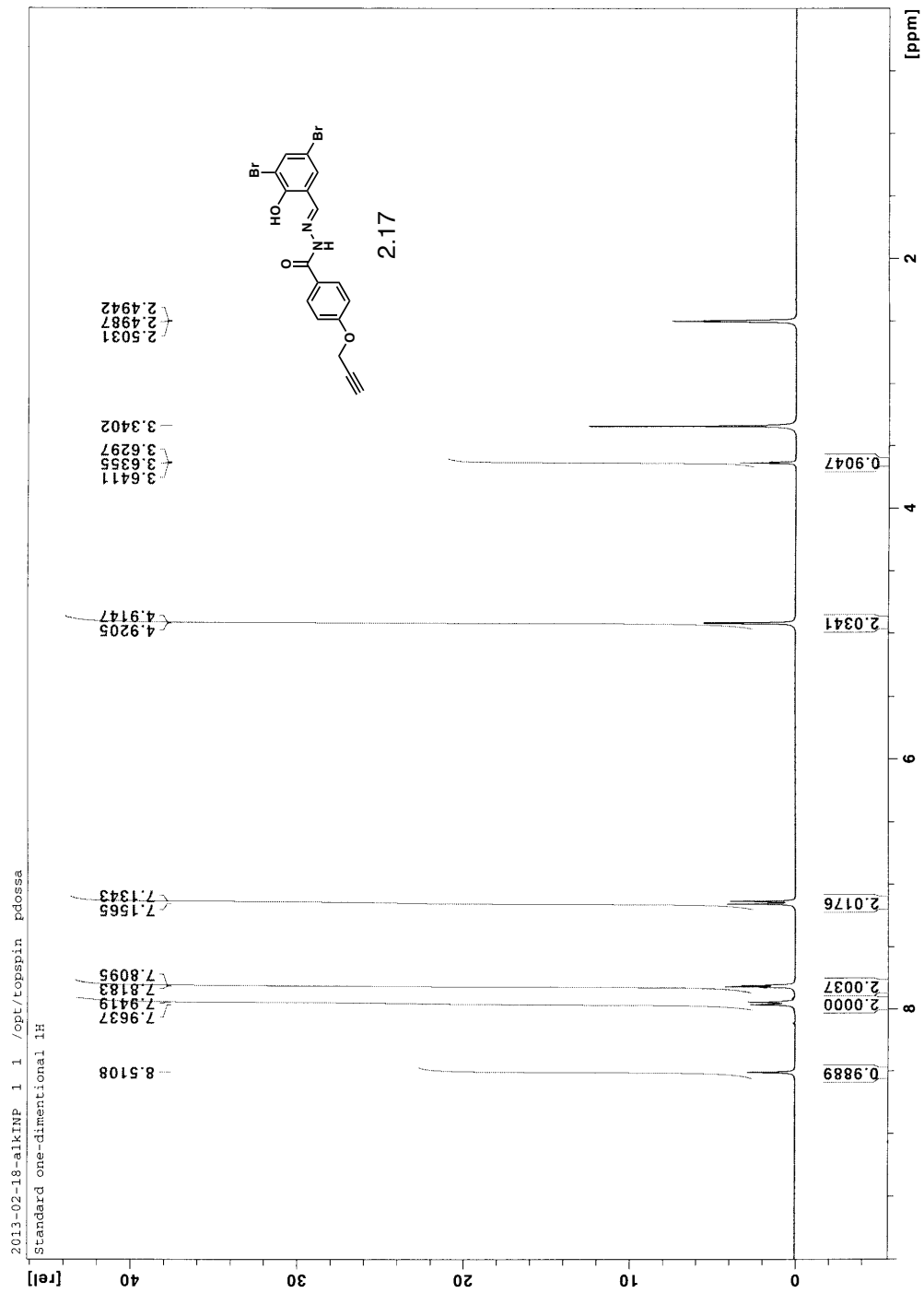


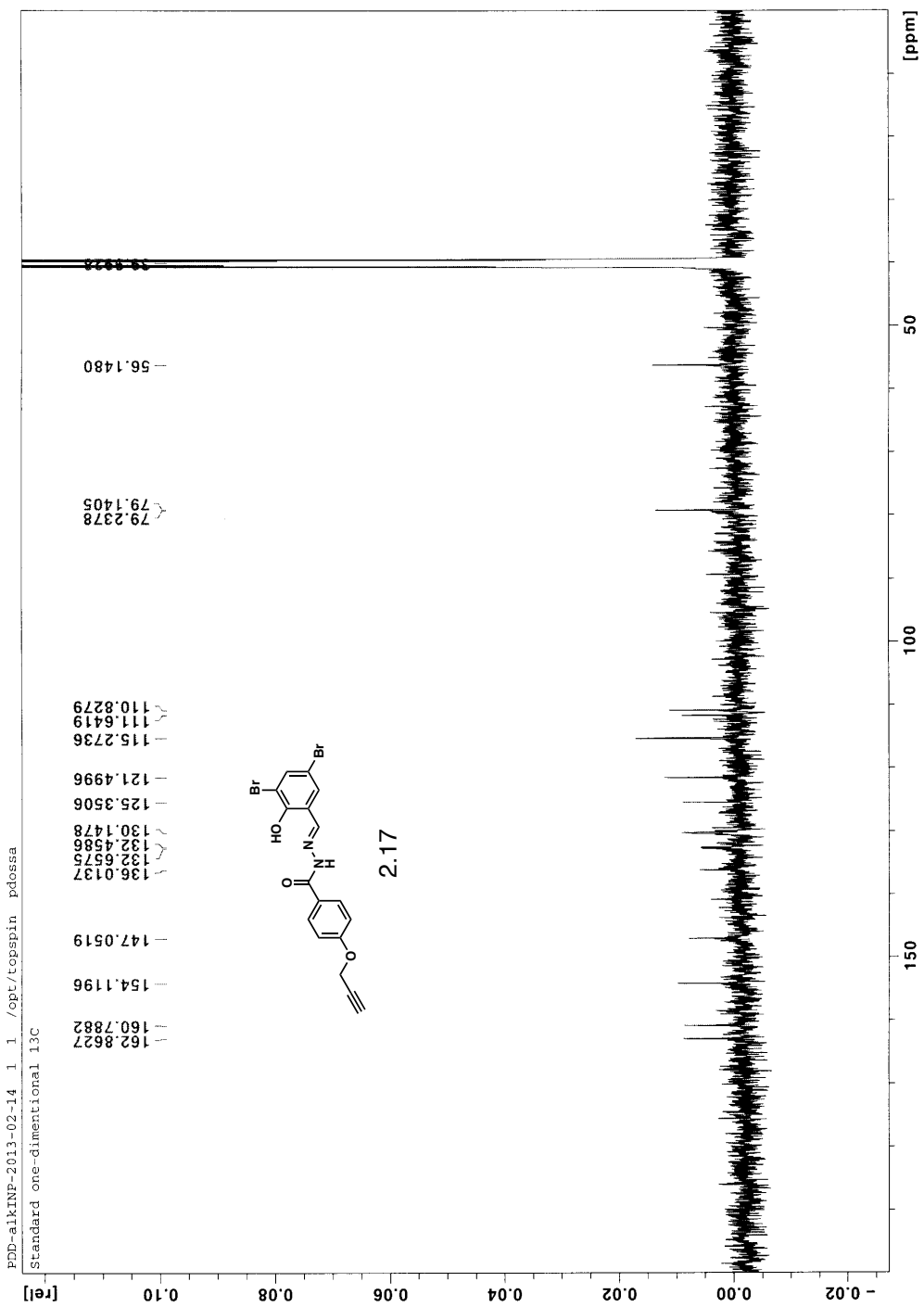


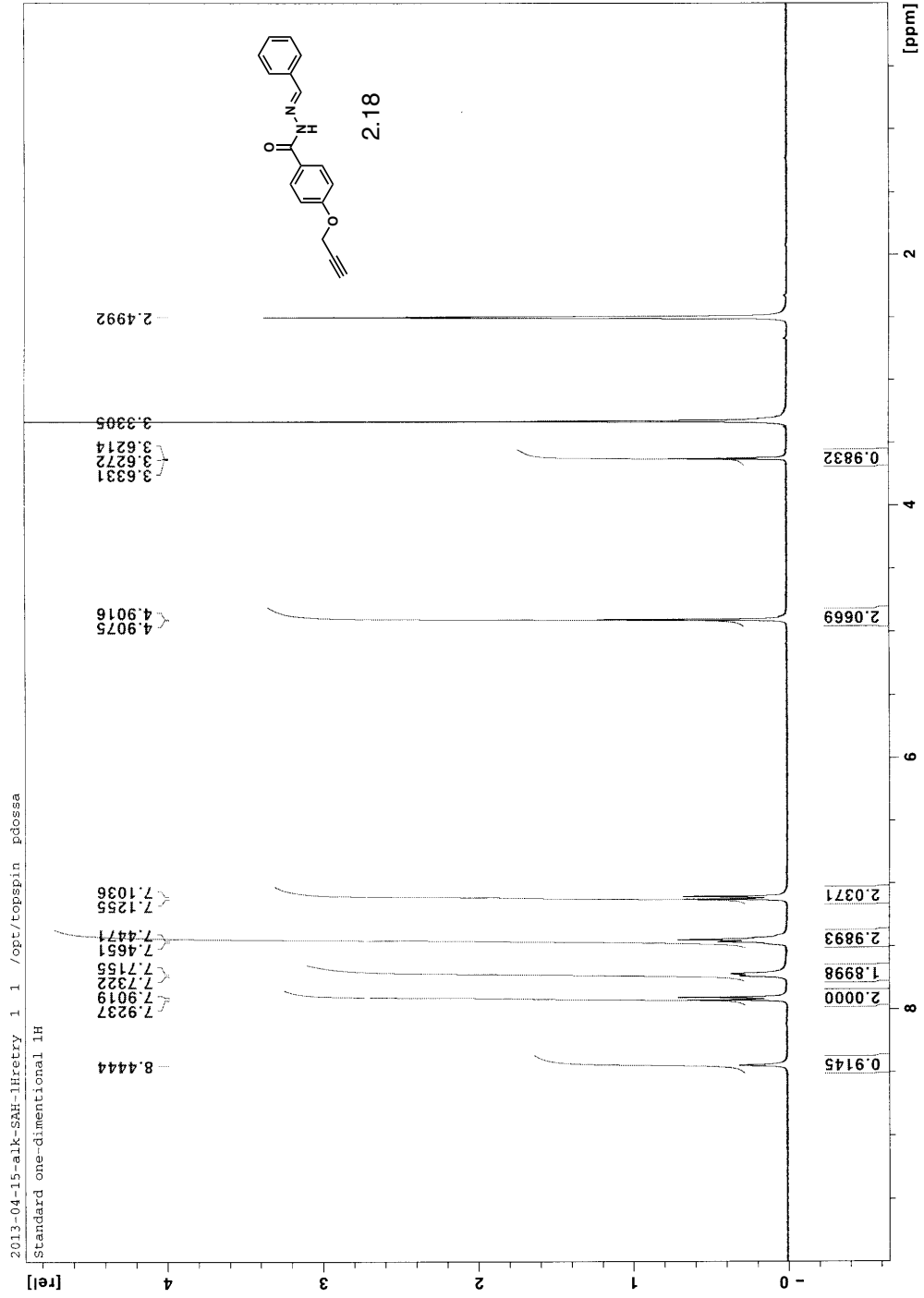


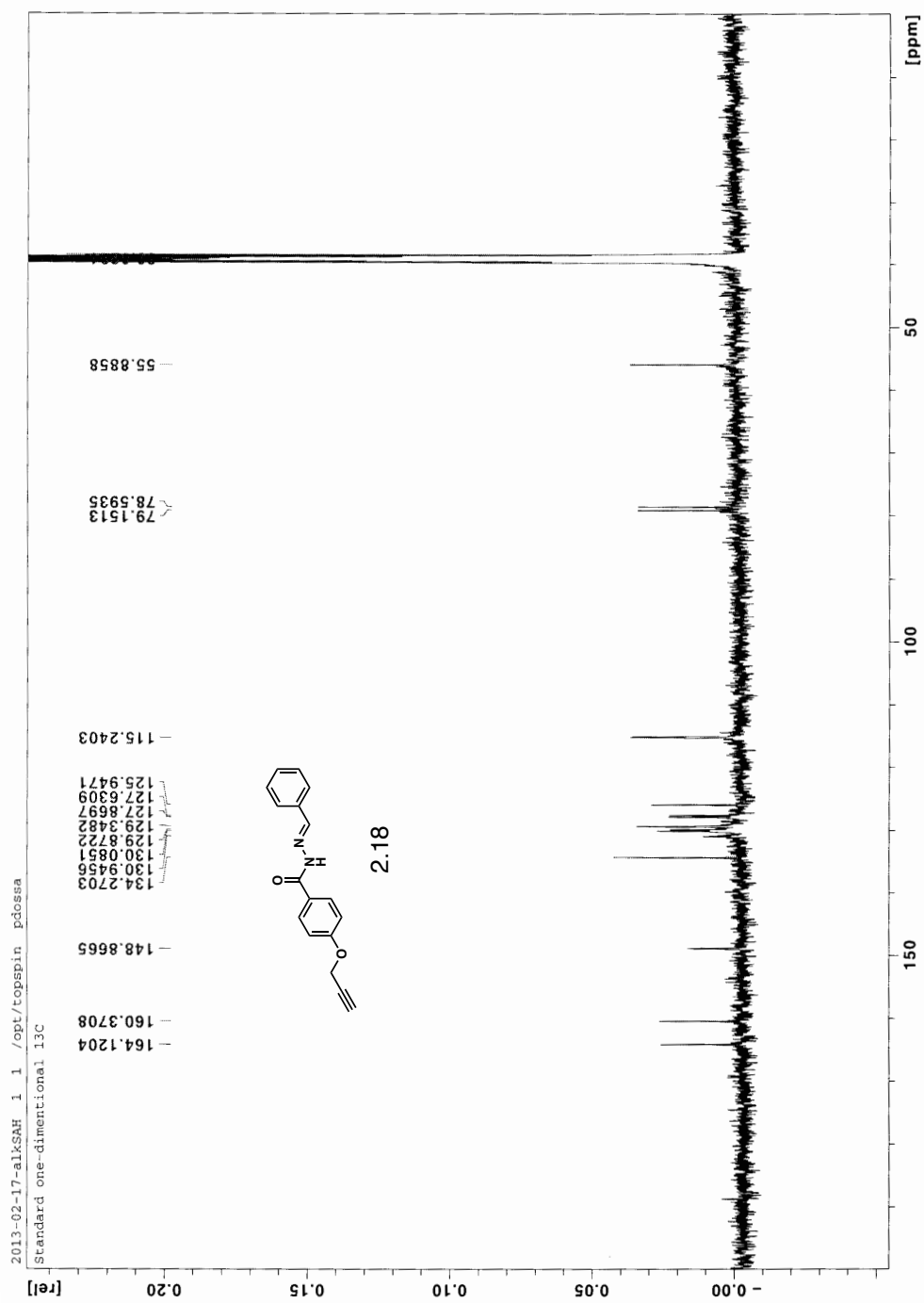


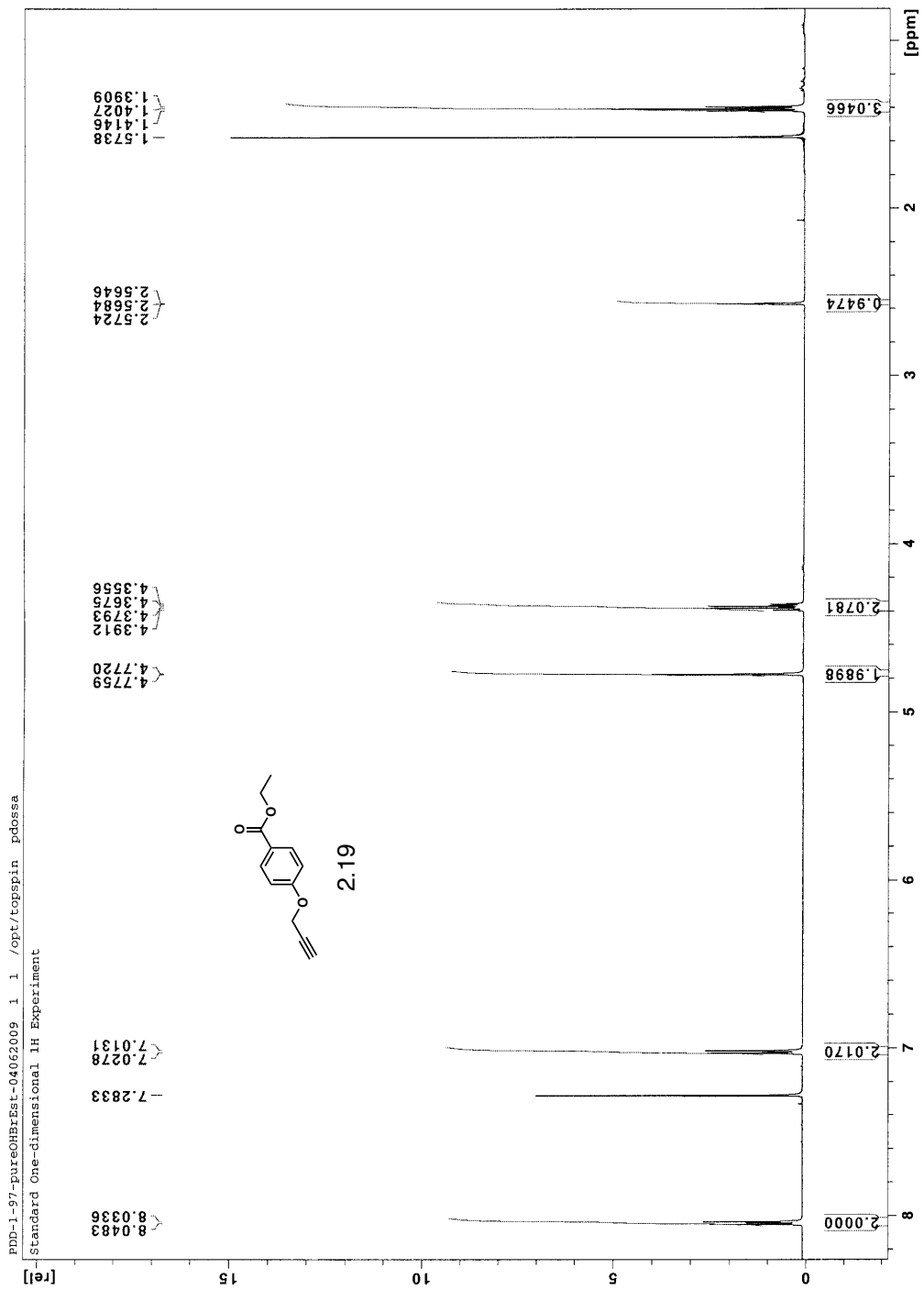


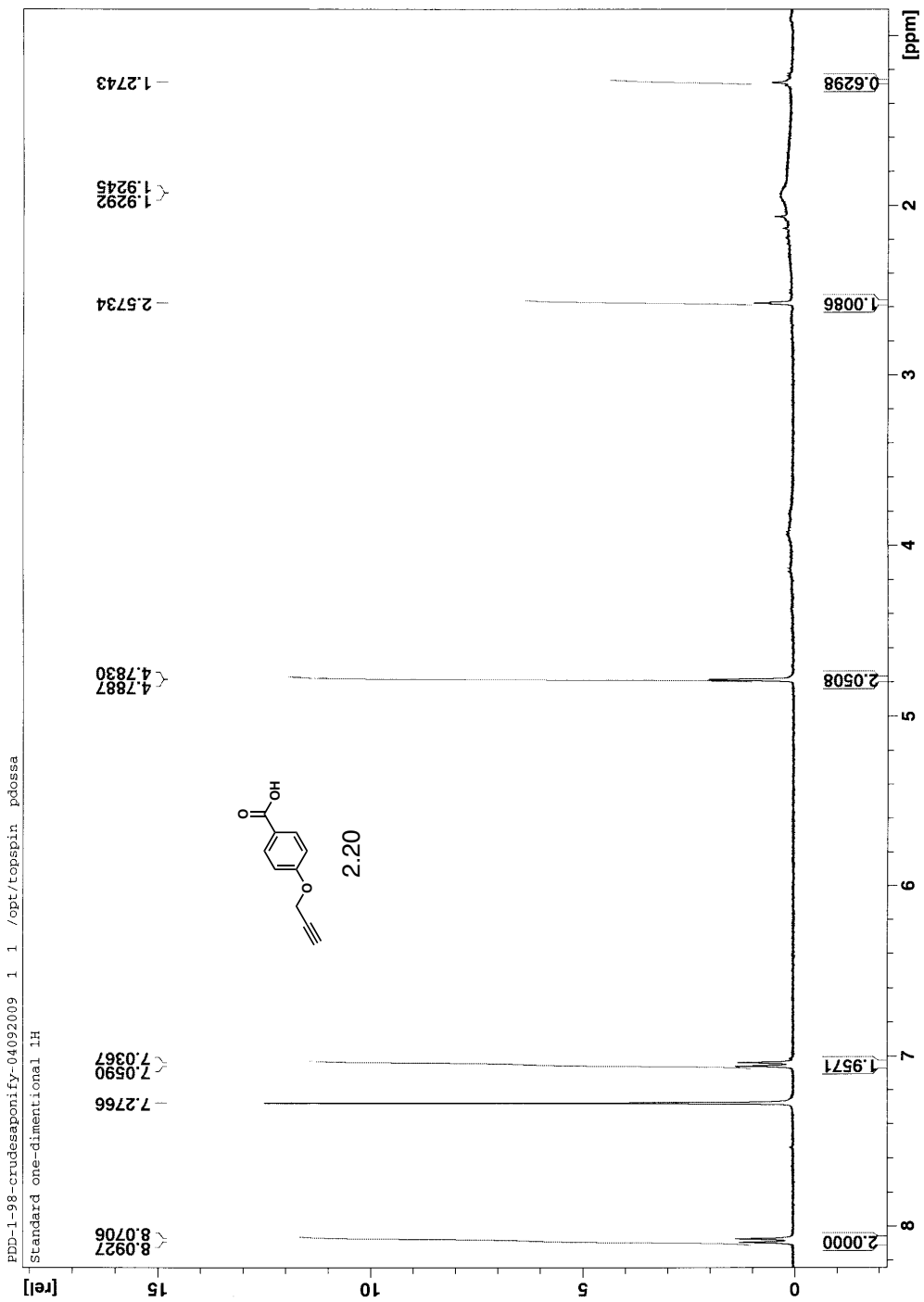




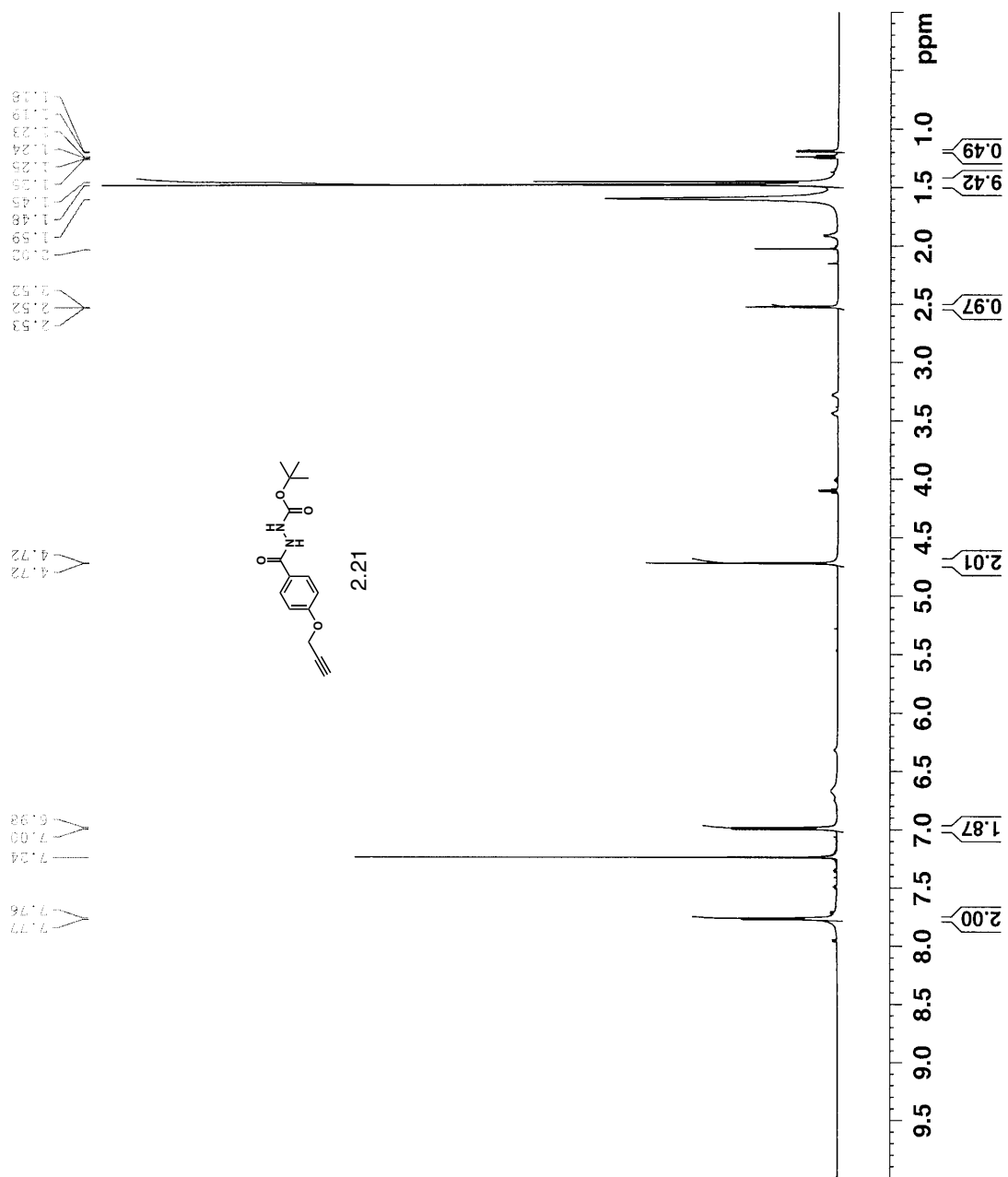


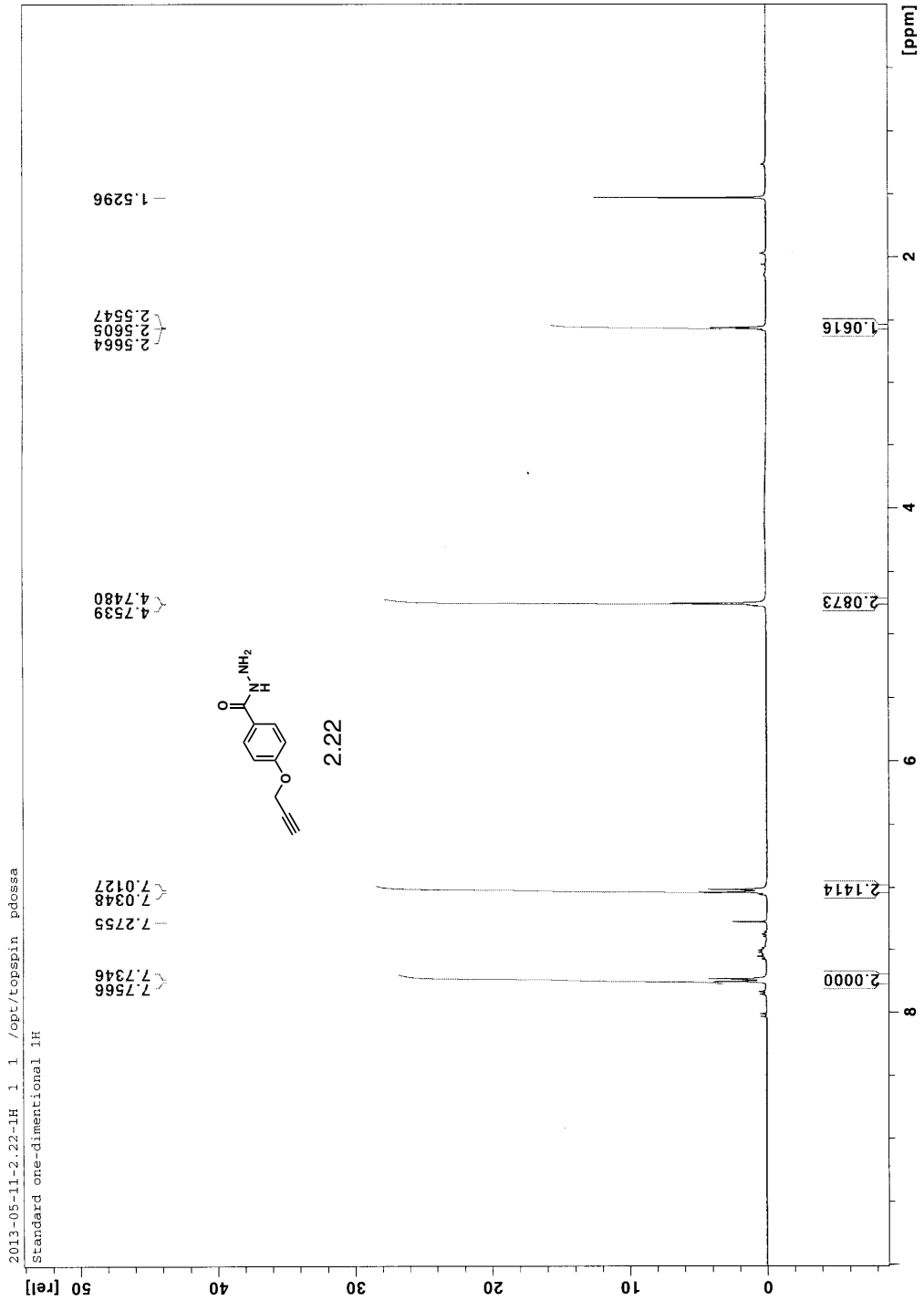


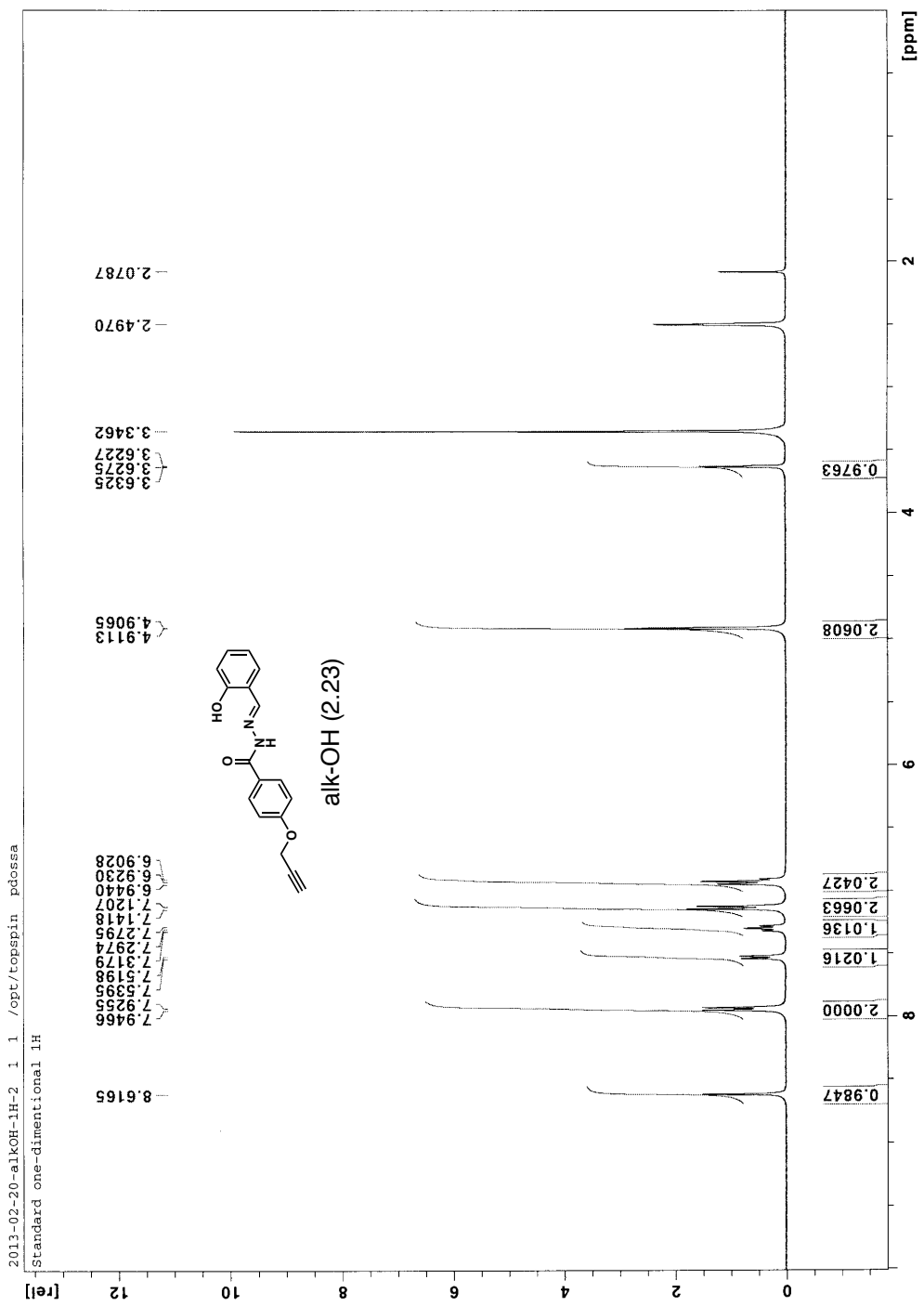


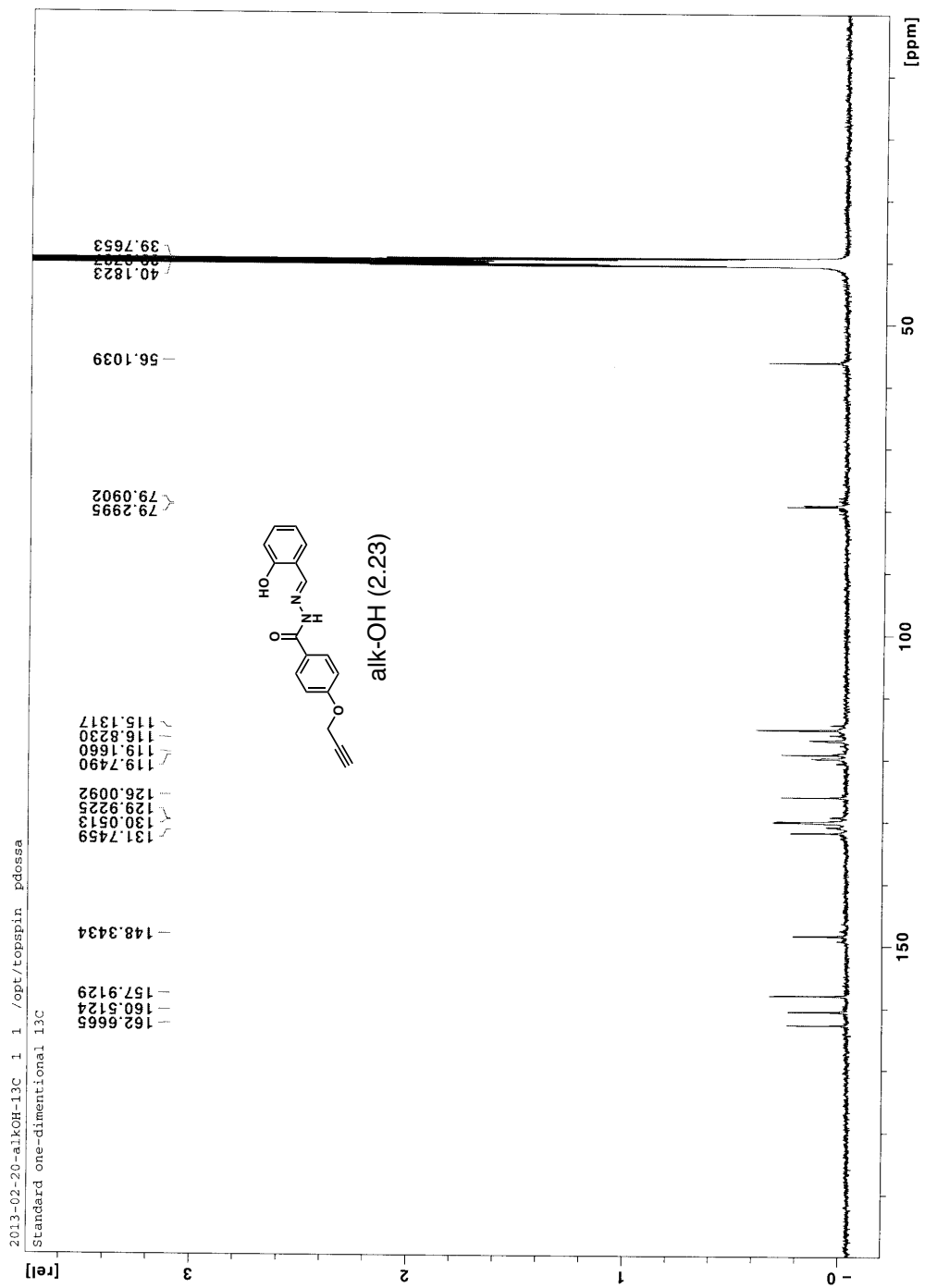


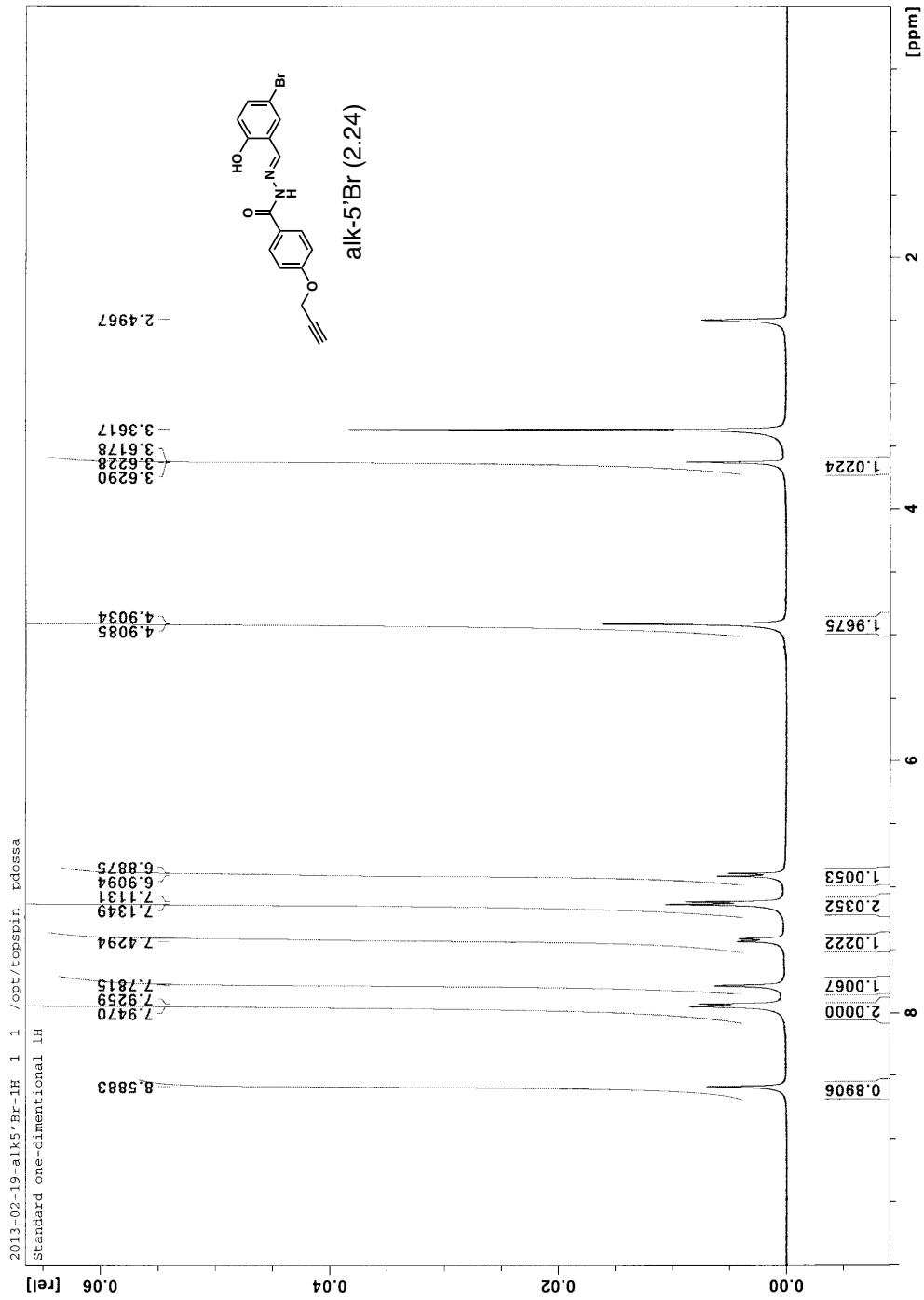
Standard One-dimensional ¹H Experiment

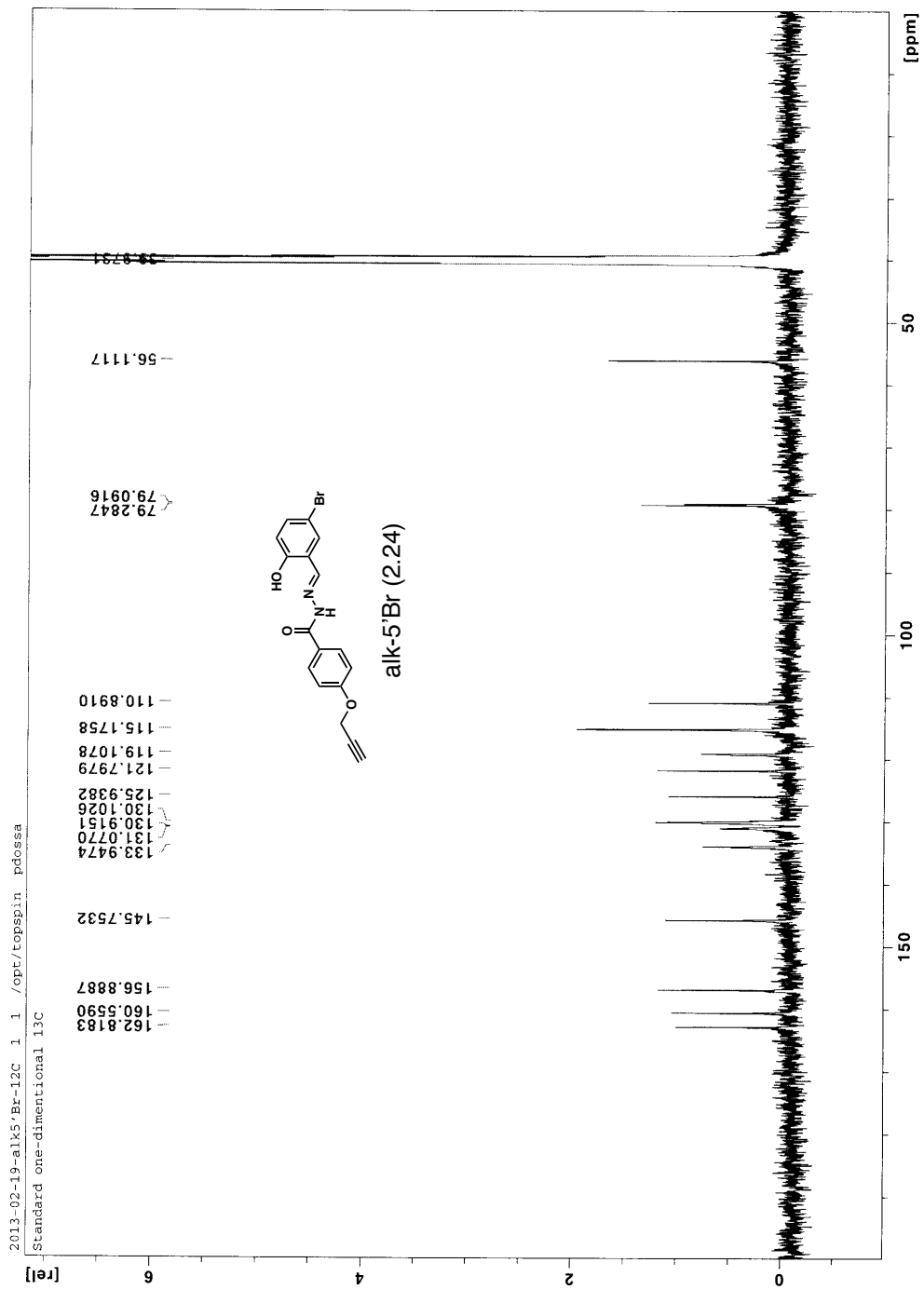


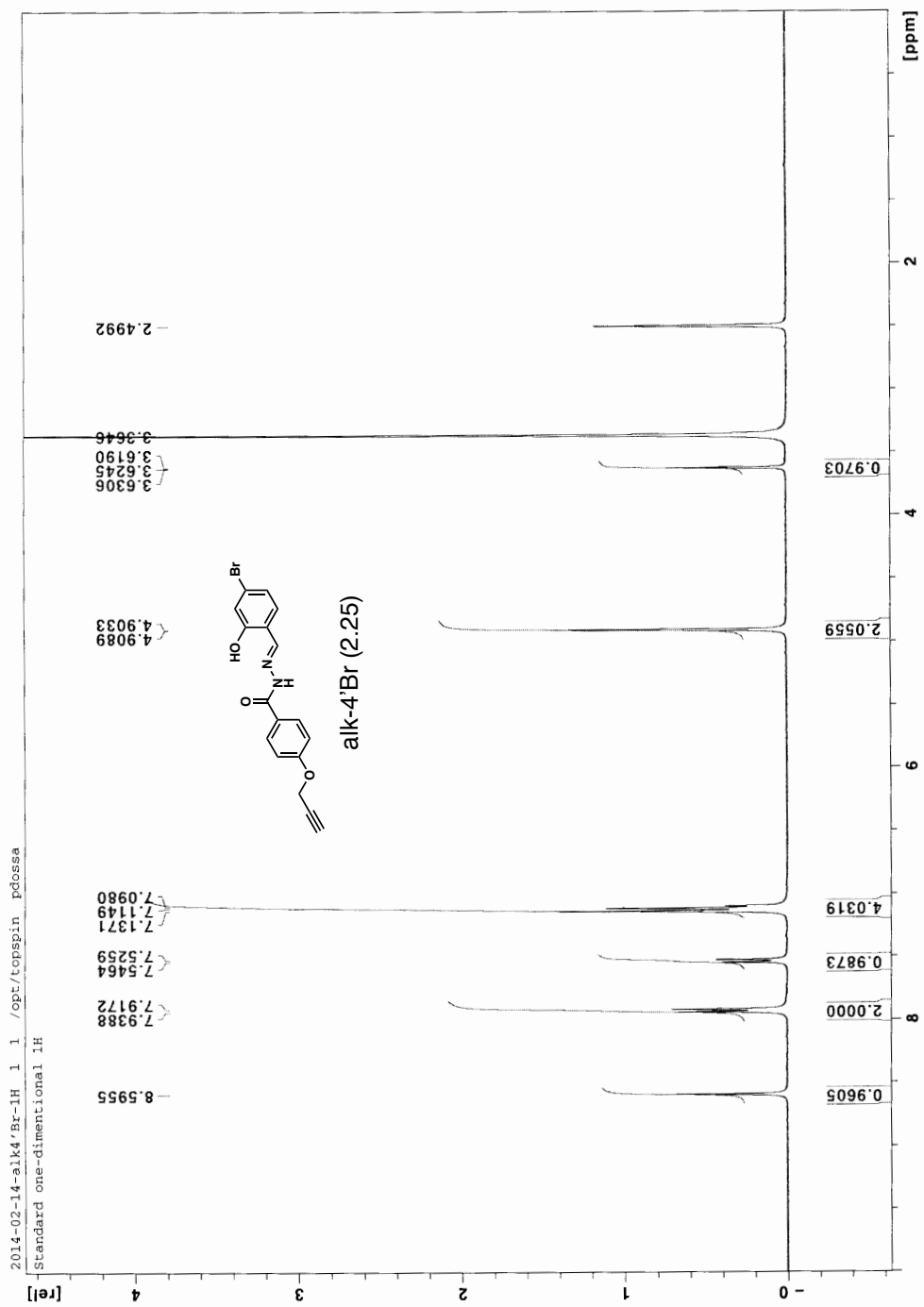


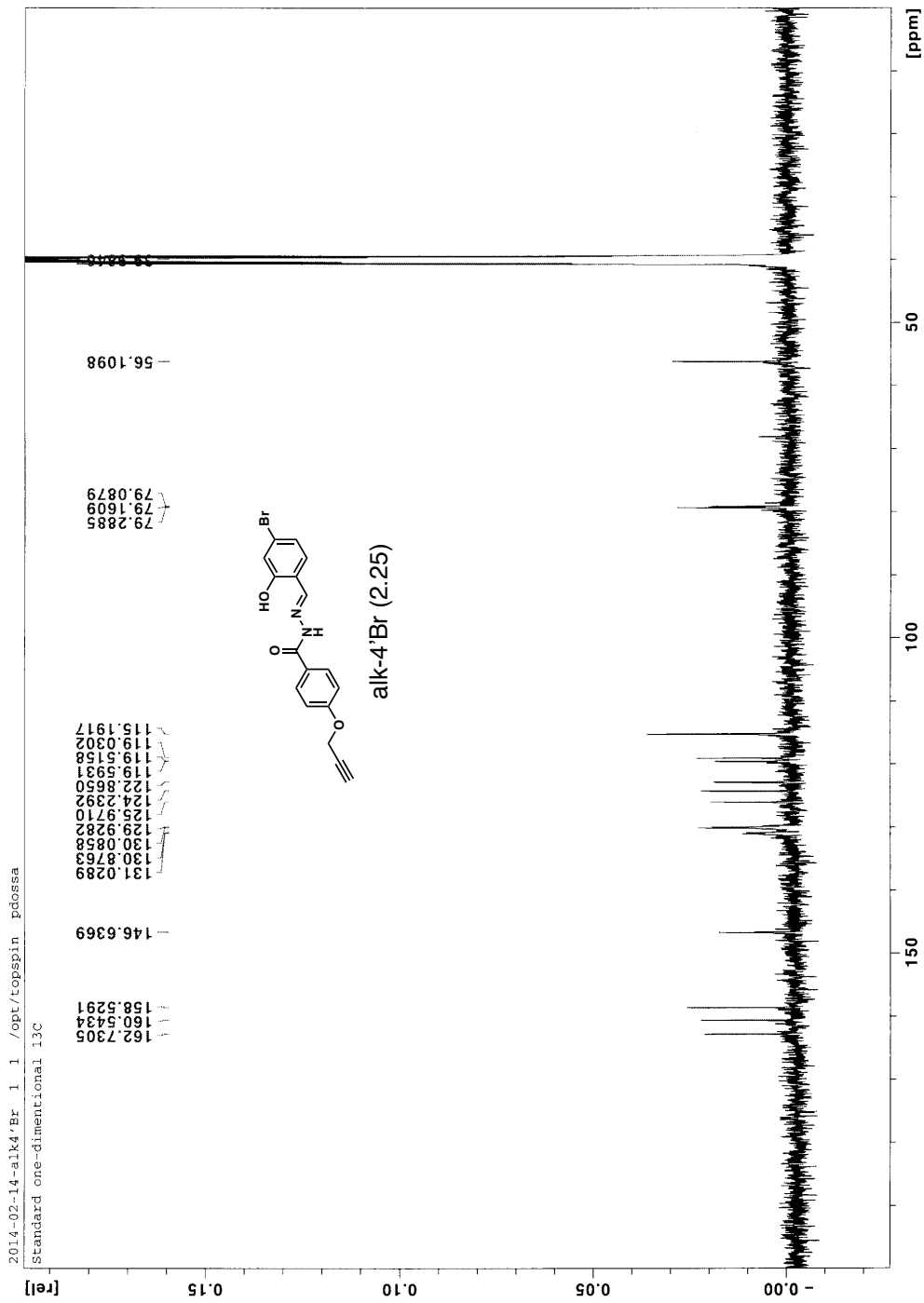


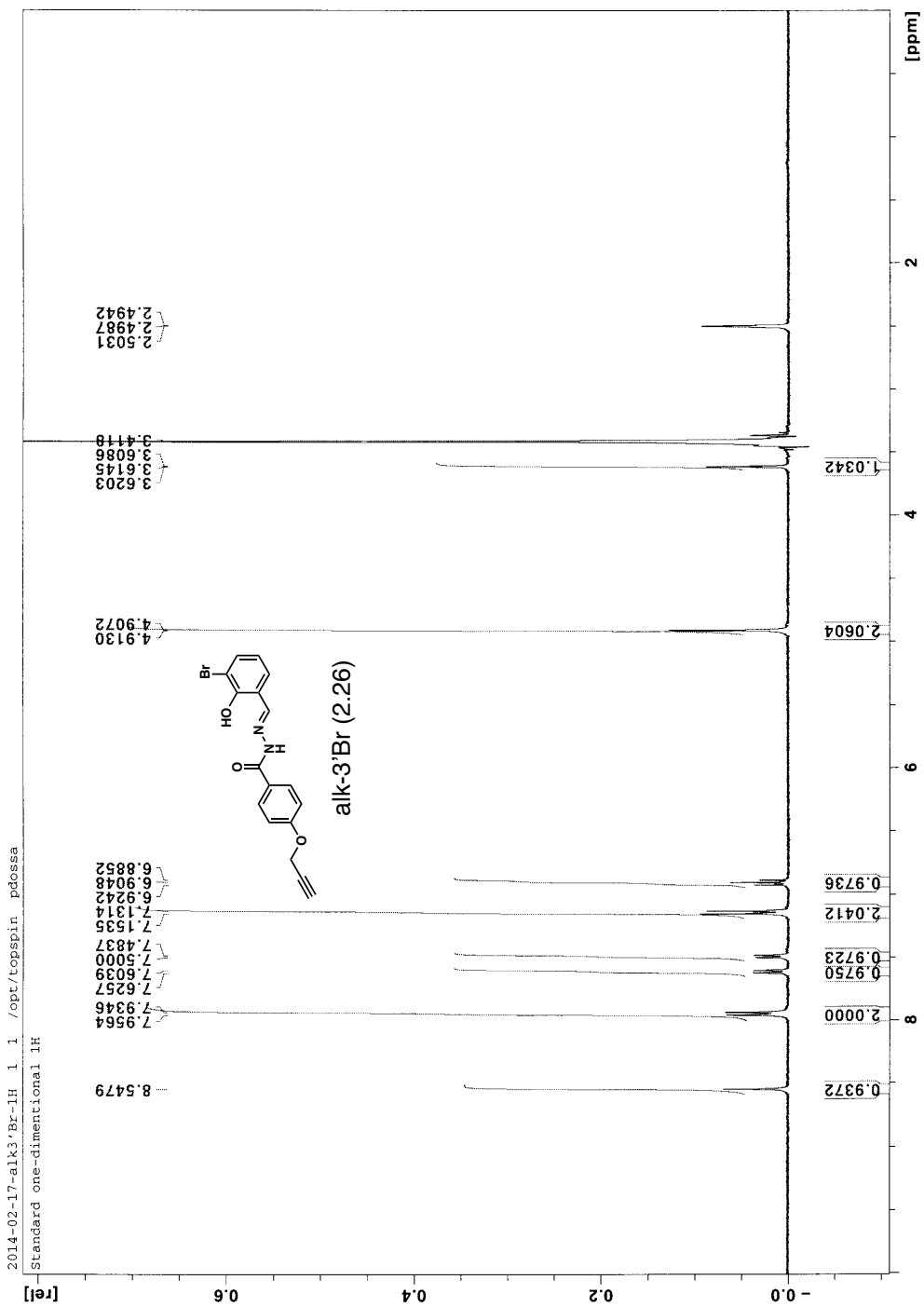


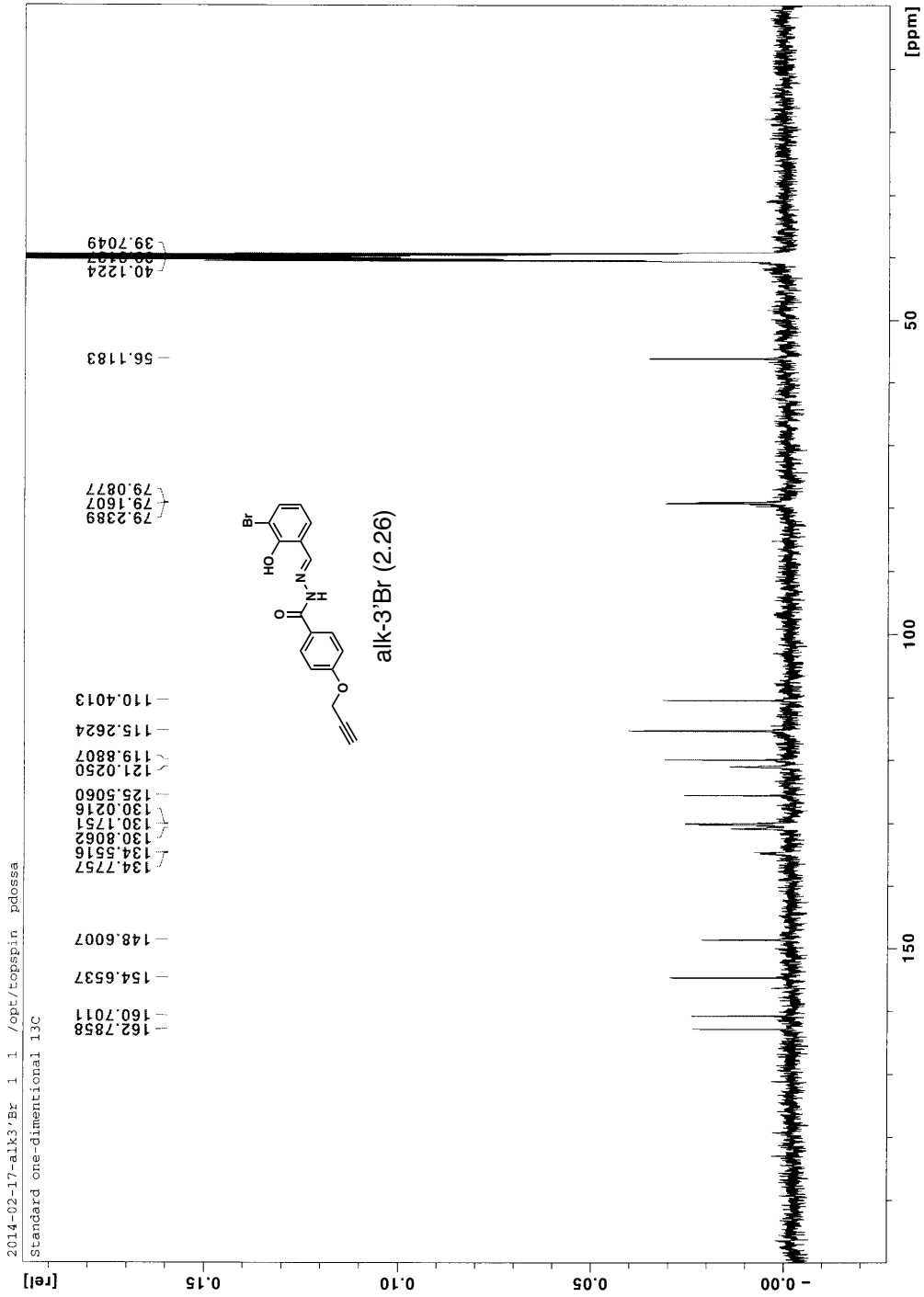


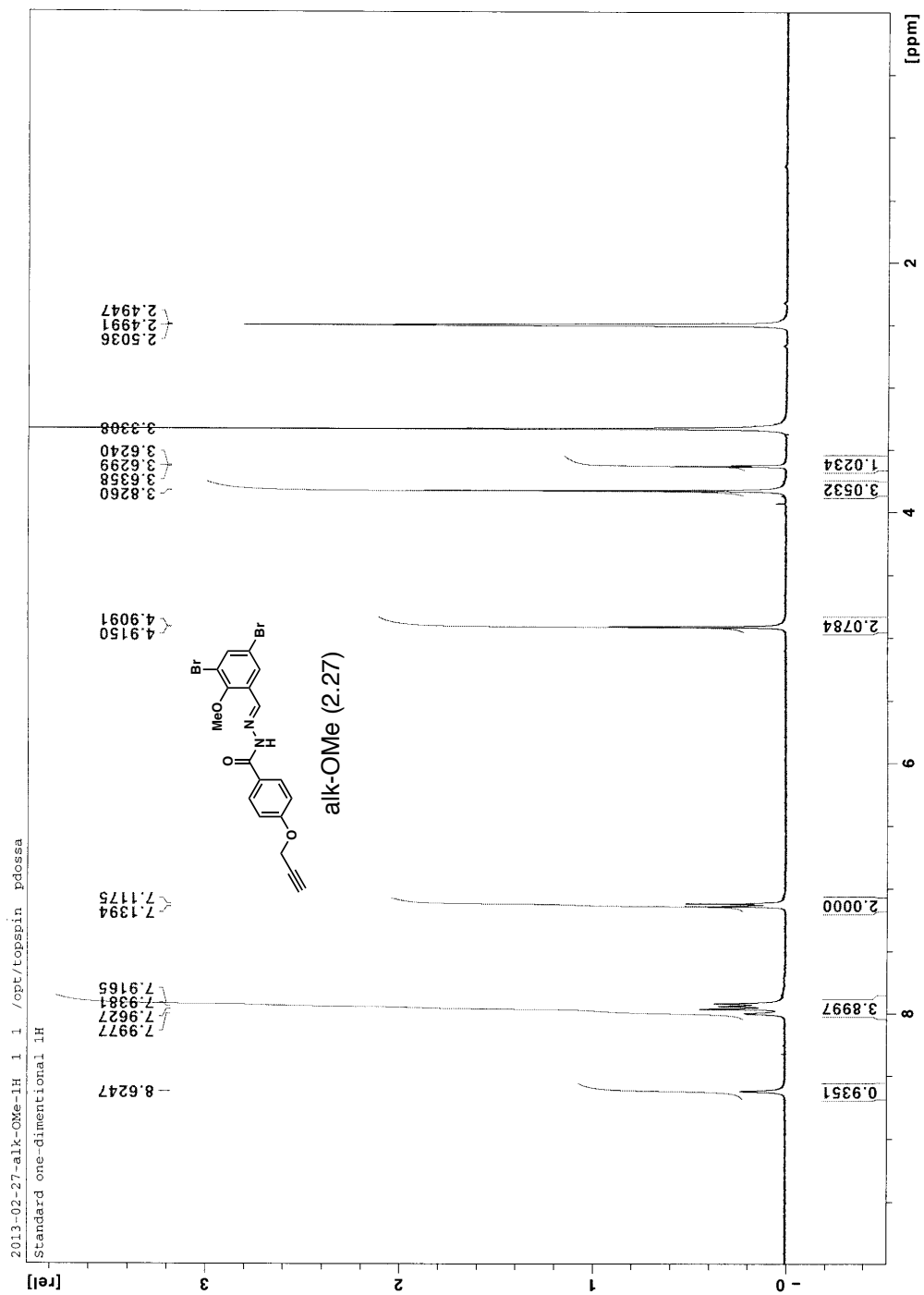


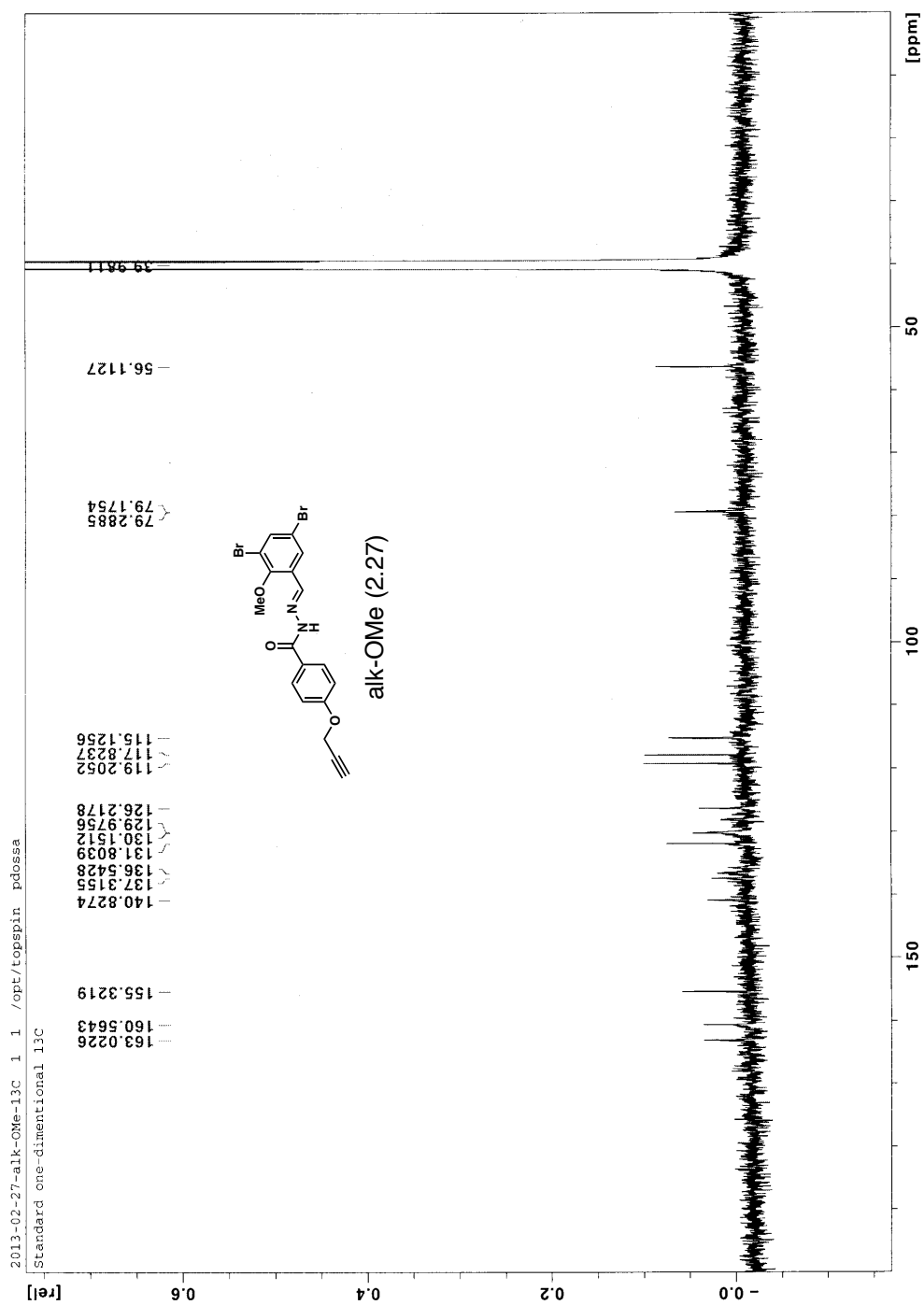


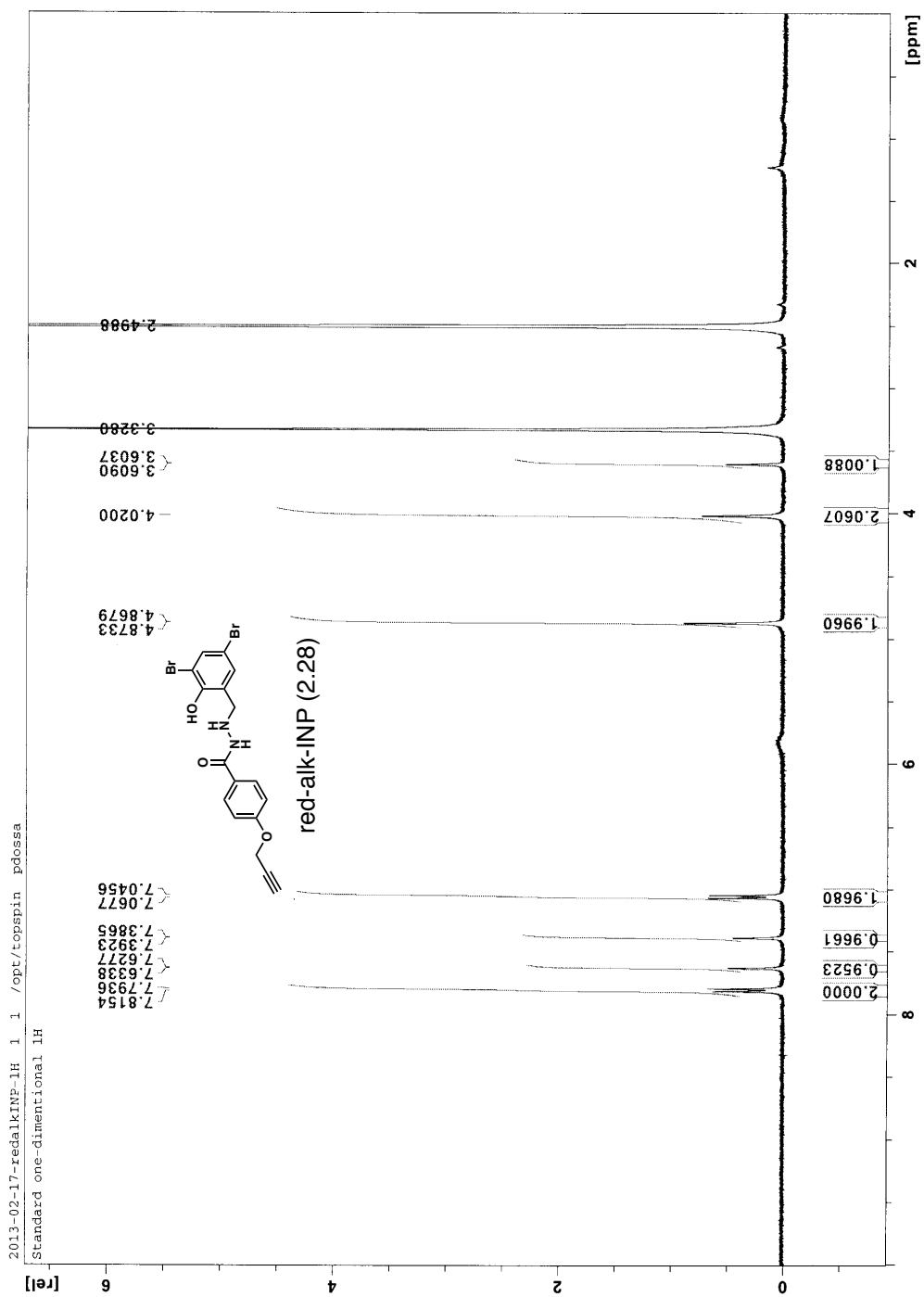


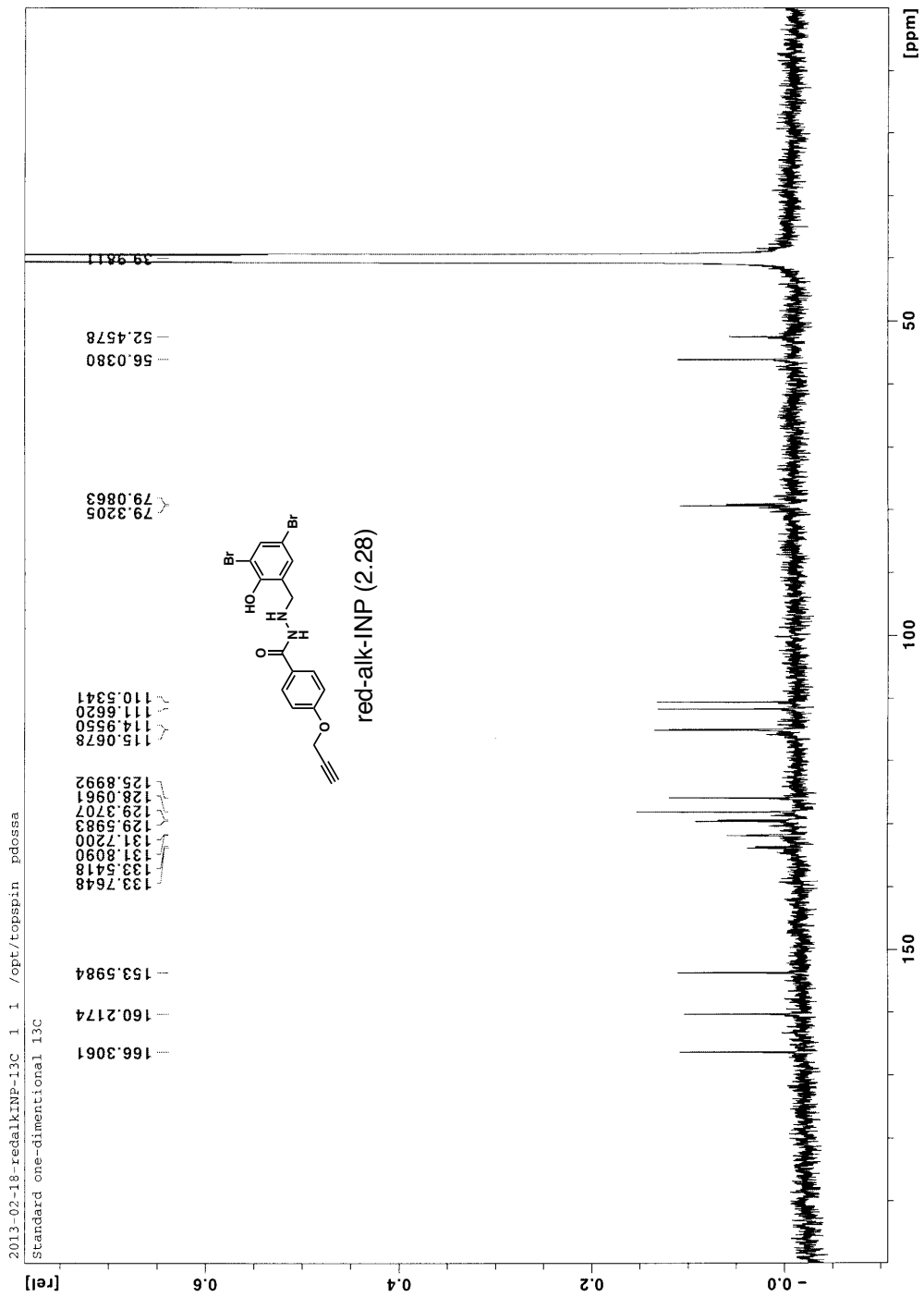












REFERENCES

1. Rasko DA, Sperandio V (2010) Anti-virulence strategies to combat bacteria-mediated disease. *Nat Rev Drug Discov* 9: 117-128.
2. Clatworthy AE, Pierson E, Hung DT (2007) Targeting virulence: a new paradigm for antimicrobial therapy. *Nat Chem Biol* 3: 541-548.
3. Hawkey PM, Jones AM (2009) The changing epidemiology of resistance. *J Antimicrob Chemother* 64 Suppl 1: i3-10.
4. Cotter PD, Stanton C, Ross RP, Hill C (2012) The impact of antibiotics on the gut microbiota as revealed by high throughput DNA sequencing. *Discov Med* 13: 193-199.
5. Hooper LV, Littman DR, Macpherson AJ (2012) Interactions between the microbiota and the immune system. *Science* 336: 1268-1273.
6. Jarchum I, Pamer EG (2011) Regulation of innate and adaptive immunity by the commensal microbiota. *Curr Opin Immunol* 23: 353-360.
7. Ubeda C, Pamer EG (2012) Antibiotics, microbiota, and immune defense. *Trends Immunol* 33: 459-466.
8. Hill DA, Artis D (2010) Intestinal bacteria and the regulation of immune cell homeostasis. *Annu Rev Immunol* 28: 623-667.
9. Clemente JC, Ursell LK, Parfrey LW, Knight R (2012) The impact of the gut microbiota on human health: an integrative view. *Cell* 148: 1258-1270.
10. Macpherson AJ, Uhr T (2004) Induction of protective IgA by intestinal dendritic cells carrying commensal bacteria. *Science* 303: 1662-1665.
11. Mazmanian SK, Liu CH, Tzianabos AO, Kasper DL (2005) An immunomodulatory molecule of symbiotic bacteria directs maturation of the host immune system. *Cell* 122: 107-118.
12. Ivanov, II, Atarashi K, Manel N, Brodie EL, Shima T, et al. (2009) Induction of intestinal Th17 cells by segmented filamentous bacteria. *Cell* 139: 485-498.
13. Willing BP, Russell SL, Finlay BB (2011) Shifting the balance: antibiotic effects on host-microbiota mutualism. *Nat Rev Microbiol* 9: 233-243.
14. Jernberg C, Lofmark S, Edlund C, Jansson JK (2010) Long-term impacts of antibiotic exposure on the human intestinal microbiota. *Microbiology* 156: 3216-3223.

15. Tedesco FJ, Barton RW, Alpers DH (1974) Clindamycin-associated colitis. A prospective study. *Ann Intern Med* 81: 429-433.
16. Sekirov I, Tam NM, Jogova M, Robertson ML, Li Y, et al. (2008) Antibiotic-induced perturbations of the intestinal microbiota alter host susceptibility to enteric infection. *Infect Immun* 76: 4726-4736.
17. Schumann A, Nutten S, Donnicola D, Comelli EM, Mansourian R, et al. (2005) Neonatal antibiotic treatment alters gastrointestinal tract developmental gene expression and intestinal barrier transcriptome. *Physiol Genomics* 23: 235-245.
18. Ma T, Thiagarajah JR, Yang H, Sonawane ND, Folli C, et al. (2002) Thiazolidinone CFTR inhibitor identified by high-throughput screening blocks cholera toxin-induced intestinal fluid secretion. *J Clin Invest* 110: 1651-1658.
19. Lebeis SL, Kalman D (2009) Aligning antimicrobial drug discovery with complex and redundant host-pathogen interactions. *Cell Host Microbe* 5: 114-122.
20. Rainey GJ, Young JA (2004) Antitoxins: novel strategies to target agents of bioterrorism. *Nat Rev Microbiol* 2: 721-726.
21. Scobie HM, Thomas D, Marlett JM, Destito G, Wigelsworth DJ, et al. (2005) A soluble receptor decoy protects rats against anthrax lethal toxin challenge. *J Infect Dis* 192: 1047-1051.
22. Miller MB, Bassler BL (2001) Quorum sensing in bacteria. *Annu Rev Microbiol* 55: 165-199.
23. Waters CM, Bassler BL (2005) Quorum sensing: cell-to-cell communication in bacteria. *Annu Rev Cell Dev Biol* 21: 319-346.
24. Geske GD, Wezeman RJ, Siegel AP, Blackwell HE (2005) Small molecule inhibitors of bacterial quorum sensing and biofilm formation. *J Am Chem Soc* 127: 12762-12763.
25. Wu H, Song Z, Hentzer M, Andersen JB, Molin S, et al. (2004) Synthetic furanones inhibit quorum-sensing and enhance bacterial clearance in *Pseudomonas aeruginosa* lung infection in mice. *J Antimicrob Chemother* 53: 1054-1061.
26. Rasko DA, Moreira CG, Li de R, Reading NC, Ritchie JM, et al. (2008) Targeting QseC signaling and virulence for antibiotic development. *Science* 321: 1078-1080.
27. Proft T, Baker EN (2009) Pili in Gram-negative and Gram-positive bacteria - structure, assembly and their role in disease. *Cell Mol Life Sci* 66: 613-635.

28. Pinkner JS, Remaut H, Buelens F, Miller E, Aberg V, et al. (2006) Rationally designed small compounds inhibit pilus biogenesis in uropathogenic bacteria. *Proc Natl Acad Sci U S A* 103: 17897-17902.
29. Svensson A, Larsson A, Emtenas H, Hedenstrom M, Fex T, et al. (2001) Design and evaluation of pilicides: potential novel antibacterial agents directed against uropathogenic *Escherichia coli*. *Chembiochem* 2: 915-918.
30. Galan JE, Wolf-Watz H (2006) Protein delivery into eukaryotic cells by type III secretion machines. *Nature* 444: 567-573.
31. Keyser P, Elofsson M, Rosell S, Wolf-Watz H (2008) Virulence blockers as alternatives to antibiotics: type III secretion inhibitors against Gram-negative bacteria. *J Intern Med* 264: 17-29.
32. Kline T, Felise HB, Sanowar S, Miller SI (2012) The type III secretion system as a source of novel antibacterial drug targets. *Curr Drug Targets* 13: 338-351.
33. Lee VT, Kessler JL (2009) Type III secretion systems as targets for novel therapeutics. *IDrugs* 12: 636-641.
34. Izore T, Job V, Dessen A (2011) Biogenesis, regulation, and targeting of the type III secretion system. *Structure* 19: 603-612.
35. Cornelis GR (2006) The type III secretion injectisome. *Nat Rev Microbiol* 4: 811-825.
36. Santiviago CA, Reynolds MM, Porwollik S, Choi SH, Long F, et al. (2009) Analysis of pools of targeted *Salmonella* deletion mutants identifies novel genes affecting fitness during competitive infection in mice. *PLoS Pathog* 5: e1000477.
37. Marlovits TC, Kubori T, Sukhan A, Thomas DR, Galan JE, et al. (2004) Structural insights into the assembly of the type III secretion needle complex. *Science* 306: 1040-1042.
38. Marlovits TC, Kubori T, Lara-Tejero M, Thomas D, Unger VM, et al. (2006) Assembly of the inner rod determines needle length in the type III secretion injectisome. *Nature* 441: 637-640.
39. Schraidt O, Marlovits TC (2011) Three-dimensional model of *Salmonella*'s needle complex at subnanometer resolution. *Science* 331: 1192-1195.
40. Schraidt O, Lefebvre MD, Brunner MJ, Schmied WH, Schmidt A, et al. (2010) Topology and organization of the *Salmonella typhimurium* type III secretion needle complex components. *PLoS Pathog* 6: e1000824.
41. Marlovits TC, Stebbins CE (2010) Type III secretion systems shape up as they ship out. *Curr Opin Microbiol* 13: 47-52.

42. Galan JE (2001) Salmonella interactions with host cells: type III secretion at work. *Annu Rev Cell Dev Biol* 17: 53-86.
43. Lara-Tejero M, Kato J, Wagner S, Liu X, Galan JE (2011) A sorting platform determines the order of protein secretion in bacterial type III systems. *Science* 331: 1188-1191.
44. Coburn B, Sekirov I, Finlay BB (2007) Type III secretion systems and disease. *Clin Microbiol Rev* 20: 535-549.
45. Hauser AR (2009) The type III secretion system of *Pseudomonas aeruginosa*: infection by injection. *Nat Rev Microbiol* 7: 654-665.
46. Galan JE (2009) Common themes in the design and function of bacterial effectors. *Cell Host Microbe* 5: 571-579.
47. Tsou LK, Dossa PD, Hang HC (2013) Small molecules aimed at type III secretion systems to inhibit bacterial virulence. *MedChemComm* 4: 68-79.
48. Kauppi AM, Nordfelth R, Uvell H, Wolf-Watz H, Elofsson M (2003) Targeting bacterial virulence: inhibitors of type III secretion in *Yersinia*. *Chem Biol* 10: 241-249.
49. Felise HB, Nguyen HV, Pfuetzner RA, Barry KC, Jackson SR, et al. (2008) An inhibitor of gram-negative bacterial virulence protein secretion. *Cell Host Microbe* 4: 325-336.
50. Yount JS, Tsou LK, Dossa PD, Kullas AL, van der Velden AW, et al. (2010) Visible fluorescence detection of type III protein secretion from bacterial pathogens. *J Am Chem Soc* 132: 8244-8245.
51. Harmon DE, Davis AJ, Castillo C, Meccas J (2010) Identification and characterization of small-molecule inhibitors of Yop translocation in *Yersinia pseudotuberculosis*. *Antimicrob Agents Chemother* 54: 3241-3254.
52. Schlumberger MC, Muller AJ, Ehrbar K, Winnen B, Duss I, et al. (2005) Real-time imaging of type III secretion: *Salmonella* SipA injection into host cells. *Proc Natl Acad Sci U S A* 102: 12548-12553.
53. Van Engelenburg SB, Palmer AE (2010) Imaging type-III secretion reveals dynamics and spatial segregation of *Salmonella* effectors. *Nat Methods* 7: 325-330.
54. Enninga J, Mounier J, Sansonetti P, Tran Van Nhieu G (2005) Secretion of type III effectors into host cells in real time. *Nat Methods* 2: 959-965.
55. Van Engelenburg SB, Palmer AE (2008) Quantification of real-time *Salmonella* effector type III secretion kinetics reveals differential secretion rates for SopE2 and SptP. *Chem Biol* 15: 619-628.

56. Simpson N, Audry L, Enninga J (2010) Tracking the secretion of fluorescently labeled type III effectors from single bacteria in real time. *Methods Mol Biol* 619: 241-256.
57. Pettersson J, Nordfelth R, Dubinina E, Bergman T, Gustafsson M, et al. (1996) Modulation of virulence factor expression by pathogen target cell contact. *Science* 273: 1231-1233.
58. Kauppi AM, Andersson CD, Norberg HA, Sundin C, Linusson A, et al. (2007) Inhibitors of type III secretion in *Yersinia*: design, synthesis and multivariate QSAR of 2-arylsulfonylamino-benzanilides. *Bioorg Med Chem* 15: 6994-7011.
59. Gauthier A, Robertson ML, Lowden M, Ibarra JA, Puente JL, et al. (2005) Transcriptional inhibitor of virulence factors in enteropathogenic *Escherichia coli*. *Antimicrob Agents Chemother* 49: 4101-4109.
60. Macielag MJ, Demers JP, Fraga-Spano SA, Hlasta DJ, Johnson SG, et al. (1998) Substituted salicylanilides as inhibitors of two-component regulatory systems in bacteria. *J Med Chem* 41: 2939-2945.
61. Nordfelth R, Kauppi AM, Norberg HA, Wolf-Watz H, Elofsson M (2005) Small-molecule inhibitors specifically targeting type III secretion. *Infect Immun* 73: 3104-3114.
62. Tree JJ, Wang D, McNally C, Mahajan A, Layton A, et al. (2009) Characterization of the effects of salicylidene acylhydrazide compounds on type III secretion in *Escherichia coli* O157:H7. *Infect Immun* 77: 4209-4220.
63. Wang D, Zetterstrom CE, Gabrielsen M, Beckham KS, Tree JJ, et al. (2011) Identification of bacterial target proteins for the salicylidene acylhydrazide class of virulence-blocking compounds. *J Biol Chem* 286: 29922-29931.
64. Gong S, Lei L, Chang X, Belland R, Zhong G (2011) *Chlamydia trachomatis* secretion of hypothetical protein CT622 into host cell cytoplasm via a secretion pathway that can be inhibited by the type III secretion system inhibitor compound 1. *Microbiology* 157: 1134-1144.
65. Muschiol S, Bailey L, Gylfe A, Sundin C, Hultenby K, et al. (2006) A small-molecule inhibitor of type III secretion inhibits different stages of the infectious cycle of *Chlamydia trachomatis*. *Proc Natl Acad Sci U S A* 103: 14566-14571.
66. Wolf K, Betts HJ, Chellas-Gery B, Hower S, Linton CN, et al. (2006) Treatment of *Chlamydia trachomatis* with a small molecule inhibitor of the *Yersinia* type III secretion system disrupts progression of the chlamydial developmental cycle. *Mol Microbiol* 61: 1543-1555.

67. Bailey L, Gylfe A, Sundin C, Muschiol S, Elofsson M, et al. (2007) Small molecule inhibitors of type III secretion in *Yersinia* block the *Chlamydia pneumoniae* infection cycle. *FEBS Lett* 581: 587-595.
68. Slepkin A, Enquist PA, Hagglund U, de la Maza LM, Elofsson M, et al. (2007) Reversal of the antichlamydial activity of putative type III secretion inhibitors by iron. *Infect Immun* 75: 3478-3489.
69. Muschiol S, Normark S, Henriques-Normark B, Subtil A (2009) Small molecule inhibitors of the *Yersinia* type III secretion system impair the development of *Chlamydia* after entry into host cells. *BMC Microbiol* 9: 75.
70. Hudson DL, Layton AN, Field TR, Bowen AJ, Wolf-Watz H, et al. (2007) Inhibition of type III secretion in *Salmonella enterica* serovar Typhimurium by small-molecule inhibitors. *Antimicrob Agents Chemother* 51: 2631-2635.
71. Negrea A, Bjur E, Ygberg SE, Elofsson M, Wolf-Watz H, et al. (2007) Salicylidene acylhydrazides that affect type III protein secretion in *Salmonella enterica* serovar typhimurium. *Antimicrob Agents Chemother* 51: 2867-2876.
72. Layton AN, Hudson DL, Thompson A, Hinton JC, Stevens JM, et al. (2010) Salicylidene acylhydrazide-mediated inhibition of type III secretion system-1 in *Salmonella enterica* serovar Typhimurium is associated with iron restriction and can be reversed by free iron. *FEMS Microbiol Lett* 302: 114-122.
73. Veenendaal AK, Sundin C, Blocker AJ (2009) Small-molecule type III secretion system inhibitors block assembly of the *Shigella* type III secretion. *J Bacteriol* 191: 563-570.
74. Ur-Rehman T, Slepkin A, Chu H, Blomgren A, Dahlgren MK, et al. (2012) Pre-clinical pharmacokinetics and anti-chlamydial activity of salicylidene acylhydrazide inhibitors of bacterial type III secretion. *J Antibiot (Tokyo)* 65: 397-404.
75. Forthal DN, Phan TB, Slepkin AV, Landucci G, Chu H, et al. (2012) In vitro anti-HIV-1 activity of salicylidene acylhydrazide compounds. *Int J Antimicrob Agents* 40: 354-360.
76. Dahlgren MK, Zetterstrom CE, Gylfe S, Linusson A, Elofsson M (2010) Statistical molecular design of a focused salicylidene acylhydrazide library and multivariate QSAR of inhibition of type III secretion in the Gram-negative bacterium *Yersinia*. *Bioorg Med Chem* 18: 2686-2703.
77. Kline T, Felise HB, Barry KC, Jackson SR, Nguyen HV, et al. (2008) Substituted 2-imino-5-arylidene-thiazolidin-4-one inhibitors of bacterial type III secretion. *J Med Chem* 51: 7065-7074.

78. Kline T, Barry KC, Jackson SR, Felise HB, Nguyen HV, et al. (2009) Tethered thiazolidinone dimers as inhibitors of the bacterial type III secretion system. *Bioorg Med Chem Lett* 19: 1340-1343.
79. Li X (2005) Inhibitors of bacterial type III secretion systems. In: patent U, editor.
80. Aiello D, Williams JD, Majgier-Baranowska H, Patel I, Peet NP, et al. (2010) Discovery and characterization of inhibitors of *Pseudomonas aeruginosa* type III secretion. *Antimicrob Agents Chemother* 54: 1988-1999.
81. Pan NJ, Brady MJ, Leong JM, Goguen JD (2009) Targeting type III secretion in *Yersinia pestis*. *Antimicrob Agents Chemother* 53: 385-392.
82. Li X, Kang F-A, Macielag MJ (2005) Triazine compounds as inhibitors of bacterial type III protein secretion systems. In: patent U, editor. US.
83. Lee VT, Pukatzki S, Sato H, Kikawada E, Kazimirova AA, et al. (2007) Pseudolipasin A is a specific inhibitor for phospholipase A2 activity of *Pseudomonas aeruginosa* cytotoxin ExoU. *Infect Immun* 75: 1089-1098.
84. Kim OK, Garrity-Ryan LK, Bartlett VJ, Grier MC, Verma AK, et al. (2009) N-hydroxybenzimidazole inhibitors of the transcription factor LcrF in *Yersinia*: novel antivirulence agents. *J Med Chem* 52: 5626-5634.
85. Garrity-Ryan LK, Kim OK, Balada-Llasat JM, Bartlett VJ, Verma AK, et al. (2010) Small molecule inhibitors of LcrF, a *Yersinia pseudotuberculosis* transcription factor, attenuate virulence and limit infection in a murine pneumonia model. *Infect Immun* 78: 4683-4690.
86. Swietnicki W, Carmany D, Retford M, Guelta M, Dorsey R, et al. (2011) Identification of small-molecule inhibitors of *Yersinia pestis* Type III secretion system YscN ATPase. *PLoS One* 6: e19716.
87. Linington RG, Robertson M, Gauthier A, Finlay BB, van Soest R, et al. (2002) Caminoside A, an antimicrobial glycolipid isolated from the marine sponge *Caminus sphaeroconia*. *Org Lett* 4: 4089-4092.
88. Linington RG, Robertson M, Gauthier A, Finlay BB, MacMillan JB, et al. (2006) Caminosides B-D, antimicrobial glycolipids isolated from the marine sponge *Caminus sphaeroconia*. *J Nat Prod* 69: 173-177.
89. Iwatsuki M, Uchida R, Yoshijima H, Ui H, Shiomi K, et al. (2008) Guadinomines, Type III secretion system inhibitors, produced by *Streptomyces* sp. K01-0509. I: taxonomy, fermentation, isolation and biological properties. *J Antibiot (Tokyo)* 61: 222-229.
90. Iwatsuki M, Uchida R, Yoshijima H, Ui H, Shiomi K, et al. (2008) Guadinomines, Type III secretion system inhibitors, produced by *Streptomyces* sp. K01-0509. II:

physico-chemical properties and structure elucidation. *J Antibiot (Tokyo)* 61: 230-236.

91. Hirose T, Sunazuka T, Tsuchiya S, Tanaka T, Kojima Y, et al. (2008) Total synthesis and determination of the absolute configuration of guadinomines B and C2. *Chemistry* 14: 8220-8238.
92. Kimura K, Iwatsuki M, Nagai T, Matsumoto A, Takahashi Y, et al. (2010) A small-molecule inhibitor of the bacterial type III secretion system protects against in vivo infection with *Citrobacter rodentium*. *J Antibiot (Tokyo)* 64: 197-203.
93. Li J, Lv C, Sun W, Li Z, Han X, et al. (2013) Cytosporone B, an Inhibitor of Type Three Secretion System of *Salmonella enterica* serovar Typhimurium. *Antimicrob Agents Chemother.*
94. Zhan Y, Du X, Chen H, Liu J, Zhao B, et al. (2008) Cytosporone B is an agonist for nuclear orphan receptor Nur77. *Nat Chem Biol* 4: 548-556.
95. Hedley D, Ogilvie L, Springer C (2007) Carboxypeptidase-G2-based gene-directed enzyme-prodrug therapy: a new weapon in the GDEPT armoury. *Nat Rev Cancer* 7: 870-879.
96. Lord SJ, Conley NR, Lee HL, Samuel R, Liu N, et al. (2008) A photoactivatable push-pull fluorophore for single-molecule imaging in live cells. *J Am Chem Soc* 130: 9204-9205.
97. Lord SJ, Conley NR, Lee HL, Nishimura SY, Pomerantz AK, et al. (2009) DCDHF fluorophores for single-molecule imaging in cells. *Chemphyschem* 10: 55-65.
98. Tsou LK, Zhang MM, Hang HC (2009) Clickable fluorescent dyes for multimodal bioorthogonal imaging. *Org Biomol Chem* 7: 5055-5058.
99. Haraga A, Ohlson MB, Miller SI (2008) *Salmonellae* interplay with host cells. *Nat Rev Microbiol* 6: 53-66.
100. Crump JA, Luby SP, Mintz ED (2004) The global burden of typhoid fever. *Bull World Health Organ* 82: 346-353.
101. Bhutta ZA, Threlfall J (2009) Addressing the global disease burden of typhoid fever. *JAMA* 302: 898-899.
102. Crump JA, Mintz ED (2010) Global trends in typhoid and paratyphoid Fever. *Clin Infect Dis* 50: 241-246.
103. Vilcheze C, Jacobs WR, Jr. (2007) The mechanism of isoniazid killing: clarity through the scope of genetics. *Annu Rev Microbiol* 61: 35-50.

104. Pootoolal J, Neu J, Wright GD (2002) Glycopeptide antibiotic resistance. *Annu Rev Pharmacol Toxicol* 42: 381-408.
105. Ito T, Ando H, Suzuki T, Ogura T, Hotta K, et al. (2010) Identification of a primary target of thalidomide teratogenicity. *Science* 327: 1345-1350.
106. Ziegler S, Pries V, Hedberg C, Waldmann H (2013) Target identification for small bioactive molecules: finding the needle in the haystack. *Angew Chem Int Ed Engl* 52: 2744-2792.
107. Ong SE, Blagoev B, Kratchmarova I, Kristensen DB, Steen H, et al. (2002) Stable isotope labeling by amino acids in cell culture, SILAC, as a simple and accurate approach to expression proteomics. *Mol Cell Proteomics* 1: 376-386.
108. Ong SE, Mann M (2005) Mass spectrometry-based proteomics turns quantitative. *Nat Chem Biol* 1: 252-262.
109. Bantscheff M, Hopf C, Savitski MM, Dittmann A, Grandi P, et al. (2011) Chemoproteomics profiling of HDAC inhibitors reveals selective targeting of HDAC complexes. *Nat Biotechnol* 29: 255-265.
110. Lallana E, Riguera R, Fernandez-Megia E (2011) Reliable and efficient procedures for the conjugation of biomolecules through Huisgen azide-alkyne cycloadditions. *Angew Chem Int Ed Engl* 50: 8794-8804.
111. Yang YY, Ascano JM, Hang HC (2010) Bioorthogonal chemical reporters for monitoring protein acetylation. *J Am Chem Soc* 132: 3640-3641.
112. Yount JS, Zhang MM, Hang HC (2011) Visualization and Identification of Fatty Acylated Proteins Using Chemical Reporters. *Curr Protoc Chem Biol* 3: 65-79.
113. Charron G, Zhang MM, Yount JS, Wilson J, Raghavan AS, et al. (2009) Robust fluorescent detection of protein fatty-acylation with chemical reporters. *J Am Chem Soc* 131: 4967-4975.
114. Rangan KJ, Yang YY, Charron G, Hang HC (2010) Rapid visualization and large-scale profiling of bacterial lipoproteins with chemical reporters. *J Am Chem Soc* 132: 10628-10629.
115. Yount JS, Moltedo B, Yang YY, Charron G, Moran TM, et al. (2010) Palmitoylome profiling reveals S-palmitoylation-dependent antiviral activity of IFITM3. *Nat Chem Biol* 6: 610-614.
116. Grammel M, Dossa PD, Taylor-Salmon E, Hang HC (2012) Cell-selective labeling of bacterial proteomes with an orthogonal phenylalanine amino acid reporter. *Chem Commun (Camb)* 48: 1473-1474.

117. Saghatelian A, Jessani N, Joseph A, Humphrey M, Cravatt BF (2004) Activity-based probes for the proteomic profiling of metalloproteases. *Proc Natl Acad Sci U S A* 101: 10000-10005.
118. Speers AE, Adam GC, Cravatt BF (2003) Activity-based protein profiling in vivo using a copper(i)-catalyzed azide-alkyne [3 + 2] cycloaddition. *J Am Chem Soc* 125: 4686-4687.
119. Cisar JS, Cravatt BF (2012) Fully functionalized small-molecule probes for integrated phenotypic screening and target identification. *J Am Chem Soc* 134: 10385-10388.
120. Nakashima H, Hashimoto M, Sadakane Y, Tomohiro T, Hatanaka Y (2006) Simple and versatile method for tagging phenyldiazirine photophores. *J Am Chem Soc* 128: 15092-15093.
121. Ainscough EW, Brodie AM, Denny WA, Finlay GJ, Gothe SA, et al. (1999) Cytotoxicity of salicylaldehyde benzoylhydrazone analogs and their transition metal complexes: quantitative structure-activity relationships. *J Inorg Biochem* 77: 125-133.
122. Mayer T, Maier ME (2007) Design and Synthesis of a Tag-Free Chemical Probe for Photoaffinity Labeling. *European Journal of Organic Chemistry* 2007: 4711-4720.
123. Singh J, Petter RC, Baillie TA, Whitty A (2011) The resurgence of covalent drugs. *Nat Rev Drug Discov* 10: 307-317.
124. Kuijl C, Savage ND, Marsman M, Tuin AW, Janssen L, et al. (2007) Intracellular bacterial growth is controlled by a kinase network around PKB/AKT1. *Nature* 450: 725-730.
125. Mochalkin I, Miller JR, Narasimhan L, Thanabal V, Erdman P, et al. (2009) Discovery of antibacterial biotin carboxylase inhibitors by virtual screening and fragment-based approaches. *ACS Chem Biol* 4: 473-483.
126. Miller JR, Dunham S, Mochalkin I, Banotai C, Bowman M, et al. (2009) A class of selective antibacterials derived from a protein kinase inhibitor pharmacophore. *Proc Natl Acad Sci U S A* 106: 1737-1742.
127. Walsh CT, Fischbach MA (2009) Repurposing libraries of eukaryotic protein kinase inhibitors for antibiotic discovery. *Proc Natl Acad Sci U S A* 106: 1689-1690.
128. Barnett SF, Defeo-Jones D, Fu S, Hancock PJ, Haskell KM, et al. (2005) Identification and characterization of pleckstrin-homology-domain-dependent and isoenzyme-specific Akt inhibitors. *Biochem J* 385: 399-408.

129. Ohlson MB, Fluhr K, Birmingham CL, Brumell JH, Miller SI (2005) SseJ deacylase activity by *Salmonella enterica* serovar Typhimurium promotes virulence in mice. *Infect Immun* 73: 6249-6259.
130. Lossi NS, Rolhion N, Magee AI, Boyle C, Holden DW (2008) The *Salmonella* SPI-2 effector SseJ exhibits eukaryotic activator-dependent phospholipase A and glycerophospholipid : cholesterol acyltransferase activity. *Microbiology* 154: 2680-2688.
131. Hirai H, Sootome H, Nakatsuru Y, Miyama K, Taguchi S, et al. MK-2206, an allosteric Akt inhibitor, enhances antitumor efficacy by standard chemotherapeutic agents or molecular targeted drugs in vitro and in vivo. *Mol Cancer Ther* 9: 1956-1967.
132. Davies SP, Reddy H, Caivano M, Cohen P (2000) Specificity and mechanism of action of some commonly used protein kinase inhibitors. *Biochem J* 351: 95-105.
133. Chiu HC, Kulp SK, Soni S, Wang D, Gunn JS, et al. (2009) Eradication of intracellular *Salmonella enterica* serovar Typhimurium with a small-molecule, host cell-directed agent. *Antimicrob Agents Chemother* 53: 5236-5244.
134. Karaman MW, Herrgard S, Treiber DK, Gallant P, Atteridge CE, et al. (2008) A quantitative analysis of kinase inhibitor selectivity. *Nat Biotechnol* 26: 127-132.
135. Rogers LD, Brown NF, Fang Y, Pelech S, Foster LJ Phosphoproteomic analysis of *Salmonella*-infected cells identifies key kinase regulators and SopB-dependent host phosphorylation events. *Sci Signal* 4: rs9.
136. Shi J, Casanova JE (2006) Invasion of host cells by *Salmonella typhimurium* requires focal adhesion kinase and p130Cas. *Mol Biol Cell* 17: 4698-4708.
137. Lochner A, Moolman JA (2006) The many faces of H89: a review. *Cardiovasc Drug Rev* 24: 261-274.
138. Moy TI, Ball AR, Anklesaria Z, Casadei G, Lewis K, et al. (2006) Identification of novel antimicrobials using a live-animal infection model. *Proc Natl Acad Sci U S A* 103: 10414-10419.
139. Moy TI, Conery AL, Larkins-Ford J, Wu G, Mazitschek R, et al. (2009) High-throughput screen for novel antimicrobials using a whole animal infection model. *ACS Chem Biol* 4: 527-533.
140. Tenor JL, McCormick BA, Ausubel FM, Aballay A (2004) *Caenorhabditis elegans*-based screen identifies *Salmonella* virulence factors required for conserved host-pathogen interactions. *Curr Biol* 14: 1018-1024.

141. Adams KN, Takaki K, Connolly LE, Wiedenhoft H, Winglee K, et al. (2011) Drug tolerance in replicating mycobacteria mediated by a macrophage-induced efflux mechanism. *Cell* 145: 39-53.
142. Pukkila-Worley R, Feinbaum R, Kirienko NV, Larkins-Ford J, Conery AL, et al. Stimulation of Host Immune Defenses by a Small Molecule Protects *C. elegans* from Bacterial Infection. *PLoS Genet* 8: e1002733.
143. Engh RA, Girod A, Kinzel V, Huber R, Bossemeyer D (1996) Crystal structures of catalytic subunit of cAMP-dependent protein kinase in complex with isoquinolinesulfonyl protein kinase inhibitors H7, H8, and H89. Structural implications for selectivity. *J Biol Chem* 271: 26157-26164.
144. Reuveni H, Livnah N, Geiger T, Klein S, Ohne O, et al. (2002) Toward a PKB inhibitor: modification of a selective PKA inhibitor by rational design. *Biochemistry* 41: 10304-10314.
145. Mitchell G, Lafrance M, Boulanger S, Seguin DL, Guay I, et al. (2012) Tomatidine acts in synergy with aminoglycoside antibiotics against multiresistant *Staphylococcus aureus* and prevents virulence gene expression. *J Antimicrob Chemother* 67: 559-568.